NRL Report 6598

Basic Aspects of Crack Growth and Fracture

November 21, 1967

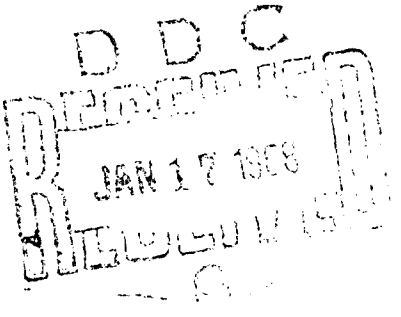

NAVAL RESEARCH LABORATORY
Washington, D.C.

82

NRL Report 6598

Basic Aspects of Crack Growth and Fracture

G. R. Irwin and J. M. Krafft

Mechanics Division

P. C. Paris

Lehigh University
Bethlehem, Pennsylvania

and

A. A. Wells

Queen's University
Belfast, North Ireland

November 21, 1967

NAVAL RESEARCH LABORATORY
Washington, D.C.

CONTENTS

ABSTRACT

A near approach to absolute fracture safety in boiling water (BW) and pressurized water (PW) nuclear reactor pressure vessels requires a very conservative fracture control plan. Such a plan must assume that any plausible cracklike defect, which has not been proved absent by inspection, may exist in the vessel. Requirements for design, materials, and inspection may then be established in a conservative way relative to estimates of progressive crack extension behavior. These estimates are assisted by elastic and plastic methods of analysis of cracks in tension. Approximate methods of assigning K_{Ic} values to measurements of crack toughness in terms of a brittle-ductile transition temperature are valuable in reviewing methods of fracture control which have received trial in the past, such as the NRL fracture analysis diagram and the leak-before-break toughness criterion.

PROGRAM STATUS

This is a final report. Unless otherwise notified the problem will be considered closed 30 days after the issuance of this report.

AUTHORIZATION

NRL Problem F01-18
USAEC Oak Ridge, Tenn., ltr ACT:WT of 9 Aug. 1966

Manuscript submitted May 22, 1967

BASIC ASPECTS OF CRACK GROWTH AND FRACTURE

GENERAL COMMENTS ON DEFECTS AND FRACTURE CONTROL

Strength failures of load-bearing structures can be either of the yielding-dominant or of the fracture-dominant type. Defects are important in both types of failure, but those of primary importance to a fracture failure differ in an extreme way from those influencing resistance to plastic flow. For the latter, the significant defects (dislocation arrays, interstitial atoms, out-of-size substitutional atoms, grain boundary spacings, bonded precipitate particles) are those which tend to warp and interrupt the crystalline lattice planes, thus interfering with easy glide of dislocations. The resistance to plastic deformation thus provided is essential to the strength of high-strength metals. Larger defects such as inclusions, porosity, surface scratches, and small cracks may influence the effective net-section bearing the load, but otherwise have no significant effect on resistance to plastic yielding.

For failures of the fracture-dominant type (fracture prior to general yielding of the net-section) the size scale of those defects which are of major significance depends upon the toughness of the material. For the common structural steels, surface scratches, regardless of sharpness, do not lower the strength of a tensile specimen unless the testing temperature is far below the NDT (small flaw, drop-weight nil-ductility temperature). The 1/4-in.-size brittle-weld-bead flaw used in NDT fracture testing and the notch depth used in V-notch Charpy fracture appearance transition temperature (FATT) evaluations are indications of the major (directly significant) flaw size for steels in the NDT to FATT temperature range, when a tensile stress equal to the dynamic yield stress is applied. Rapid crack propagation at smaller stresses or smaller loading speed would require cracks of larger size. The minor flaws influencing the fracturing process range downward toward smaller sizes. The minute flaws controlling resistance to plastic flow are of interest in studying macroscopic fracture behaviors primarily because resistance to plastic flow is related to crack toughness.

At temperatures near or above the NDT a structural component of interest for this report must contain at least one cracklike flaw of substantial size before fracture can occur prior to general yielding. The size necessary for crack propagation is a function of toughness and average tensile stress and can be estimated by the methods of fracture mechanics, as will be explained later. Depending upon the size and shape characteristics of a structural component and upon its stress-environment history during service use, a critical condition for crack propagation may develop gradually because of (a) crack growth by fatigue, (b) crack growth by stress corrosion (or hydrogen), or (c) reductions of crack toughness, for example, by radiation damage.

It is unlikely that a crack large enough for propagation by a normal service load would be introduced during fabrication. In any case, the pressure vessels of interest will be pretested with pressures higher (by 25%, say) than the largest expected during service. Thus, the attention of a fracture control plan can focus on achieving a satisfactory time duration of fracture-safe operation relative to the three dangers stated above. These can occur in various combinations. The "safe life" depends upon suitable limiting of these dangers in any way possible.

Unfortunately, interest in studies of crack growth rate for fatigue and stress corrosion conditions is comparatively recent, and data directly applicable to the materials

and conditions of interest are quite limited. Some assurance can, however, be obtained if conservative estimates of stable growth added to the plausible initial crack sizes still leave situations well removed from rapid crack propagation. Also, the possibilities for stable cracks large enough to allow leakage through the vessel wall can be examined. In this way, the principal elements of a fracture control plan can be illustrated, and the kinds of information necessary for more accurate predictions can be understood. Comments bearing on the anticipated kinds of initial defects and their possible sizes at the outset of service life of a vessel are discussed next.

The gross defects which can be identified both in hot-worked steels and in welded joints may be divided into geometrical forms which are one, two, and three dimensional. Stringers of nonmetallic inclusions in rolled plate are one-dimensional, laminar inclusions and cracks are two-dimensional, and distributions of porosity are three-dimensional. Planar defects and cracks are important because they may extend in area when the surrounding material is stressed in tension. Stringers and globular defects represent comparatively weaker stress concentrations. They are undesirable when present in clustered groups, because these regions have a weakened resistance to the development and extension of a crack. A more serious consideration is the contribution of such segregations to the weakness of solidification boundaries in a welded region. Defects of the volume type, those in the nature of holes, do not represent a fracture initiation hazard unless, combined with other holes or inclusions, they assist the low-stress extension of a separation through a damaged region. Holes are readily detected by radiography if they present a nonmetallic path length exceeding 2% of the metal thickness. Conversely, the detection of planar defects by radiography is difficult. A flat, open separation aligned with the radiation and giving a sharp linear indication on the radiographic film is rare. More often, such defects are not flat and are not well enough aligned with the radiation so that the film record permits recognition of the defect. Furthermore, little confidence can be given to estimates of crack size from the radiographic indications that are seen. An increasing hindrance to radiographic crack detection results from increasing wall thickness.

Inspection methods using ultrasonic waves are more sensitive than radiography in revealing cracks and have greater improvement potential for that purpose. It is recognized that present specifications for the pressure vessels of interest do not require advanced, shear-wave type, ultrasonic inspections. However, the degree of fracture safety which AEC will want in future, large-size boiling water (BW) and pressurized water (PW) vessels suggests that the development and systematic use of these methods would be desirable. In the case of heavy rotating components for large steam turbine generators extensive ultrasonic inspection studies were conducted by the large producers. Ultrasonic inspection methods suitable for the specialized regions of most interest were developed, are routinely used, and are essential to the large-steam-turbine-generator fracture control plan (1,2).

Longitudinal-wave pulse-echo methods are currently used in the inspection of plates for lamination defects. However, the cracks these methods disclose are those nearly parallel to, rather than normal to, the largest expected tension in service. The seriousness of a crack left after inspection is roughly proportional to the short dimension of the crack area times the square of the tensile stress normal to the crack. A low-toughness condition of the region containing the crack contributes additionally to the chance of crack extension. Surface cracks are usually transverse and thus have a dangerous orientation relative to the expected tension. Magnetic-powder and dye-penetrant methods are used to find such cracks and are better for this purpose than radiography. However, a high degree of detection accuracy requires smooth surfaces devoid of the troughs and ridges commonly present on as-welded surfaces. In addition, only a crude indication of crack size, particularly of crack depth, is possible.

In simple concept, one might imagine that, after all fabrication is complete and a successful hydrotest has been passed, meticulous direct inspection could be employed to guarantee absence of any significantly dangerous crack. The effect of the heating cycles and hydrotest would be to open any overlooked cracks and make them more easily seen in inspection. However, many parts of the vessel are much easier to inspect in detail at an intermediate stage of assembly and cladding. For this reason, considerable reliance is placed on intermediate inspections. This means that the fabrication process must be trustworthy with regard to avoidance of cracking in previously inspected parts.

A major contribution to the control of cracklike flaws in nuclear pressure vessels is obtained through the general practice of using clean vacuum-degassed steel for shell and forging stock. Thus, hydrogen in the steel is restricted to the transient concentrations which may result if some hydrogen is introduced during welding. The stirring action of the degassing treatment tends to restrict impurity segregation, and the amounts of impurity are reduced by the lowered dependency on chemical action for deoxidation. At the same time, the amounts of sulphur and phosphorus allowed in the final composition are relatively small. The advantages thus achieved, in terms of freedom from hydrogen-induced slow crack extension and by reduced segregation at solidification boundaries during welding, is an essential part of the program for minimizing the presence and danger of cracklike flaws in the final pressure vessel.

In view of the fabrication care and intermediate inspections pertaining to steel used for shell and nozzles, the greatest chance for prior cracklike defects of transverse orientation and significant size is in the welded regions. Some concern must be reserved for regions away from the welds which are subjected to tension during straightening, for unexpected damage, such as arc strikes from poor control of prods used for magnetic-particle inspection, and for cracks under handling tabs.

The welding methods anticipated are mainly electroslag welding and submerged arc welding. From past experience, both methods have produced cracklike defects. The causes are thermal stress, residual stress, coarse dendritic solidification, and impurities in various combinations. Cracks along the borders of a submerged arc weld have sometimes occurred, particularly when the top surface of the weld bead is permitted to join the base metal with a relatively sharp angle. Cracks of this nature having substantial size can remain undetected unless the weld border is ground to a smooth contour. Since these cracks are open to the surface and are in a region of obvious suspicion, in the presence of good inspection conditions, only very small cracks of this kind should escape notice. Cracks may be introduced during the process of overlaying the internal surface of the pressure vessel with a stainless steel coating. Since a residual tensile stress is probable in and near the solidified layer, some cracks might form through this layer after a time delay assisted by any hydrogen inserted during the overlaying process, or by stress corrosion extension of small prior cracks.

Cracklike defects produced within a large solidifying segment of welding represent a special danger. Impurities such as sulphur and phosphorus tend to segregate on the solidification boundaries. In multiple-pass welding of the tungsten inert gas (TIG) type the solidification structure is often on a relatively fine scale. This lessens the impurity segregation. Furthermore, some homogenization and grain refinement are introduced by the temperature cycle from subsequent adjacent weld beads. In the submerged arc welding process fewer passes and larger masses of solidifying metal are customary; hence, there is a greater danger that weak solidification boundaries may be formed. Such defects may not be pulled open until subjected to a tensile stress. Even when opened they are difficult to recognize in radiographic inspection. When solidification defects of this kind present an opening to the surface, the defect size may be much larger than the size suggested by the irregular elements of separation visible at the surface.

In the case of electroslag welding the solidification pattern is gross, much larger than for multiple-pass submerged arc welding. A subsequent quench and temper treatment is used to refine the grain size and improve the properties. Despite the coarse-grained nature of the electroslag weldment, a considerable success has been achieved with this method. Nevertheless, undesirable amounts of center-line weakness, where impurity segregation is most serious, have sometimes occurred. It may be correct to assume that significant degrees of center-line weakness can be eliminated by careful control of the electroslag welding process and the impurity level. However, the term "significant degree" is not yet clear, and studies of how to recognize intolerable amounts of this defective condition by inspection are needed.

When a welded region is subjected to a heat treatment after welding, experience has indicated that nondestructive inspection is more sensitive to defects after the heat treatment than before, and post-heat-treatment inspection would be expected for the pressure vessels of interest here. The inspection advantages provided by some opening of defects during heat treatment are additionally enhanced by the stress applied during internal pressure testing prior to service. An increased detection sensitivity for flaws in the weak solidification boundary type is needed. Therefore, repetition of certain inspections, after hydrotesting, with the assistance of ultrasonic techniques, deserves careful study.

The transverse cracklike defects previously discussed were primarily those which are oriented to favor crack extension parallel to the line of welding, either at the weld border or within the weld. Cracks may also be formed in the heat affected zone (HAZ) region, normal to the direction of welding, particularly when the preheating and post-heating are inadequate. Cracks of this type, which have extended through the zone of residual stress and have arrested, are often observed where two stiff steel members are joined by a line of tack welding. Cracks of this general class have caused fracture failures in numerous field-welded structures. The danger of such a crack is increased first by the fact that, once instability by stable growth or stress elevation is achieved, the crack extends immediately through and beyond the region of residual tensile stress bordering the weld. A second enhancement of danger results from the moving nature of the crack, which means that crack arrest is resisted only by the minimum, dynamic, crack toughness of the steel.

The development of weld cracks prior to the pressurization of the vessel is essentially eliminated in thick-walled BW and PW pressure vessels because of the slow heating and cooling rates and the postwelding stress relief. However, the fabrication plan may require making a girth weld across a previously completed longitudinal seam weld. In this case small welding defects in the seam weld may be opened. The danger of such new cracks would be increased by any residual tensile stress parallel to the girth weld remaining after the girth welding operation.

Numerous fracture failure examination records resulted from the hydrotest failures of high-strength-steel solid-propellant rocket chambers. Several comments from these may be of interest here (3). Initially, attachments of small brackets needed to support test equipment or guidance mechanisms were attempted by tack welding. It was not feasible either to reliably detect cracks produced by the welding beneath the bracket or to avoid making such cracks. Prior to adoption of different joining methods (brazing, for example) a significant fraction of the hydrotest fractures initiated beneath small tack welded attachments. Repair welding might seem an unrelated cause for fractures. However, in both cases a welding operation was contemplated on a component already fabricated to the desired size and shape. Apprehension over possible alteration of dimensions furnished an incentive toward preheating and postheating treatments, which were inadequate. As a result, many of the fractures which originated in a longitudinal seam weld started in a region of repair welding.

Full cooperation in the development of improved inspection for cracks in steel rocket chambers was initially difficult to obtain. Presumably, a "zero defects" rating was wanted, and the fabricator preferred an inspection system which detected only the flaws of "significant" size. In the case of the Polaris and Minuteman rocket chambers, wall thicknesses were generally less than 0.2 in. Flush grinding of the seam and girth welds plus careful radiography sufficed to furnish the sensitivity needed; therefore, cracks of insignificant size could often be observed in those regions and could be seen clearly enough to permit sensible decisions regarding the need for repair welding.

For nuclear BW and PW pressure vessels it is desirable not only to detect cracks of marginal size relative to significance but also to "see" these cracks well enough, say with ultrasonic shear waves, to obtain estimates of their dimensions. Inspection procedures have not, so far, attempted to do this in a systematic way, and considerable additional study is certainly required. Meanwhile, estimates of the sizes of unseen cracks, which we should assume are allowed by present construction and inspection methods, will be difficult to fix. The estimates depend on confidence in the fabrication controls and on confidence in the direct inspections. For example, there is evidence that surface cracks about 0.5-in. long and 0.2-in. deep might be overlooked by present inspection methods, even with the advantage of smooth ground surfaces. Whether or not cracks of 0.5-in. depth are discovered with negligible error might be questioned. However, in regions where cladding is applied to shell or nozzle base metal, such a choice of maximum crack depth seems reasonable simply because of the small thickness of the added metal and the considerable experience and machine control now available for cladding nuclear pressure vessels. A larger estimate of maximum prior crack size, say 3/4 in., might be best for surface regions of welds.

Transverse cracks of substantially larger sizes than those suggested above are less significant if located near the midpoint of the wall thickness because (a) exposure of a crack to a free surface essentially doubles its effective size relative to stress elevation near the leading edge, (b) the midthickness crack does not feel stress elevations due to superimposed bending, and (c) stable extension of the midthickness crack cannot be assisted by contact with the water inside the vessel or with the water vapor outside.

The most reliable indicator of the kinds of defects likely to cause serious fracturing of thick-walled BW and PW pressure vessels would be an extensive experience of internal pressure testing conducted on vessels of similar wall thickness, geometry, materials, and construction methods. Such a test program would not, however, settle all doubts. Various reasons such as differences of design, size, location, and construction date, cause each large nuclear reactor pressure vessel to possess certain fabrication problems individual to that particular vessel. Unquestionably, more experience will be quite helpful, but a requirement for nearly absolute fracture safety suggests that the experience should be supplemented by a very conservative fracture control plan. Such a plan must assume that any cracklike defect which is plausible and which has not been proved absent by inspection may actually exist in the vessel. The plan must then establish methods of estimating fracture-safe life based upon stable crack growth data, service environment, and service stress cycles. Additional confidence can be predicted if the toughness and stress level at the end of the safe life correspond to a leak-before-break condition (4). A complete specification of such a fracture control plan requires a more detailed understanding of progressive fracturing than currently exists. However, present fracture mechanics technology provides general features of the control plan and a number of answers which are interesting. Subsequent sections of this report will discuss current knowledge of progressive crack extension, largely in terms of fracture mechanics, and will illustrate the application of this information to the planning of fracture control.

LINEAR-ELASTIC MODELING OF CRACKS

Progressive Crack Extension

The nature of the fracture behavior for which a suitable analysis is needed is termed progressive crack extension. A brief description of this is given first. The distribution of a tensile load across a region containing a crack (normal to the tension) results in elevated tension adjacent to the perimeter or leading edge of the crack. The tension at the leading edge is somewhat relaxed by local plastic strains. This local change in the stress distribution eliminates the linear-analysis stress infinity but causes very large strains adjacent to leading elements of the opened crack. The combination of local plastic strains, advance separations, elastic constraint, and tension near the leading edge may be sufficient, or less than sufficient, to cause sudden rapid spreading of the crack. If less than sufficient, then with the aid of repeated changes of stress during service, plastic strain reversals in the material near the leading edge may occur and cause stable forward growth of the crack by fatigue. In addition, the environment, with or without fatigue assistance, may cause stable spreading of the crack by stress corrosion cracking. Liquid water or water vapor suffices for this purpose, in the case of many structural metals. Hydrogen in the steel also assists slow stable extension of a crack subjected to tensile stress. When a structural member containing such a crack is in general tension, as the wall of a vessel containing internal pressure, extension of the crack area results in larger stress elevation near the leading edge and hastens the pace of stable growth. Onset of rapid crack extension provides a relatively abrupt endpoint for the stable growth period. To appreciate how this can happen at a nominal tensile stress well below the yield strength, it is best to focus attention on the leading edge stress elevation associated with a crack, rather than upon brittleness per se, because large local plastic strains occur as an essential part of progressive crack extension in the customary structural metals, even when their behavior is somewhat brittle.

Studies of running cracks have been conducted using a variety of techniques to measure crack speed and the stresses near the crack. Such studies are more easily done with glass and brittle plastics. However, for a brittle crack traversing a plate of steel, Wells (5) observed the temperature rise parallel to the path of the crack. From these observations the separation region was found to be acting as a heat source with the strength increasing with crack length. Edge-notched plates were used, as in later work by Wells and Post (6), in which the rate of strain energy release was calculated from photoelastic observations and was proportional to crack length. At the time of Wells' thermal observations the evolved thermal energy seemed somewhat higher than the stress field energy release, but this was not regarded as significant in view of experimental uncertainties. Currently available stress analysis information applied to the experiment would increase the estimate of the rate of strain energy release and would reduce the moderate difference of this estimate from the observed rate of thermal energy production.

In terms of the old, modified Griffith theory (7,8) the condition critical for onset of rapid fracture was a point of stable balance, between stress-field energy release rate and rate of plastic work near the crack, to be followed by a region of unstable rapid crack propagation. However, study of the implications from Wells' thermal measurements suggested, quite oppositely, that the point of onset of rapid fracture was an abrupt instability point followed by a stable region in which work rate and loss of stress-field energy were balanced through a considerable range of crack speeds. Indeed, the instability point could be preceded by a slow region of crack extension in which the crack extension process was also stable. From these facts it was not clear that writing an equality between rate of strain energy release and plastic work rate would be helpful as a means for understanding the sudden onset of fast crack extension.

The preceding conclusions have been verified by numerous subsequent observations of running crack behavior. The latest results of this kind are discussed in a recent paper by Clark and Irwin (9). During the mid 1950's the effect was to shift the emphasis of fracture mechanics toward characterization as the primary task. In the modified Griffith theory characterization of onset of fast progressive fracturing was linked, unnecessarily, with an energy balance relationship which was uncertain in terms of both usefulness and validity at the measurement point. The dubious validity aspect is discussed by McClintock and Irwin (10a), where calculations using a plasticity model are used for illustration.

Progressive crack-extension behaviors range from several kinds of slow-stable extension through the fast-stable region. At very high crack speeds one observes a limiting velocity followed by crack division tendencies, when the tensile driving force is still further increased. A single service fracture failure may exhibit all these crack extension behaviors. To understand and prevent such fractures, appropriate use of experimental data from laboratory testing is essential. The characterization plan should permit application of laboratory fracture testing data to service components in the simplest adequate way. Linear-elastic fracture mechanics provides an appropriate and simple characterization method applicable to any component in which we have a reasonable idea of the stress distribution. With some care regarding interpretation, the linear analysis method retains usefulness as the stress level approaches a general yielding condition. The method is not suitable for use at higher stresses.

Linear Crack Stress Field Analysis

For purposes of linear stress analysis a crack is regarded as a flat separation bounded within the material by a leading edge which is approximated by a simple curve. For example, if a sharp groove of small length is cut into one face of a metal plate and subjected to fatigue stressing, a leading-edge contour resembling half of an ellipse is produced. At a relatively small tensile stress across the cracked region, plastic strains are confined to a small zone, as shown schematically by the shaded area in Fig. 1. The plane of Fig. 1 is normal both to the crack and to its leading edge and represents only a small segment of the leading edge. Following the practice customary for stress analysis near a crystalline dislocation line, the region containing plastic strains is regarded as a line disturbance zone. The natural locus for the leading edge of the linear analysis

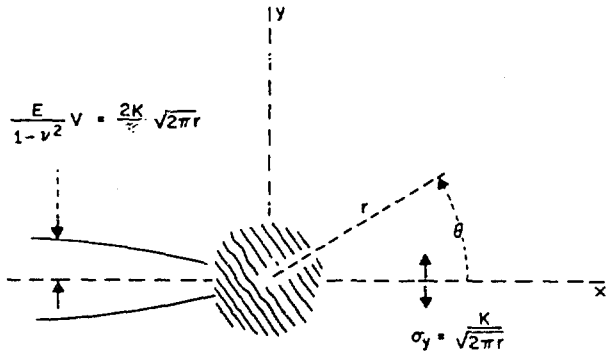

$\mathcal{J} = (\frac{1}{E})K$, PLANE STRESS

$\mathcal{J} = (\frac{1-\nu^2}{E})K^2$, PLANE STRAIN

Fig. 1 - The leading edge of a crack

model crack is a central position within the plastic zone, not the left side of this zone where the leading separational elements are situated. We will return to this aspect later. At this point of our discussion, since the plastic zone is assumed to be very small relative to the crack size, the above difference of crack border location for analysis purposes is not important.

For the region of a tensile crack shown in Fig. 1 (close to the leading edge) the stress distribution is two-dimensional, and from linear analysis the stresses are

$$\sigma_y = \frac{K}{\sqrt{2\pi r}} \cos\frac{\theta}{2}\left(1 + \sin\frac{\theta}{2}\sin\frac{3\theta}{2}\right), \tag{1a}$$

$$\sigma_x = \frac{K}{\sqrt{2\pi r}} \cos\frac{\theta}{2}\left(1 - \sin\frac{\theta}{2}\sin\frac{3\theta}{2}\right), \tag{1b}$$

$$\tau_{xy} = \frac{K}{\sqrt{2\pi r}} \sin\frac{\theta}{2}\cos\frac{\theta}{2}\cos\frac{3\theta}{2}, \tag{1c}$$

and

$$\sigma_z = \nu(\sigma_y + \sigma_x) \quad \text{(plane-strain)}, \tag{2}$$

where the coordinates are as shown in Fig. 1 and ν is Poisson's ratio.

The y-direction displacements v at the crack plane, from which crack opening size would be estimated, are given by

$$Ev = \frac{2K}{\pi}(1 - \nu^2)\sqrt{2\pi r}, \tag{3}$$

where E is Young's modulus. From Eqs. (1) and (3) computation of the work done in an increment of crack closure shows that the Griffith theory strain energy release rate $\mathcal{G}$ is proportional in a simple way to K^2.

The terms on the right side of the above equations are the leading terms of the linear stress analysis solution, which would be completed by adding terms proportional to higher powers of the ratio r/a (where a is a length factor indicative of crack size). In the limit of small enough values of r/a, the terms shown dominate and form a leading-edge stress system characteristic of Mode I (tensile) cracks. The parameter K is proportional to the applied tensile load and is a function of the crack, specimen size, and shape factors. The stress intensity factor K, termed K_I for the opening (tensile) mode of crack surface displacements, provides a simple one-parameter characterization of the stresses tending to cause crack extension. Use of the $\mathcal{G}_I$ value corresponding to K_I, for characterization purposes, is optional and equivalent. A well-known example of characterization is the determination of the critical value K_{Ic} for onset of fast crack extension.

A general mathematical treatment would refer to Mode II (forward shear) and Mode III (parallel shear) stress equations to represent stresses developed by application of shears parallel to the crack plane. This complexity is unnecessary here, since we are primarily concerned with tensile cracking in which the stresses τ_{xy} and τ_{zy} on the plane of expected crack extension (ahead of the leading edge) are zero. An article by Paris and Sih (10b) provides a comprehensive summary of linear-crack stress-field analysis.

The tensile crack stress field near the leading edge of a crack is regarded as either of the plane-strain or of the plane-stress type. The plane-strain model is three-dimensional, in the sense that the stress conditions must be uniform in the z-direction

across a leading-edge region which is large compared to the size of the zone containing plastic strains. The plastic zone is then held within a plane-strain stress system with its size somewhat reduced by elastic constraint. Of course, if the crack is what we term a "through-crack" with leading edges right through the plate thickness, even if the plastic zone is small, a plane-strain condition near the free surfaces is not possible. Customarily the linear analysis applied to crack problems of this kind is the one termed generalized plane stress in which $\sigma_z = 0$ is assumed. In this case Eqs. (1) remain applicable with the stresses interpreted as averages through the plate thickness. Such a model is two-dimensional, since the z-direction dimension plays no role in the analysis. The effect of assuming $\sigma_z = 0$, instead of Eq. (2), is to eliminate the factor $(1 - \nu^2)$ from Eq. (3). The two-dimensional plane-stress situation permits larger shear stresses and thus a larger plastic zone size than would occur, with the same stresses in the x, y plane, for plane-strain. The relation of this to the brittle-ductile change in fracture toughness is discussed later.

From Eqs. (1) K is the limiting value on $\theta = 0$ of the product $\sigma_y\sqrt{2\pi r}$ as r approaches zero. Given any valid stress analysis solution for σ_y, even though it is not expressed in the r, a power series form, the preceding limiting process may be used to obtain the value of K. In fact, if a small-flank-angle notch of root radius ρ is subjected to the nominal stress σ_N, and if the stress concentration factor K_{th} is available as a function of ρ, then

$$K = \lim_{\rho \to 0} 1/2\, \sigma_N K_{th} \sqrt{\pi\rho} \,. \tag{4}$$

In calculating K_{Ic} from tensile fractures of circumferentially notched round bars, Eq. (4) along with published stress concentration factors pertaining to that geometrical shape, furnished the first approximate answers. The procedure is reviewed by Paris and Sih (10b).

The same basic analysis rules apply to determinations of K for a laboratory specimen, with a crack of controlled size and shape inserted for testing, as are used to determine K for a crack in a service component. However, for the most used types of laboratory specimens the analysis accuracy has been improved by considerable numerical work. In the case of cracks in service components the estimates used are usually of the "engineering approximation" type based upon one or more of the crack stress field results discussed next.

For an infinite plate subjected to an in-plane uniform stress σ perpendicular to a through-the-thickness crack of length $2a$,

$$K = \sigma\sqrt{\pi a} \,. \tag{5}$$

Cutting this configuration in half results in a through-crack of length a into the edge of a semi-infinite plate with the stress σ parallel to the edge, where

$$K = 1.13\, \sigma\sqrt{\pi a} \,. \tag{6}$$

The 1.13 factor may be regarded as the correction factor for increased crack opening due to the free surface.

For a strip of width W with a central crack of length $2a$ perpendicular to a longitudinally applied stress σ, approximate values of K can be obtained from

$$K = \sigma\sqrt{\pi a \sec\frac{\pi a}{W}} \,, \tag{7}$$

where $a \leq 0.3W$.

Returning to the idea of calculating K as a limit, the addition of any uniform tension or compression to a crack stress field solution would not change the value of K, because this would not change the limit of the product $\sigma_y \sqrt{2\pi r}$ as r approaches zero. Thus, if a uniform compressive stress numerically equal to σ is superimposed on the problem of Eq. (5), the K value is not changed. However, the stress σ at infinity is thereby canceled, and a uniform pressure numerically equal to σ is placed on the crack surfaces. In this way we see that Eq. (5), with σ replaced by p, provides the answer to the problem of a two-dimensional crack of length $2a$ opened by an internal pressure p. If both σ (at infinity) and p (on the crack surfaces) act at the same time, the K value is obtained by substituting $\sigma + p$ for σ in Eq. (5). Similar comments pertain to the influence of internal pressure, say from hydrogen, in connection with the three-dimensional problems discussed next.

For a circular (penny-shaped) crack of radius a imbedded in an infinite, three-dimensional body with uniform stress σ applied perpendicular to the crack,

$$K = \frac{2}{\pi} \sigma \sqrt{\pi a} \ . \tag{8}$$

This is really a special case of a similarly oriented elliptical crack of semiminor axis a and semimajor axis b. At the semiminor axis, where K is largest,

$$K = \frac{\sigma \sqrt{\pi a}}{\Phi_0} \tag{9a}$$

and

$$\Phi_0 = \int_0^{\pi/2} \sqrt{1 - \frac{b^2 - a^2}{b^2} \sin^2\theta} \, d\theta \ .$$

where Φ_0 is recognized as the complete elliptic integral function whose values are: a/b = 0, 0.1, 0.2, 0.3, 0.4, 0.5, 0.6, 0.7, 0.8, 0.9, and 1; Φ_0 = 1.0, 1.016, 1.051, 1.097, 1.151, 1.211, 1.277, 1.345, 1.418, 1.493, and $\pi/2$. For the extreme values of a/b Eq. (9a) leads to Eq. (5) or to Eq. (8), as would be necessary. Thus, Φ_0 can be regarded as a correction factor for the elliptical nature of the crack shape.

Influences upon the K value of proximity to a free surface and changes of crack shape can often be approximated in a simple way with good enough accuracy for practical applications. Equation (6) is known to be the free-surface modification of Eq. (5) from numerical calculations. Equation (7) is simply an approximate empirical representation of the results from numerical calculations for a central two-dimensional crack in a finite-width plate. Comparisons to accurate numerical results, when these became available, showed Eq. (7) was preferable to a tangent function representation previously used.

Often the shape of a surface crack suggests representation of the crack as half of an ellipse with the principal dimension at the surface of the plate. The analysis problem is a difficult three-dimensional calculation, and exact numerical results are not available. However, from comparisons of test results, the controlling K value for this problem can be estimated using the equation

$$K = \frac{1.12 \sigma \sqrt{\pi a}}{\Phi_0} \ . \tag{9b}$$

The factor 1.12 was guessed from comparison to the problems represented by Eqs. (5) and (6) at a time when the third significant figure of the coefficient in Eq. (6) was not well determined (11). Careful measurements of K_{Ic} using semielliptical cracks and

Eq. (9b) have agreed well with K_{Ic} values from other methods, so long as the value of a was not more than half the plate thickness (10c).

Experimental Fracture Mechanics Analysis

In view of the inherent difficulty of some three-dimensional crack stress field problems, experimental methods of determining K will be briefly reviewed. The first of these employs compliance measurements and leads directly to values of $\mathcal{G}$ rather than K. For tensile cracks the relationships connecting $\mathcal{G}$ and K are

$$\mathcal{G} = \frac{K^2}{E}(1-\nu^2)(\text{plane strain}) \tag{10}$$

and

$$\mathcal{G} = \frac{K^2}{E}(\text{plane stress}). \tag{11}$$

Figure 2 shows a single-edge-notched plate specimen sometimes used for crack toughness measurements. This is a through-crack problem for which a generalized plane-stress analysis viewpoint is natural. The experiment consists in repeated measurements of specimen compliance with the crack-notch depth into the specimen fixed at a series of values, say from $0.1W$ to $0.7W$, where W is the specimen width. If P is the applied load and ℓ is the total load displacement (between the two loading points) the compliance C is given by

$$C = \ell/P. \tag{12}$$

In a graph of P as a function of ℓ, for a series of increasing crack depths a, each load-unload line would have a slope $1/C$ which would be a decreasing function of the depth a. Simple analysis of the strain energy lost from the specimen in a small increment da of crack extension shows that energy loss per unit of plate thickness B is given by

$$G = \frac{1}{2}\frac{P^2}{B}\left(\frac{dC}{da}\right). \tag{13}$$

The expression for K^2 can be written in the form

$$K^2 = \frac{1}{2W}\left(\frac{P^2}{B}\right)\frac{d(EBC)}{d(a/W)}. \tag{14}$$

where the final derivative term is dimensionless and, for a long specimen, depends only on the relative crack depth a/W. As discussed by Brown and Strawley (10d) comparisons of K from compliance measurements to numerical collocation-analysis values of K can be done with sufficient accuracy to show agreement within about 3% for the specimen of Fig. 2, and equivalent agreement has been found using notched bend specimens. When this method is applied in a simple way to three-dimensional problems and K does not have a constant value along the entire leading edge of the crack, the method provides only the average value of K^2 across the leading edge.

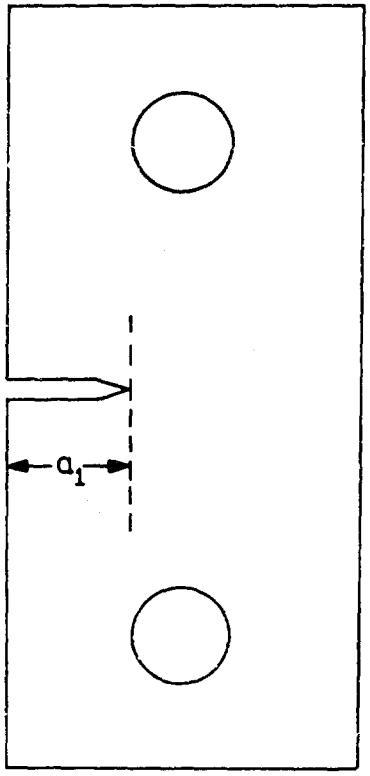

Fig. 2 - Single-edge-notch specimen

Attempts to measure K based upon determinations of stress near the leading edge of the crack, either with photoelasticity or with bonded strain gauge methods, have not been equally successful. Approximate answers can be achieved, but errors of 10% to 15% have been apparent in work of this nature to date. The reason is probably the dependency of the definition of K upon a limiting process in which the distance r must approach zero. In the compliance technique an uncertainty as to the exact location of the leading edge contributes only a small error. However, the leading edge location is of critical importance to the photoelastic and bonded-strain-gauge methods. Further study of the positioning of the leading edge of the crack for analysis purposes will be required to reduce the existing analysis uncertainties.

Other experimental methods are possible which may well be more accurate than those discussed above but which have received very little trial. Two such methods would proceed as follows: (a) Calibrate a test material for fatigue striation spacing as a function of K in tension-tension fatigue; then use measurements of striation spacing to measure K values for crack geometries of interest. (b) Form a model of the component of interest from glass or another suitable transparent material. Move a crack into the model as desired using a fixed, low humidity to assist stable crack extension. Measure crack opening displacement as a function of distance from the leading edge using optical techniques and interference fringes. Use Eq. (3) to obtain K.

Except for reservations based upon accuracy troubles, frozen-stress photoelasticity methods might seem well suited to the determination of ratios of K to applied nominal stress for, say, deep cracks in the throat regions of nozzles. The results from frozen stress methods would have improved value if these results could be checked using a different technique such as one of those suggested above.

When artificially inserted increments of crack extension are used, along with the compliance technique, to determine K values for the specimen of Fig. 2, the extensions are straight across the plate, because this is the natural path for tensile mode crack extension. In general, the natural trajectory for a moving tensile crack may be a curved surface. Where this surface is not known in advance, it can usually be determined by three-dimensional model studies, using fatigue or stress corrosion to produce stable extension of the crack. The determination of K for a crack or slot which does not correspond to a natural tensile mode crack surface is complicated by the fact that the leading edge stress system will contain contributions from Mode II and Mode III stress fields. In the case of the single-edge-notched plate or a notched bend bar K_{Ic} test, available analysis methods provide only the average value of K^2 along the nearly straight leading edge of the crack. The actual value of K_I^2 in central regions should be larger than the average value of K^2, but the amount is uncertain. Some investigators estimate the increase factor as the reciprocal of $(1 - \nu^2)$. Others report a value of K_{Ic} which may be conservative (possibly by as much as 5%) by taking the central region K_I^2 value as equal to the average K^2 across the specimen. The difference is of small practical importance, since replicate test results tend to vary by amounts in the range of 5% to 10%.

PLASTICITY ANALYSIS CONCEPTS FOR CRACKS

Studies of fracture suggest that a close relationship to plastic flow properties exists. It is impossible to explore interests of this kind in a quantitative manner without using analysis models to define properties which can be computed as well as observed and discussed. Exact elastic-plastic solutions are not available for the tensile cracks which are of interest. Furthermore, the structural metals possess fine-scale imhomogeneities, and this limits the realistic accuracy of any continuum mechanics representation. Despite these difficulties, significant progress has been made with the aid of several relatively simple analytical methods. Three elementary and widely used plasticity analysis concepts for cracks are described next.

The r_y Plasticity Adjustment Factor

Critical values $\mathcal{G}_c$ for onset of rapid fracture in high-strength aluminum alloy sheets were among the first crack toughness measurements attempted. These employed tensile sheets of various size with a central, sharp-ended slot to represent the initial crack. Results showed a trend for $\mathcal{G}_c$ to increase with the lateral dimensions of the specimen, which was nearly eliminated by adding a plasticity adjustment r_y to the crack size (12).

No specific model of the plastic zone was attempted. The idea was simply to remove a leading edge positioning error from the linear elastic analysis model. A central position inside the plastic zone, as shown in Fig. 1, was assumed to be a better location for the analysis model leading edge than the apparent tip of the crack at the left side of this zone. From Eqs. (1a) with $\theta = 0$,

$$\sigma_y = K/\sqrt{2\pi r} \quad . \tag{15}$$

It was assumed that the distance r_y from the central location to the elastic plastic boundary could be estimated by inserting a critical yield stress value σ_Y for σ_y in Eq. (15) and that this distance could also be taken as the separation of the analysis model leading edge from the apparent tip of the crack (13). From these rules

$$r_y = \frac{1}{2\pi}\left(\frac{K}{\sigma_Y}\right)^2 \quad . \tag{16}$$

In fracture testing applications the value of σ_Y was taken to be the 0.2%-offset uniaxial tensile yield strength σ_{YS} for situations of plane stress. The length factor $2r_y$ was used as an approximate estimate of the size of the plastic zone. The influence of plane-strain conditions in elevating the tensile stress necessary for yielding was assumed representable by taking $\sigma_Y \cong \sqrt{3}\ \sigma_{YS}$.

Crack toughness testing of the plane stress kind is not yet carefully defined. Within the limited accuracy of available results for onset of rapid crack extension in high-strength metal sheets, use of the leading edge positioning adjustment r_y results in $\mathcal{G}_c$ values which are essentially constant with change of test sheet size, so long as the net section stress is less than σ_{YS}.

Historically, the length factor $2r_y$ was used as an approximate estimate of the plastic zone size. Studies of the change in the ratio of $2r_y$ to test-plate thickness across the brittle-ductile fracture mode transition range showed clearly the dominating influence of elastic constraint and led to interpretation of this fracture transition as a change from plane strain to plane stress in the leading-edge plastic zone (13). Clark (14) investigated the apparent size of the plastic zone in silicon iron both for plane-stress and plane-strain conditions and at a stress level where the net-section stress was well below σ_{YS}. He concluded that the size estimates provided by calculating $2r_y$ for plane stress and plane strain were approximately correct both in magnitude and in terms of the 3-to-1 size ratio for the two conditions of elastic constraint.

Substitution of r_y for r in Eq. (3) permits calculation of a crack opening dimension which is interesting for various fracture analysis applications. Wells (15) has used terms such as crack opening displacement and crack opening dislocation for the crack opening size $2v = \delta$ estimated in this way. He noted that one obtains the result $4\mathcal{G}/\pi\sigma_Y$ regardless of whether or not a plane-stress or plane-strain condition is assumed.

The Strip-Yield Zone Concept

Linear analysis of stresses near a crack can always be formally done by solving the stress problem, ignoring the crack, and then superimposing a solution which contains forces at the crack plane just sufficient to restore free surface conditions. The analysis can be adjusted so that, adjacent to the leading edge, the crack surfaces are not force-free but are subject to crack closure forces arising, say, from attraction between opposite crack surfaces. Barenblatt (16) assumed that such a system of crack closure forces always exists near the leading edge. The closure tensions and their distribution were balanced, so as to eliminate the linear analysis stress infinity.

Dugdale (17) noted that this idea could be applied to representation of the plane-stress yield zone for a crack in a thin metallic sheet. In this application the force system became simply a constant tensile stress across the linear yield zone equal to the tensile yield strength. Since Dugdale's analysis ignores the sheet thickness, the analysis model plastic zone is simply a line segment extending ahead of the apparent tip of the crack. Concentration of all the plastic strain into a line results in a representation which permits calculations of the opening displacement discontinuity but does not permit calculations of plastic strains.

Interest in this type of representation also developed among dislocation scholars who saw that a strip yield zone could be thought of in terms of a continuous distribution of dislocations. A criterion for onset of rapid crack extension based upon a critical value of crack opening displacement might, it seemed, provide a way to connect macroscopic fracturing directly with dislocation mechanics (18). Modifications toward greater realism are possible by assuming various line patterns of concentrated yielding at the expense of greatly increased analytical complexity.

For those with less ambitious analytical objectives there are other reasons for interest in the strip-yield model. For example, a single line of yielding can be analyzed with only moderate computational difficulty for certain tensile fracture specimens which might be used for crack toughness evaluation. Wells' crack opening displacement δ could be estimated for such tests from the strip-yield analysis model in terms of observations of applied load and crack size, until the yield zone extends completely across the net section. Only theoretical studies of this kind have been done. These resulted in δ values not significantly different from the value of $(\mathcal{G}/\sigma_Y)$ resulting from a linear analysis with the usual r_y positioning adjustment (19).

When the size b_0 of the strip-yield plastic zone is small relative to crack size and net section size, the following relationships hold:

$$\delta = \mathcal{G}/\sigma_Y \tag{17}$$

and

$$K = \frac{2\sigma_Y}{\pi}\sqrt{2\pi b_0} \ . \tag{18}$$

Examination of stress and opening displacement equations for the strip-yield model, in the small plastic zone limit, shows that the "best fit" location for the leading edge of a linear analysis model crack is at the distance $b_0/3$ from the apparent leading edge of the crack. Comparison of

$$\frac{b_0}{3} = \frac{\pi}{24}\left(\frac{K}{\sigma_Y}\right)^2 \tag{19}$$

to Eq. (16) shows that $b_0/3$ is smaller than r_y by only 18%.

Compression of all the yielding into a thin layer ahead of the crack might seem too unrealistic to be valuable for thick-section tensile fracturing of metals. However, it is helpful to learn what concepts associated with various models of the plastic zone have magnitudes which are nearly independent of plastic strain distribution. Comparison of Eqs. (17) and (19) to the r_y values from Eq. (16) suggest that the linear analysis positioning adjustment r_y and the crack opening displacement δ are two concepts possessing a considerable degree of strain distribution invariance.

The Mode III Elastic-Plastic Treatment

The system of deformations near the crack border, termed Mode III, is a distribution of shear strains such that all the particle displacements are parallel to the leading edge of the crack. Limitation of displacements to a single coordinate direction reduces the mathematical difficulty for linear analysis (with yielding suppressed) and for strip-yield analysis (with yielding confined to a line segment). In fact, Mode III elastic-plastic solutions can be done without arbitrary restriction of the region of yielding and, for zero work hardening, with a degree of mathematical difficulty only moderately greater than that for the strip-yield analysis. The Mode III plasticity analysis idea introduced by McClintock and associates (20-22) became of increasing interest as the inherent difficulty of the corresponding Mode I analysis became evident. The reason for this is the need for analytical representation of plastic strains very close to the leading separational elements of the crack.

If one assumes zero work hardening and either the Von Mises or Tresca criterion for yielding, Mode III plasticity analysis predicts a distribution of shear strains representable in the form

$$\vec{\gamma} = \gamma_{yz} + i\gamma_{xz}, \tag{20}$$

where

$$\gamma_{xz} = -\gamma_Y \frac{R}{r_1} \cos \theta_1, \tag{21}$$

$$\gamma_{xz} = -\gamma_Y \frac{R}{r_1} \sin \theta_1, \tag{22}$$

and $\gamma_Y = \tau_Y/\mu$ is the shear strain at the elastic-plastic boundary.

The coordinates r_1 and θ_1 are the cylindrical coordinates about an axis coincident with the apparent leading edge. R is the value of r_1 if the latter is extended to the elastic-plastic boundary. The preceding result is not generally valid. However, it is valid for any series of equally spaced, equal-length, two-dimensional cracks on the x-z plane and for a uniform stress $\tau_{yz} = \tau$ acting a remote distance from this plane. This problem has received study, because it can be regarded as the Mode III analog for centrally cracked, symmetrically edge cracked, and finite-width tensile specimens used for crack toughness evaluation.

Analytical considerations (10a) show that as the plastic zone reduces in relative size the elastic-plastic boundary approaches the shape of a circle (or cylinder) with the coordinate axis of θ_1 at the left extreme of the x-direction diameter as suggested by Fig. 1. The size R_0 of this diameter is expressed by

$$R_0 = \frac{1}{\pi} \left(\frac{K_{III}}{\tau_Y} \right)^2. \tag{23}$$

For comparison, the leading-edge equations for the elastic strains predicted by linear analysis in Mode III are

$$\gamma_{yz} = \gamma_Y \frac{K_{III}}{\tau_Y} \frac{\cos(\theta/2)}{\sqrt{2\pi r}} \tag{24}$$

and

$$\gamma_{xz} = -\gamma_Y \frac{K_{III}}{\tau_Y} \frac{\sin(\theta/2)}{\sqrt{2\pi r}} . \tag{25}$$

If we locate the origin of the r, θ coordinates at the center of the plastic zone and put $r = R_0/2$, Eqs. (24) and (25) predict the same strain as do Eqs. (21) and (22). Thus, the linear-analysis value of r_Y for this problem is

$$r_Y = \frac{R_0}{2} = \frac{1}{2\pi} \left(\frac{K_{III}}{\tau_Y} \right)^2 . \tag{26}$$

Clearly, Eq. (16) is the tensile analog of Eq. (26).

If we assume $R = R_0 \cos\theta_1$, corresponding to the small plastic zone situation, integration of the total strain γ around the elastic-plastic boundary provides the result

$$\delta = \frac{2}{\pi} \gamma_Y \left(\frac{K_{III}}{\tau_Y} \right)^2 . \tag{27}$$

Using $2\mu\mathcal{G}_{III} = K_{III}^2$, this equation becomes

$$\delta = 4\mathcal{G}/\pi\tau_Y . \tag{28}$$

Equation (28), with σ_Y in place of τ_Y, is the same as the value for δ in the case of the tensile mode, when the linear analysis approach was used, supplemented by the leading-edge positioning adjustment r_Y.

For the Mode III elastic-plastic problem of a finite-width plate, such as was indicated above, values of δ have been calculated by Rice (23) as a function of τ and crack size a for various levels of net-section stress. From comparisons to these results one finds that the value of δ provided by Eq. (28) is still accurate to better than 5% when the net section stress is $0.95\tau_Y$.

An additional result of interest from studies by Rice (24) pertains to the influence of strain hardening. Using a nonlinear stress-strain law in the plastic range of the type

$$\tau_Y = \tau_0(\gamma)^n \tag{29}$$

Rice was able to study the shape of the Mode III crack opening and the shift of the elastic-plastic boundary for the small plastic-zone situation with a work hardening influence present. He found that the elastic-plastic boundary remained circular. The diameter was still given by Eq. (23), and the crack opening at the intersection of the elastic-plastic boundary with the crack was given by Eq. (28).

Fracture Characterization Problems in Relation to Plastic Analysis

As noted in previous sections, much has been learned about progressive crack extension through direct observation of the behavior trends as functions of K (or $\mathcal{G}$). The degree of success thus achieved resulted from giving primary analysis attention to the region close to the leading edge. Intuitively, a similar procedure should be followed in plasticity studies. Primary attention should be given to regions of the plastic zone close to the leading separational elements of the crack. The K or $\mathcal{G}$ value represents a controlling aspect of the elastic stress field. Presumably, a controlling aspect associated with plastic strain would be appropriate in the case of plasticity studies. However, the task of selecting a simple characterization plan based upon plasticity analysis can only be done, at present, on a judgment basis. Essentially, one needs the answer which is sought in order to find this answer, a dilemma not uncommon in exploratory science. Two judgment type answers are as follows:

1. Characterization in Terms of the Crack Opening Displacement δ. Intuitively, an average strain of some kind would seem most promising as a single-parameter characterization of critical "state of strain" for onset of rapid crack extension. One special kind of averaging, potentially suitable, would be that which is measured by the value of the crack opening displacement δ. Although, conceptually, values of δ might be obtained by direct observation, the feasibility of doing these measurements with useful accuracy is still not clear. Calculations of δ can be made, based upon a specific elastic-plastic model, as the integral around the elastic-plastic boundary of the extensional strain normal to the crack. A simpler plan would be to compute δ as equal to $\mathcal{G}/\sigma_{ys}$. Both methods become inapplicable after development of general yielding. Beyond general yielding, estimates of δ can be made using a rigid-plastic slip-field viewpoint. Obviously, somewhat different values of δ would be obtained with different methods, and use of δ as a characterization parameter in a consistent way would require arbitrary standardization of the calculation procedures.

2. Characterization in Terms of a Critical Average Strain ϵ_1 for Plastic Instability. This procedure is based upon Krafft's correlations between K_{Ic} and strain hardening, which suggest that local plastic instability is a significant controlling aspect for onset of rapid crack extension (25). In the calculation plan used by Krafft the critical average strain ϵ_1 is assumed given by

$$\epsilon_1 = \frac{K_{Ic}}{E\sqrt{2\pi d_T}} . \tag{30}$$

The length factor d_T for a given test material was determined, Ref. 25, by assuming ϵ_1 equal to the strain hardening exponent n for isothermal conditions of straining. Direct measurement comparisons of K_{Ic} and n for similar conditions of strain rate and temperature then permitted finding a best-fit proportionality factor. More recently, following suggestions by Williams and Turner (26), Krafft assumes

$$\epsilon_1 = \frac{n}{2} + \frac{2\sigma_{ys}}{E} , \tag{31}$$

where the terms on the right represent the influence of an assumed specific type of elastic constraint on the critical strain for plastic instability (27).

It is possible to arrive at somewhat similar equations by defining an average strain close to the leading edge in terms of the Mode III elastic-plastic model, Eqs. (21) and (22), as follows. From the preceding equations, the maximum shear strain at a point (r_1, θ_1) is given by

$$\cdot \quad {}_{Y}\frac{R}{r_1} \cdot \tag{32}$$

Assuming $R \quad 2r_1 \cos {}_1$, the average strain along a vertical line at $x = x_1$, where $x_1 \quad 2r_1$ is given by

$$\quad {}_{Y}\left(\frac{}{2}\sqrt{\frac{2r_Y}{x_1}} \quad 1\right) \tag{33}$$

$$\quad \frac{}{2}\frac{K_{III}}{\sqrt{x_1}} \quad \frac{_Y}{} \cdot \tag{34}$$

The tensile analog of Eq. (34) is

$$_1 \quad \frac{K_{Ic}}{2E\sqrt{x_1}} \quad \frac{_{YS}}{E} \cdot \tag{35}$$

In this calculation plan the elastic constraint might be assumed representable by $_1 = n$ 2 to derive a relationship between K_{Ic} and n similar to that provided by Eqs. (30) and (31).

At present, correlation studies between plastic flow properties and crack toughness need additional support from plasticity analysis. Equation (35) is of no special importance in itself, but the derivation has illustrative values. Plasticity investigations intended to assist extension of fracture mechanics toward basic factors at finer scale should provide help of that kind in terms of better plasticity models. Previous calculations of plastic strain fields near a tensile crack using computer programs have not been planned so as to assist the characterization task either in terms of a crack opening displacement concept or along the lines of the K_{Ic} - n correlation.

SLOW-STABLE CRACK GROWTH

Crack Growth Rates With Fatigue

In assessing the severity of flaws in a structure the possibility of their growth to a dangerous size from the effects of repeated loading, including cyclic thermal stresses and/or environment, should be considered. Two related approaches have been adopted for making this assessment. They are (a) to give attention to an analysis of the growth rates of subcritical flaws (28,29) which can subsequently be used to estimate a "life" from an initial flaw size to the critical size and (b) to give attention to a direct analysis of the "life" of typical flaws (10c).

Of the two approaches the former is more detailed and fundamental and, consequently, lead to a better understanding of service behavior. On the other hand, the latter approach is simpler and has been demonstrated to be adequate for certain analyses of the life of pressure vessels of very-high-strength metal alloys, such as rocket engine cases (10c). For a full understanding of flaw growth considerations in the design and behavior of pressure vessels, both viewpoints of the two approaches should be employed.

In the initiation of subcritical growth of flaws due to fatigue, planar defects are most likely to develop into growing fatigue cracks. However, in a conservative assessment of the danger all flaws and defects are potentially growing cracks with a slight amount of sharpening. As one might expect, the most severe flaws are normally those which are largest, in the most highly stressed regions of a structure, and often those in material which is degraded in the process of fabrication.

The analysis of the growth rates of flaws, from sizes which are too small to find in normal inspection to those of critical size for unstable running fracture, proceeds on a similar basis of analysis as that for final failure itself. The increment of crack growth experienced in a cycle of loading depends upon the corresponding excursion in the stresses surrounding the crack tip, as measured by K.

For a given material and environment the rate of crack growth, da/dn, depends primarily on the stress intensity factor range ΔK and secondarily on the relative mean value γ of the stress intensity factor K_m (or relative mean load P_m), i.e.,

$$\gamma = \frac{K_M}{\Delta K} = \frac{P_M}{\Delta P} . \tag{36}$$

Also of secondary (but not negligible) importance are the frequency of loading, plate thickness effects, and processing of material, which should be assessed in a refined analysis (30,31).

Since growth rates can be correlated by stress intensity factors, the effect of the location of applying the loading and solid body and crack configuration are then known, provided the growth rates are known for some laboratory test configuration at the corresponding ΔK level. This means that plotting da/dn vs ΔK may be regarded as a basic way to represent a material's crack growth rate behavior and that the effect of secondary variables is to cause shifts in the curve so obtained.

Many such plots of da/dn vs ΔK (or K) for steels are available in the literature (29-33). If the plots for steel are superimposed, a curious result occurs. For zero-tension loading ($\gamma = 0.5$) all the data for steels fall very close to each other, i.e., within a factor of 2 (or perhaps at most 3) in the growth rate for a given ΔK. For example, Brothers' data (32) on low-alloy medium-strength rotor steels are very close to Carman's data on high-alloy very-high-strength rocket engine pressure vessel steels. Moreover, the meager data available on low-strength steels for pressure vessels, such as A302B (34), indicate that they are no exception. (See Fig. 3.)

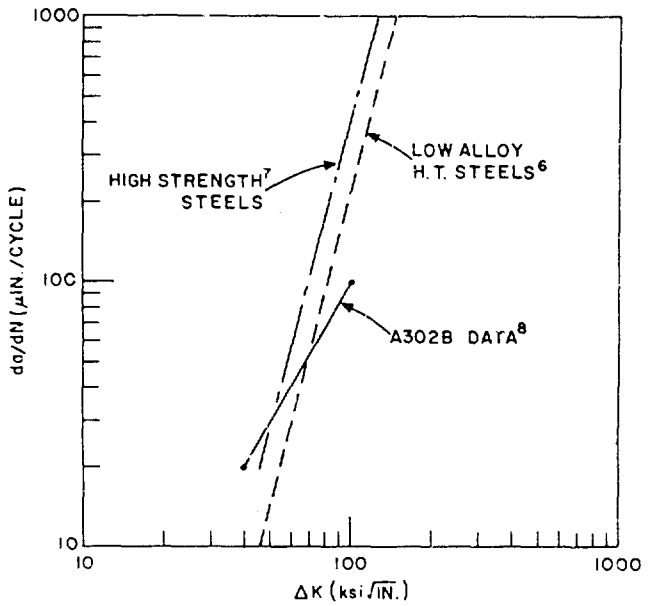

Fig. 3 - Crack growth rate da/dN as a function of fatigue cycle range of the K value ΔK

Consequently, from the steel data which are now available a rather crude empirical relationship may be devised to describe the normal rates of growth of cracks in all steels in air at room temperature (29,30,32-34). It is

$$\frac{da}{dN} = C(\Delta K)^4, \tag{37}$$

where, referring to Fig. 3,

$C_1 = 1.0\times 10^{-12}$ (for mean data on medium and low-strength steel),

$C_2 = 1.6\times 10^{-12}$ (for mean data on all steel),

$C_3 = 2.0\times 10^{-12}$ (for conservative estimating of fastest rates on all steels),

da/dN = in./cycle,

and

ΔK = ksi $\sqrt{\text{in.}}$

Equation (37) gives a reasonable estimate for growth rates from 10^{-6} in./cycle up to final failure, provided the cyclic K stays below K_{Ic} for the material and the cyclic nominal stress is below the static yield point. These restrictions normally offer no loss, in general, in describing flaw behavior in relatively thick pressure vessels of conservative design.

This crude relationship, Eq. (37), may at least be used to estimate whether fatigue crack growth is a real problem or not for an anticipated flaw in a steel pressure vessel. For example, for a known or anticipated flaw one may estimate the stress range and, subsequently, the range of K (or ΔK). Using Eq. (37), an anticipated rate of growth may then be estimated. The relative severity of flaws of various sizes and locations may thus be estimated also. In this manner Eq. (37) provides useful information of fatigue crack growth rates expected in vessels.

However, Eq. (37) is not recommended for actual estimates of the fatigue life of vessels. By itself it is too crude an empirical relationship for this purpose. It does not contain the effects of mean load, frequency, environment, or temperature, which surely play a role in the flaw growth fatigue life of vessels. For estimating flaw growth lives with some precision one must revert to the fundamental concept of measuring fatigue crack growth rates in laboratory tests which simulate the ΔK-levels under conditions of mean load, environment, and temperature expected in a vessel. Under the expected conditions the rate of crack growth da/dN vs the stress intensity factor range ΔK may be plotted to give the basic behavioral pattern of the material being tested. Differences in materials may be readily observed by comparisons of such curves. Moreover, carefully obtained data as represented on these curves may be used to estimate the fatigue crack growth life of a vessel. A numerical integration of crack growth rates from the initial flaw size to the critical size precipitating failure is all that is required to make such estimates (30,33).

Data on fatigue crack growth rates under expected environmental conditions are not yet available for pressure-vessel steels. Nevertheless, data which are available on aircraft materials (30,35) and some data taken on pressure-vessel steels (36) with an unfortunate choice of specimen configuration (the K levels cannot be computed) allow some tentative conclusions to be drawn on the effect of environment on fatigue crack growth rates. The presence of water (or high humidity) tends to accelerate fatigue crack growth rates in pressure-vessel steels, as well as others. For example, data (37) on A302B indicate that simulated boiler water increases the rates of fatigue crack growth by a maximum factor of 2.5, whereas for salt water the factor is about 3. (See Fig. 4.) Data

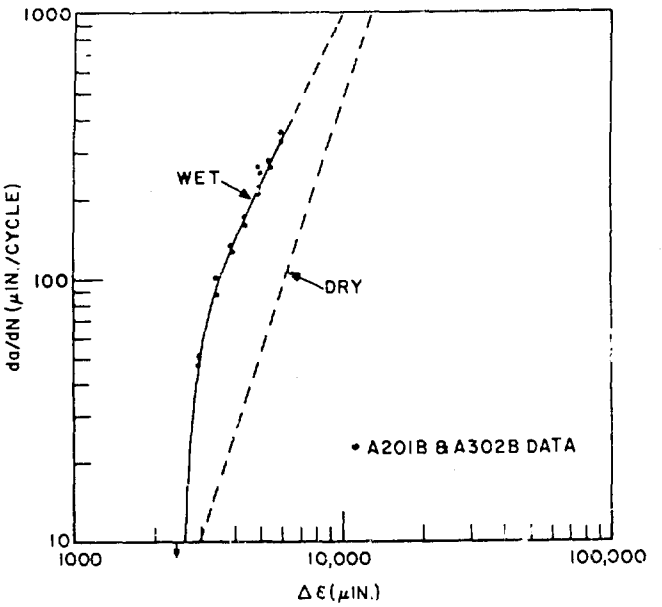

Fig. 4 - Crack growth rate da/dN as a function of displacement range in low-cycle fatigue testing. Data from Crooker and Lange (11).

on A201B show virtually identical behavior, which leads one to conclude that a factor of 3 is rather reasonable for A302B. These factors may be directly applied to the estimates for crack growth rates made using Eq. (37) discussed earlier. Though this factor of 3 is an approximation, since it is obtained from a test for which stress intensity factors cannot be computed, its precision is at best consistent with the precision of Eq. (37) itself.

The more precise and fundamental approach of simply gathering and plotting data on a da/dN vs K basis is preferred. It is implied that

$$da/dN = F(K) , \tag{38}$$

where $F(K)$ is a function which depends on the material and environmental conditions. Equation (37) is representative of the gross features of the function $F(K)$, which shows the main trend but not the details.

Similarly, one may recall that the stress intensity factor formula for any given solid-body configuration depends linearly upon the load P and also in some way upon the crack size, i.e.,

$$K = Pf(a) . \tag{39}$$

In general, Eq. (39) may be substituted into Eq. (38), which may be integrated to give the "life" N_F of a given configuration of a given material and environmental conditions. The life N_F can be written as a function of the load P and, alternatively, either the initial and final crack size or stress intensity factor values. The form is

$$N_F = H_1(P, a_i, a_c) \tag{40a}$$

or

$$N_F = H_2(P, K_i, K_c) . \tag{40b}$$

where H_1 and H_2 depend upon the material and the environment and upon the effect of the configuration through the form of the variation in its stress intensity factor with crack size.

From Ref. 10b and others on stress intensity factor formulas, it may be casually noted that for flaws which are relatively small compared to other body dimension, the formulas take the form

$$K = C_4 \sigma \sqrt{a} , \tag{41}$$

where σ is the nominal stress on the crack plane and C_4 takes on values from $2\sqrt{\pi}$ for an embedded circular crack of radius a to $1.12\sqrt{\pi}$ for a long surface crack of depth a or an edge crack in a sheet. For typical flaws which cause concern in pressure vessels, e.g., surface flaws which are of fairly similar proportions, the coefficient C_4 is nearly always the same value. It is therefore reasonable as well as informative to combine Eqs. (37) and (41) to observe the broad trends of variables in life calculations as implied by Eqs. (40). Making the substitution of Eq. (37) into Eq. (41) gives

$$\frac{da}{dN} = C'(\Delta\sigma)^4 a^2 .$$

Rearranging and integrating leads to

$$\int_{a_i}^{a_c} \frac{da}{a^2} = C'(\Delta\sigma)^4 \int_0^{N_F} dN$$

or

$$N_F = \frac{1}{C'(\Delta\sigma)^4} \left[\frac{1}{a_i} - \frac{1}{a_c}\right], \tag{42}$$

or again making use of Eq. (41)

$$N_F = \frac{1}{C''(\Delta\sigma)^2} \left[\frac{1}{K_i^2} - \frac{1}{K_c^2}\right]. \tag{43}$$

Note that Eqs. (42) and (43) are the rough approximations of the forms of Eqs. (4′ , where C' and C'' are constants which depend upon the material and environment l to a lesser degree on the configuration of the flaw or crack.

Some important conclusions on flaw growth life may be extracted from Eqs. (42) and (43). First, if the initial flaw size a_i (or K_i) is small compared to the critical size a_c (or K_c), then moderate changes in the critical fracture toughness K_c (or a_c) have little effect on the flaw growth life. This is the case of moderately "high cycle fatigue." It is only in the case where the initial flaw size is nearly the order of magnitude of the critical size that the critical size or K_c becomes important. This case is relatively "low cycle fatigue." Moreover, Eq. (43), upon lumping the material constant K_c^2 into C'', becomes

$$N_F = \frac{1}{C''(\Delta\sigma)^2} \left(\frac{K_c^2}{K_i^2} - 1\right). \tag{44}$$

Quite independently of the derivation of Eq. (44), Tiffany (10c) and others have observed that data on the lives N_F of flawed laboratory test specimens and typical structures of a

given material are correlated very well in terms of K_i, K_c, provided that the stress ranges $\Delta\sigma$ were roughly comparable. Moreover, Eq. (44) has a certain measure of appeal to those who follow the Coffin-Manson type of approach to low cycle fatigue, where the relationship $(\Delta\epsilon)^2 N_F$ = constant is observed to correlate data for many materials. Equation (44) implies agreement to this relationship and that "life" also depends strongly on initial flaw size a_i or stress intensity level K_i.

Equation (44) is only the result of crude approximations for the detailed behavior of flaws growing by fatigue loading, Eqs. (37) and (41). Though it would be inadvisable to apply it directly, using it to study the significant variables and to understand their relative roles is quite appropriate. That is perhaps best done as originally suggested by Tiffany (10c) through plotting test data on K_i/K_c vs N_F to observe effects of flaw size, environment, etc., in a way which lends itself to selecting proper materials and assessing directly the severity of subcritical flaws. Again, some preliminary data (34) on flaw lives in A302B are shown in Fig. 5. These data indicate lives of thousands of cycles for flaws about 4 in. or more in depth a and breadth b when cycled at half the yield strength in A302B base metal plates tested dry at room temperature. Similar tests should be performed on welded plates and with various typical environments for pressure vessels.

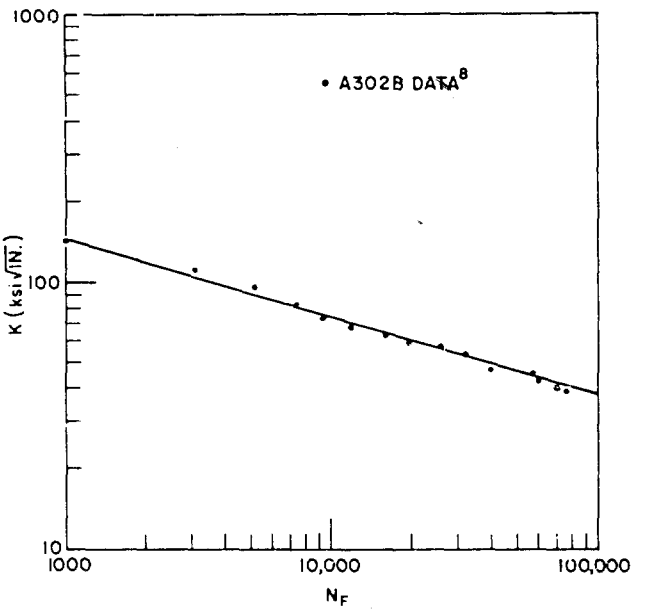

Fig. 5 - Cycles to failure as a function of the initial K value K_i. Data from Clark and Wessel (8).

The method of plotting data on Fig. 5 also implies the value to overload proof testing in assessing the remaining cyclic life (10c). Since K is proportional to load P, if any flaw survives an overload the overload K must be less than K_c; or, as a consequence, its initial K at operating load K_i must be less than K_c multiplied by the ratio of the operating load to the proof load P/P_p, i.e.,

$$\frac{K_i}{K_c} < \frac{P}{P_p} . \tag{45}$$

Moreover, the proof load can be deliberately applied at a lower temperature where K_c (low temperature) is lower. Assuming the K_c values are known at both temperatures, then

$$\frac{K_i}{K_c} = \frac{P}{P_p} \frac{K_c\,(\text{low temperature})}{K_c} \quad (46)$$

From a fracture mechanics flaw growth viewpoint there are no known disadvantages of proof testing. On the contrary, Eq. (46) combined with data in the form of Fig. 5 offer decided advantages by quantitatively guaranteeing a certain flaw growth life independent of other inspection procedures.

Crack Growth Rates With Environment

The growth of cracks in corrosive environment may be analyzed in much the same manner as fatigue crack growth, using the stress intensity factor K as the local stress variable for the "driving effect" of stress near the crack tip.

In stress-corrosion crack propagation relatively weak environments, such as water, often have pronounced effects. In certain materials the same environment may have very small effects on pitting-corrosion (i.e., crack initiation from a smooth surface under stress). Moreover, the crack tip stress state (plane stress vs plane strain) has marked effects on the growth of stress corrosion cracks. This means that where the plate thickness is large compared to the plastic zone size (plane strain) the conditions for environmental crack growth are much more severe than for relatively thin plates. Since most past stress corrosion tests have been performed on thin, smooth samples of materials for both of the preceding reasons, most ordinary stress corrosion data are of doubtful value for assessing the possibility of crack growth in the design of thick-walled pressure vessels with flaws.

In some work on high-strength steel alloys (28,35,38), it has been shown that environmental flaw growth data can be correlated in terms of stress intensity factors, implying the form

$$da/dt = H_3(K) . \quad (47)$$

This equation is analogous to Eq. (38), but here statically applied loads and environment are present (or fatigue loading and environment) with a stress state of plane strain (thick plates). For the case of a statically applied load for each material and environment combination, there appears to be a threshold level K_{ISCC} below which crack growth does not occur. This is also evident in other recent works (10c,39,40) which, in addition, have shown that the K_{ISCC} value is substantially elevated under stress conditions tending toward plane stress (thin plates). On the other hand, under repeated (fatigue) loading (of a few cycles per second) no threshold level seems to exist (35). However, the normal case in reactor vessels is probably the former, where the occasional changes in load do not significantly alter the rate of progress of a stress corrosion crack.

In low-strength high-toughness steel alloys the K_{ISCC} stress-corrosion-cracking threshold level is likely to be nearly as high as K_{Ic} itself (40). Consequently, it appears that it may be possible to completely avoid static-load stress-corrosion-cracking in reactor vessels simply by judicious choice of materials. The tests of the materials should be for the absence of any crack growth over long periods of time under environments and load variations (K-variations) anticipated in service. Currently, in such tests, fatigue-cracked notches are used as simulated flaws, and examination for absence of growth is by fractographic examination upon completion of the test and breaking open the specimen. Other techniques using sectioning of the crack-tip region showing blunting of the crack are perhaps even more convincing.

However, if the K_{ISCC} is determined to be significantly below K_{Ic}, then several alternative considerations must be suggested. First, the time to failure (or rates of growth) for cracks with applied K levels above K_{ISCC} should be determined (10c 39,40). Normally, these times are relatively short, i.e., a matter of minutes or a few hours from first load application. Consequently, a reactor vessel with a flaw stressed above K_{ISCC} would fail in a short time unless it is protected from the environment, or unless plane stress conditions prevail for cracks through the wall. In some cases protection is possible, but it is not in general. In the cases where protection is not possible, the fatigue analysis should obviously be terminated at K_{ISCC} (i.e., replace K_c in Eqs. (40) through (46) with K_{ISCC} with a corresponding change in interpretation). Above K_{ISCC}, either there is no significant life remaining or, if plane stress conditions occur at K-levels between K_{ISCC} and K_{Ic}, there is some chance of arrest or inhibition of static stress corrosion crack growth, whereupon the fatigue crack growth mechanism might again prevail. Again, this is an area where little work has been done, especially on low-strength high-toughness materials.

In summary, for corrosion considerations K_{ISCC} or its equivalent should be established for the materials considered in reactor vessels. Hopefully, K_{ISCC} will be very close to K_{Ic}, and no special provision for stress corrosion cracking need be made in addition to that in the fatigue crack growth analysis (with environment). However, if K_{ISCC} is appreciably below K_{Ic}, then either K_{ISCC} should be used as the "failure level" in design, or special procedures must be developed to assess the remaining life.

CRACK PROPAGATION AND FRACTURE TOUGHNESS

Measurements of K_c and K_{Ic} for Very-High-Strength Metals

Crack toughness measurements based upon linear crack stress field analysis lead to critical values of the stress intensity factor K for either onset of rapid fracture or crack arrest. Measurements of crack arrest K values are less common, mainly because such tests require larger amounts of material. Similarly, for reasons of convenience, the testing speed most often used has been slow. The loading time to fracture in slow testing is usually about 2 min. The primary interests supporting K_c and K_{Ic} test development pertained to very-high-strength metals for use in rocket or ordnance applications. Reference 10 provides an adequate review of this subject and this discussion will summarize only selected major points.

Onset of rapid fracture and crack arrest are naturally of interest for use as crack toughness measurement points, in part because they tend to occur abruptly and in part because present knowledge suggests no alternative choices. In the slow-stable and fast-stable regions of crack extension the average crack speed changes continuously in response to changes in the value of K or G. The in-between points called onset of rapid fracture and crack arrest, under ideally brittle conditions, appear to be true instability points at which there is an abrupt upward or downward jump in the crack speed. As toughness increases and the plastic zone grows in size, the crack length for onset of rapid fracture becomes more difficult to select unambiguously in a simple way. Even for plane-strain K_{Ic} testing, material properties leading to unexpected amounts of stable crack extension prior to onset of rapid fracture sometimes occur. After some years of study the ASTM E-24 Committee recently approved for trial, as a tentative K_{Ic} testing standard, a method remindful of a percent-offset tensile yield strength testing practice.

In K_c and K_{Ic} testing some stable crack growth prior to the measurement point is expected, because the natural contour of the leading edge of the crack at the fracture load usually differs from the crack shape inserted, say by low stress fatigue. When the specimen has a through-crack as in Fig. 2, plastic yielding near the plate surfaces results in added stress on central regions of the leading edge. The central region then advances.

Whether this advance takes the form of an unstable plane-strain "pop-in" or appears gradually depends upon the length of the leading edge segment, which becomes nearly unstable at the time of forward movement. From experience, a pop-in often occurs when the plate thickness B is more than 4 times the plane-stress value of $2r_y$ and nearly always occurs when B is more than $10(2r_y)$. Also, from testing experience, a substantial stable forward motion of central regions of the crack can be assumed to be governed by a K_{Ic} level of K so long as environment effects, which would cause continuing stable crack extension, are absent.

In K_c testing of very-high-strength steel and aluminum alloys, the test method of Ref. 41 employed an ink-staining technique to mark the region of slow stable extension prior to onset of rapid fracture. Analysis of these results showed stable extensions rarely less than r_y and rarely more than $2r_y$ (10a), where these length factors were computed on a plane-stress basis regardless of the degree of plane-strain influencing the test result. The presence of water in the ink no doubt assisted the observed stable extensions. However, most of these tests used Elox notches (about 0.002 in. root radius), and this tended to reduce the stable growth. Generally, a stable crack extension about r_y in size is expected as normal behavior and represents, primarily, readjustment of the leading edge contour toward the shape most natural for the onset of rapid fracture instability which severs the specimen.

Roughly speaking, the present K_{Ic} testing method favored by ASTM E-24 assumes that, when the load-deflection curve indicates stable crack growth of more than r_y, a load corresponding to the K_{Ic} value has been achieved. Other details of the test method tend to encourage use of large enough test specimens so that most tests will terminate with an abrupt onset of rapid fracture prior to visible indications of stable growth. No change in the average level of K_{Ic} test results from those using presently customary methods is expected.

During the past 8 years many thousands of K_c and K_{Ic} test results were reported from test methods suggested by the currently available technical literature. Results reported in Refs. 10 and 27 are typical. One finds the scatter band for a group of results from similar specimens of the same plate material usually extends from 5% to 10% above and below the mean value. Welded regions tend to have larger variations of microstructure and impurities, and the scatter range of test results is larger. The K_{Ic} values reported by Kies et al. (10e) for various welds in ultrahigh-strength maraging steel show ±15% to ±25% scatter bands for central regions of the welds. They reported that these variations correlated with variations in quality of microstructure in the local region tested.

The difference in test result scatter between fracture toughness tests and tensile yield-strength tests corresponds in part to the contrasting influences of small defects upon these properties, as discussed previously in this section. The larger defects, which tend to be less uniform in distribution, influence the crack toughness but do not influence resistance to plastic deformation. An additional factor is related to the test-volume size.

When the size of the fracture toughness specimen is increased, the leading edge of the crack samples a larger volume of material. The result is a reduction in the absolute size of the test-result scatter zone. A corresponding reduction of average critical K value should occur in accordance with a "worst flaw" statistical treatment of the problem. In the case of K_{Ic} evaluations using through-crack type specimens, one dimension of the test volume is the plate thickness, diminished by regions comparable in size to $2r_y$ (plane stress) adjacent to the test-plate surfaces. The area one would use in completing the test volume estimate would be the square of a small dimension intermediate in size between r_y and r_y (plane-strain) and might be guessed as simply the product of these length factors. Such a test volume is quite small. Yield-strength tests respond to the

average critical stress through a test volume comparable in size to the cube of the test-bar diameter, a volume several orders of magnitude larger than can participate in determining a K_{Ic} test result.

The substantial scatter of test results inherent to crack toughness measurements has a definite bearing on a fracture control plan which assumes that certain levels of crack toughness, established by testing, will be present as a barrier to crack propagation. There are no conventional methods for selecting a worst K_{Ic} value for a particular application on a probability basis, other than straightforward statistical theory.

On the basis of statistical theory, suppose K_{Ic} tests, say of an electroslag seam weld, have been done in sufficient number to permit determination of the standard deviation $\bar{\sigma}$. Then a Weibul theory flaw distribution exponent m can be estimated (41) from the equation

$$\frac{\bar{\sigma}}{(K_{Ic})_{average}} = \frac{1.2}{m} . \tag{48}$$

From the statistical theory the average K_{Ic} for a large crack through the wall thickness B should be less than that for the small test cracks in specimens of thickness B_0, in accordance with the equation

$$K_{Ic} = (K_{Ic})_{average} \left(\frac{B_0}{B}\right)^{1/m} . \tag{49}$$

The value of $\bar{\sigma}$ applicable to the large cracks would be reduced in size by the same factor $(B_0/B)^{1/m}$. Several times this reduced $\bar{\sigma}$ value would then be subtracted from the large-crack K_{Ic} to determine a conservative estimate for the service vessel. The details of this would depend upon judgment factors best settled at a later point in fracture control planning.

The Brittle-Ductile Fracture Transition

During fracture investigations associated with welded steel rocket chambers for the Polaris and Minuteman programs, K_c measurements were made on a variety of ultrahigh-strength metals. It was noted that the percentage of oblique shear on the fracture surface showed a trend-type correlation with the dimensionless ratio

$$\beta_c = \frac{1}{B}\left(\frac{K_c}{\sigma_{YS}}\right)^2_{plane\ stress} \tag{50}$$

Since

$$2r_Y = \frac{1}{\pi}\left(\frac{K_c}{\sigma_{YS}}\right)^2 \tag{51}$$

is regarded as a formal measure of plastic zone size, the ratio of plastic zone size to plate thickness was β_c/π. As was noted in Refs. 13 and 42, less than 50% oblique shear was usually present when $\beta_c < \pi$. Furthermore, the condition $\beta_c = \pi$ represented one in which the value of K_c, as a function of β_c, was increasing rapidly. Clearly, $\beta_c = \pi$ represented a midrange condition for the change from a flat-tensile fracture with relatively small shear lips to an oblique-shear fracture with substantially increased fracture toughness. The $\beta_c = \pi$ criterion for midrange behavior was the same regardless of whether the fracture transition was induced by changing the testing temperature or by

changing the test-plate thickness. In the case of high-strength aluminum, K_c did not change appreciably with temperature (excluding temperatures below -250° F) but occurred with changes of test-plate thickness in the same manner as for steels.

At the time of Ref. 13, fracture toughness data for several rotor steels at about 100 ksi yield strength were available. These showed the same behavior pattern relative to the brittle-ductile transition as did the high-strength metals. With regard to low-strength mild steel plate material, only approximate estimates of fracture toughness based upon crack arrest tests were available. However, rough estimates of K_c using an elevated dynamic yield strength were made. The same correlation between K_c and fracture transition was again evidenced.

A clear mechanism exists for the control of the brittle-ductile transition in terms of the plastic zone size. For a plate in tension containing a round hole straight through the plate thickness, the thickness direction stress close to the hole at midthickness of the plate shows a large amount of plane-stress relaxation, unless the hole diameter is less than half the plate thickness (43). From this, we expect that plane-strain confinement of the plastic zone will disappear as we increase the plastic zone size factor $2r_y$ relative to the thickness of the fracture test specimen. If we allow the open hole a moderate advantage over the crack tip plastic zone in causing thickness direction stress relaxation, the $2r_y = t$ criterion for a midrange fracture transition condition is quite plausible.

The crack opening displacement δ decreases with testing temperature for a steel and thus changes in size relative to the grain size and relative to Krafft's d_T. Alterations of this kind may have a bearing on the appearance features of a flat-tensile fracture, for example, upon the fraction of the exposed fracture surface composed of cleavage facets. However, the role of fracture appearances in relation to macroscopic fracture toughness is still not very clear. Notched bar fracture tests of steels conducted at a series of temperatures and with a series of specimen sizes do not show one fracture transition associated with crystalline cleavage and a second transition associated with the relative size of the plastic zone. Only the transition associated with relative plastic zone size is consistently observed.

Several tensile fracture tests were performed at the Naval Research Laboratory using 60-in.-wide 3/4-in.-thick 2024-T3 aluminum plates, centrally notched. The toughness was so large that the average net-section stress roughly equaled the yield strength at the load for crack propagation. However, the first test produced a flat-tensile fracture normal to the plate surface extending nearly to the side boundaries of the specimen. In a second trial, the hacksaw extension of the central slot was tilted to 45 degrees with the plate surfaces. This time the fracture was entirely oblique shear, but the load and net-section stress did not differ significantly from that for the first test plate. According to J.G. Kaufman (Alcoa Research Laboratory, New Kensington, Pa.) similar observations have been made at his laboratory. Formal reports of this curious behavior do not seem to be available. The rapid room temperature aging of 2024 aluminum after plastic straining is thought to be a factor.

Anomalous flat-tensile fracturing also occurred with certain rotor steel alloys tested in the form of centrally notched 4 in. and 6 in. thick spin disks at the General Electric Co., Large Steam Turbine Division (44). A thickness reduction at the root of the notch indicative of large plastic strains was observed, and the computed fracture toughness was high; but the fracture showed shear lips which were of almost negligible size. In these tests one could usually see an arrest line on the fracture surface marking the zone in which an oblique-shear fracture, if present, would have provided normal behavior. The temperature range for these tests was from room temperature to 450° F, and the anomalous flat-tensile fractures tended to occur in the upper half of this range. A report of recent fracture tests of berillium plates states that large amounts of plane-stress yielding accompanied a flat-tensile fracture appearance (45).

The interest in K_{Ic} testing has led to the use of brittle boundary coatings and face notching to assist establishment of plane-strain fracturing. The results show that shear lips can be eliminated in this way. However, the results also show that a fracture transition, in terms of plastic zone size and fracture toughness, occurs despite elimination of the shear lips. From such observations as these, one concludes that the position of a fracture toughness test relative to elevation of toughness by plane-stress yielding is best judged by direct measurements of thickness reduction, or in terms of a parameter such as r_y, rather than solely from appearance aspects of the fracture surface.

Double Cantilever and Face-Grooved Specimens

The single-edge-notched bend and tensile specimens most used for fracture toughness evaluations are well described in Ref. 10. For investigations of rate-sensitive materials and for other special purposes, specimens sometimes referred to as "double-cantilever" and sometimes as "crack-line loaded" are of interest and will be discussed here. The testing advantage sought in this type of specimen is control of the K value. In remotely loaded tensile and bend specimens the increase of K with crack length at onset of rapid crack extension is too fast, and continued crack extension by the loading system is beyond control.

Figure 6 shows a double-cantilever specimen of simple design. If the beam depth h is small compared to the crack length a, an adaptation of St. Venant's principle suggests an approximate but useful method of analysis. Since the section above the leading edge of the crack is remote from the applied force P, one can estimate the load-displacement l from a simple beam-theory stress distribution across the beam near the leading edge of the crack. So long as the assumed stress distribution possesses a bending moment equal to the applied moment $P(a + a_0)$, ignoring the stress singularity causes only a relatively small error. Using customary equations for beam deflections (46),

$$l = CP = \frac{8}{E}(x^3 + x)\frac{P}{B}, \tag{52}$$

where

$$x = \frac{a + a_0}{h} \tag{53}$$

and a is the crack length as measured from a point close to the applied load. Then from Eq. (13),

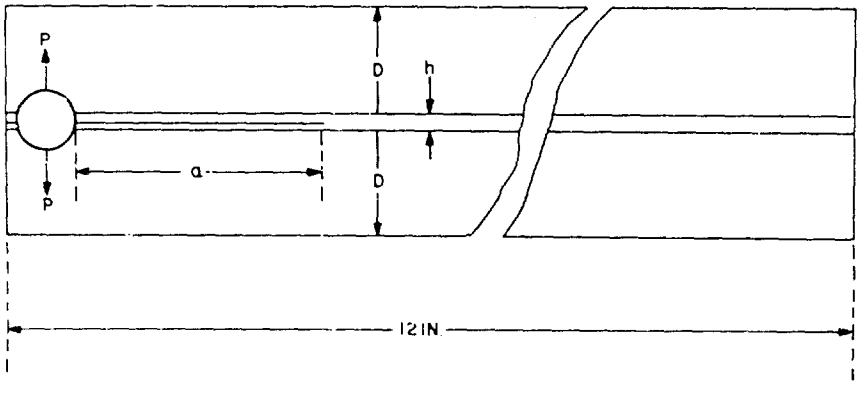

Fig. 6 - Double-cantilever specimen

$$\mathcal{G} = \frac{4P^2}{EhB^2}(3x^2 + 1) . \tag{54}$$

Using $K^2 = E\mathcal{G}$ provides the value of K. Adjustment of the small length correction a_0 with the aid of several direct observations of C permits approximate representation of K across a substantial range of crack lengths. Because of the relatively large compliance of the specimen, a careful experimental calibration for improved accuracy is not difficult.

From a study of the way beam stiffness factors influence Eq. (54) one can see that the beam depth contributes only in terms of its value near the leading edge of the crack and that a tapered contour, with beam depth increasing in the direction of crack extension, can be devised such that the coefficient of P^2 in Eq. (54) is held at a constant value. Tapered specimen contours of this kind have been developed by Ripling and Mostovoy (47). For these specimens the $\mathcal{G}$ or K value depends only upon the applied load and does not depend upon the length of the crack.

Reference 46 discusses applications of specimens similar to Fig. 6 in studies of separational behavior of adhesive joints. For a layer of relatively low modulus adhesive between two metal bars, x-direction strains in the direction of crack extension are suppressed. Thus the stress σ_y normal to the adhesive layer readily dominates in controlling orientation of the tensile crack. Unless the interface regions are weak, the crack moves straight ahead nearly at the midpoint of the layer thickness. Usually the load-displacement speed can be adjusted so that crack extension consists of a series of abrupt run-arrest sequents. As many as a dozen or so samplings of the K value for onset of rapid fracture and for crack arrest can sometimes be obtained using a single specimen.

A specimen which permits repeated observations of K for onset and arrest of rapid fracture is of natural interest for studies of crack extension in metals, particularly for the rate-sensitive metals. However, unless a very stiff specimen is used with the beam depth large relative to crack size, the desired path for the crack, straightforward along the plane of the initial starting-crack slot, is unstable. For specimens similar to Fig. 6, at a short distance from the crack, σ_x is so large compared to σ_y that a slight turning of the crack from the line of symmetry is enough to start a cracking path which breaks off one arm of the specimen.

By machining the faces of the specimen along a strip containing the symmetry plane, a situation similar to that for the adhesive layer between metal bars can be restored. Essentially, the σ_y/σ_x ratio can be increased sufficiently in this way so that the stress system controls the crack plane to lie in a region near the middle of the reduced-thickness strip.

Face grooves of moderate depth (10% of specimen thickness or less) and moderate sharpness (0.1 mm root radius or more) have seemed to improve the abruptness of onset of rapid fracture for K_{Ic} testing using single-edged-notched tensile and bend specimens. For face-notched specimens of these types the test-result K value is simply the K computed without regard to the face grooves multiplied by the square root of B/B_n, where B_n is the specimen thickness at the crack plane.

Use of face grooves with double-cantilever specimens requires more careful study. In addition to reducing the size and influence of shear lips the face groove is expected to control the direction of crack extension. These are two separate tasks and must be done in a cautious manner relative to the following points.

1. The compliance calibration (or two-dimensional analysis) furnishes the average of $\mathcal{G}$ across the specimen thickness at the leading edge of the crack. The total strain energy release rate can be divided by the reduced section thickness to obtain the $\mathcal{G}$ value

applicable to the leading edge of the crack under observation with about the same accuracy as for situations with no face grooving, so long as the crack front maintains a normal shape. A normal crack front shape for plane strain would lead slightly at midthickness in a way corresponding to the anticlastic curvature of the crack surfaces. If the face groove is very sharp and produces a crack front leading at the side boundaries, there are several barriers to clear interpretation of results. One of these is the need for a three-dimensional analysis, which is currently not available.

2. Unless the reduced section thickness B_n is greater than $\alpha(2r_y)$ (plane stress), a significant elevation of toughness from thickness-reduction yielding may be present. The value of α needs investigation. For deep notches a probable result would be $\alpha = 3$.

3. The effects of too much depth and sharpness of the face grooves and too little net-section thickness tend to offset one another in their contributions to the formally computed K value. Thus, comparisons showing K_{Ic} from deeply face-grooved specimens equal to K_{Ic} from large test specimens (known to be of adequate size for plane-strain control of test results) do not prove that the face-grooved specimens are testing the material in the desired manner. Thickness-reduction yielding may have occurred far enough in advance of the crack so that test results are influenced by a nontypical distribution of plastic strains. In addition, the crack front shape may require a different stress analysis than the one usually assumed, as suggested in 1.

General Aspects of Dynamic Crack Stress Field Analysis

A stress distribution was published by Yoffe (48) for a two-dimensional crack of constant length $2a$ moving at a fixed crack speed in an infinite solid with the tension σ acting normal to the crack at infinity. The value of K for the leading edge of this crack was $\sigma\sqrt{\pi a}$, the same as for the similar static problem. Since Yoffe's analysis assumed a crack closure action proceeding at the same speed as the opening process, the usefulness of this solution was not at first clear. However, after some study, one can see that the prediction from Yoffe's analysis, that the limit to the speed of a crack fixed by inertia is the Rayleigh wave velocity, is generally correct. A stable crack speed higher than this would not be possible, because a fixed pattern of crack opening displacements could not then advance as fast as the leading edge of the crack. Thus, the limiting velocity of a brittle crack from purely inertial limitations is about $0.9c_2$, where c_2 is the elastic shear wave speed. In addition, the pattern of stresses and strains very close to the leading edge of the Yoffe crack can be assumed to apply generally to a running brittle crack, because this stress field is dominated by the leading edge stress singularity local to the region under consideration. In the dynamic leading-edge stress pattern the principal change from the static pattern is a tendency for the maximum value of σ_y, at about $\sigma = 60°$ from the crack plane, to become more pronounced with increase of crack speed. The change is gradual, and no alterations worth attention occur when the crack velocity is below $0.4c_2$.

The highest crack velocities so far observed were found in nearly pure silica glass and were about $0.6c_2$ (9). More often, the limiting velocity is about $0.5c_2$ and is far enough below $0.9c_2$ so that only a moderate dynamic influence can be found in the calculated stress pattern for cracks moving at maximum real crack speeds. For low-velocity cracks, less than 3000 ft/sec for steels, the elastic stress pattern around the plastic zone of the crack does not differ from that for a stationary crack in tension.

In concept, the stresses near a running crack in a structural component might be found in the following way. The leading-edge stress pattern (dominated by the singularity terms) could be assumed given by the Yoffe solution. This pattern would have a one-parameter K-value characterization. Drawing a small circle around the crack tip to establish a boundary for the assumed crack tip stress field, one would next construct stress

waves (in the y-direction, primarily tensile unloading waves) from the crack tip stress field and wave reflections from the boundaries in sufficient detail to establish the K value for the crack. No accurate solution of a problem of this nature is known.

Such analysis as has been given to practical dynamic fracturing problems, for example, crack arrest studies in large welded test plates, has been of the static kind. There is some evidence from data consistency that errors incurred from not using a dynamic treatment have been relatively small. These observations are discussed later.

For the running crack, the inertia of surrounding plate material delays interaction of the crack-tip stress field with the points of load application and specimen boundaries. The effect of this delay is a moderate reduction of the K value below the static estimate. Essentially, the plate material inertia provides a short-specimen fixed-grip condition to a partial degree. Subsequent reflection of tensile unloading waves might add positive increments to K if free boundaries existed directly above and below the crack. However, such a situation is not expected for the tensile direction of loading.

After arrest of the crack, restoration of the original load results in a total stress-field energy in the structure larger than the original amount. Suppose the total energy consumed in crack extension is $U_R + U_L$, where U_R comes from the weld residual stress field and U_L comes from the superimposed stresses due to loads on the structure. Roughly, the increase of stress field energy in the structure is U_L, and the loading forces have added twice U_L during a short period following crack arrest. During this time period the K value must change from a dynamic arrest value, somewhat lowered by the inertial effects, to the static value. Occasionally, several arrest markings are visible close to a position of final arrest, suggesting that added crack extension may occur during the transient time interval prior to the final static stress distribution.

In summary, static methods of analysis serve well enough for purposes of estimating the crack arrest possibilities in a structure. The error from not using a dynamic analysis method is probably small and probably conservative. Run-arrest segments of crack extension comparable in size to the wall thickness would not be expected in carefully fabricated BW and PW nuclear pressure vessels. This phenomenon requires a local region of large residual tensile stress, say from welding without stress relief, or a substantial-size local region where resistance to crack extension has been lost for some reason (for example an extensive concentration of undesirable impurities). Both conditions should be eliminated by fabrication and inspection controls, as discussed previously.

The Fracture Process Zone, Time Rate Effects, and Minimum Fracture Toughness

The term "fracture process zone" is here used for the region at the leading edge of the crack, within which small separational elements form and within which plastic strain conditions critical for their rapid joining develop. The length factor δ seems a large enough estimate of the size of this zone. Krafft's d_T length factor is smaller and is thought of as the spacing of the fine-scale elements of separation.

A rough estimate can be made of a time t_A necessary for a substantial degree of temperature equalization across a distance r in a metal, using the equation

$$t_A = \frac{r^2}{\alpha} , \tag{55}$$

where the thermal diffusion coefficient α is the ratio of the thermal conductivity to the product of density times specific heat.

Consider the value of t_A if we use for r an opening dislocation δ, which would be typical for A302B steel at onset of rapid fracture (plane strain) and for rapid load application in a time of several milliseconds at room temperature. For these conditions K_{Ic} = 75 ksi $\sqrt{\text{in.}}$ can be assumed. The yield strength will be taken as 62 ksi plus 20 ksi for elevation by rapid loading. The sum of these times $\sqrt{3}$ for plane-strain constraint gives σ_Y = 142 ksi. Thus,

$$\delta = \frac{K^2}{E\sigma_Y} = \frac{(75 \times 10^3)^2}{30 \times 10^6 \times 142 \times 10^3} = 1.3 \times 10^{-3} \text{ in.} \tag{56}$$

If we assume α = 0.16 cm^2/sec = 0.025 in.^{2}/sec, then

$$t_A = \frac{(1.3 \times 10^{-3})^2}{0.025} = 68 \times 10^{-6} \text{ sec.} \tag{57}$$

The resulting value of t_A is so small in comparison to the loading time of several milliseconds that we can be sure a fracture process zone comparable in size to δ is quenched, by surrounding metal, to an isothermal condition.

For a running plane-strain crack in the same metal approaching an arrest point, a K value of 70 ksi $\sqrt{\text{in.}}$ and a minimum crack speed of 50 ft/sec would be reasonable estimates. The estimate of loading time for a zone of size δ near the leading edge of the running crack will be approximated as δ divided by 600 in./sec. Because of the shortening of the loading time, σ_Y is estimated as $\sqrt{3}$ (62 + 40) = 178 ksi. Thus,

$$\delta = \frac{(70 \times 10^3)^2}{30 \times 10^6 \times 178 \times 10^3} = 0.92 \times 10^{-3} \text{ in.} \tag{58}$$

and

$$t_A = 34 \times 10^{-6} \text{ sec.} \tag{59}$$

However, the loading time is only

$$\frac{0.92 \times 10^{-3} \text{ in.}}{600 \text{ in./sec}} = 1.5 \times 10^{-6} \text{ sec.} \tag{60}$$

This time is so short compared to t_A that one can be sure thermal gradients will be maintained, corresponding to differences in local plastic work across dimensions in the metal substantially smaller than δ.

Use of d_T in place of δ in the preceding illustrations would not have changed the conclusions. For metals, quite generally, the most rapid loadings feasible with testing equipment (2 msec for fast hydraulic testers and 0.2 msec to 0.5 msec for drop weight and Charpy impact testing) are not fast enough to prevent quenching of the fracture-process zone of the stationary crack to an isothermal condition. In contrast, the smallest speeds which have been observed for cracks approaching an arrest in a rate-sensitive steel are equivalent to loading times so short that the fracture process zone has an adiabatic thermal condition down to length factors as small as d_T.

The running crack approaching a crack arrest point and a stationary crack approaching instability due to rising tensile load are clearly different in terms of thermal conditions. Nevertheless, a strain-rate comparison is of some interest. Characterization of the fracture process zone in terms of an average strain concept ϵ_1 has already been discussed. It will be assumed that attention can be restricted to the fracture process zone

and that only the strain rate pertaining to ϵ_1 need be considered. For this purpose the relation suggested by Krafft serves well enough. Thus, the critical strain ϵ_1 for the fracture process zone is represented in the form

$$\epsilon_1 = \frac{K}{E\sqrt{2\pi d_T}} . \tag{61}$$

For a K_{Ic} test conducted with a linear increase of load with time up to the fracture point, the strain rate $\dot{\epsilon}$ is given by

$$\dot{\epsilon} = \frac{\epsilon_1}{t} = \epsilon_1 \frac{\dot{K}}{K_{Ic}} . \tag{62}$$

As noted before, other representations of ϵ_1 are possible. An averaging procedure which would predict proportionality of ϵ_1 to K^2 could be shown. However, this would merely insert a factor of 2 in the numerator of the last term of Eq. (62), and changes occur slowly enough with strain rate so that a factor of 2 error in $\dot{\epsilon}$ would not be serious in correlation studies.

Consider next the strain rate for a crack traveling at some relatively low constant speed $\dot{a}$. As in the case of the thermal estimate, the time for elevation of the strain to ϵ_1 at a fixed point approached by the process zone will be taken to be $\delta/\dot{a}$. Thus, the strain rate for the running crack becomes

$$\dot{\epsilon} = \frac{\dot{a}\epsilon_1}{\delta} . \tag{63}$$

A match between strain rates for the stationary and moving cracks, except for difference in values of ϵ_1, would occur for a loading time equal to $\delta/\dot{a}$. In the case of the 50-ft/sec crack in A302B, employed for a thermal condition illustration, this time was found to be only 1.5 μsec, 300 times smaller than the loading time estimate for a notched-bar impact fracture test. Actually, K-value estimates from studies of crack arrest in strain-rate-sensitive steels do not seem to differ from K_{Ic} values derived from notched-bar impact tests, despite the difference in the corresponding estimates of strain rate.

Figure 7 provides a concise summary of plane-strain crack extension behaviors in schematic form. A solid curve and a dash-dot curve show the fast-stable and slow-stable regions in terms of $\log \dot{a}$ as a function of $\log \mathcal{G}$. The vertical line segment forming the lower left portion of the solid curve represents the tendency of crack arrest, in rate-sensitive materials, to occur abruptly from a certain minimum velocity. This vertical portion should be thought of as a stretched-out endpoint of the fast-stable region. Crack extension is stable only where the slope of the line is positive and finite. In terms of a loading-speed scale at the right of the graph, $\log \dot{K}$, the dashed line represents the tendency of $\mathcal{G}_{Ic}$, for onset of rapid fracture, to decrease with increase of strain rate. All the behaviors are for a fixed temperature. With increase of temperature the slow-stable curve would tend to shift upward, while the fast-stable and $\mathcal{G}_{Ic}$ curves would shift to the right. For a rate-insensitive metal such as 7075-T4 aluminum, the $\mathcal{G}_{Ic}$ curve would coincide with the left vertical portion of the solid curve, which would, then, not shift appreciably over the temperature range of rate insensitivity.

For tests of layers of epoxy adhesive between metal bars in the double-cantilever specimen form, the crack speed has been measured using vibration-induced ripples on the fracture surface (46), and the observed behavior corresponds to the crack arrest curve shown in Fig. 8. The load-time curves for these tests showed a saw-tooth appearance. Each run-arrest burst produced a vertical segment of load drop which was followed by a slant upward reloading line to the next instability point. With increase of

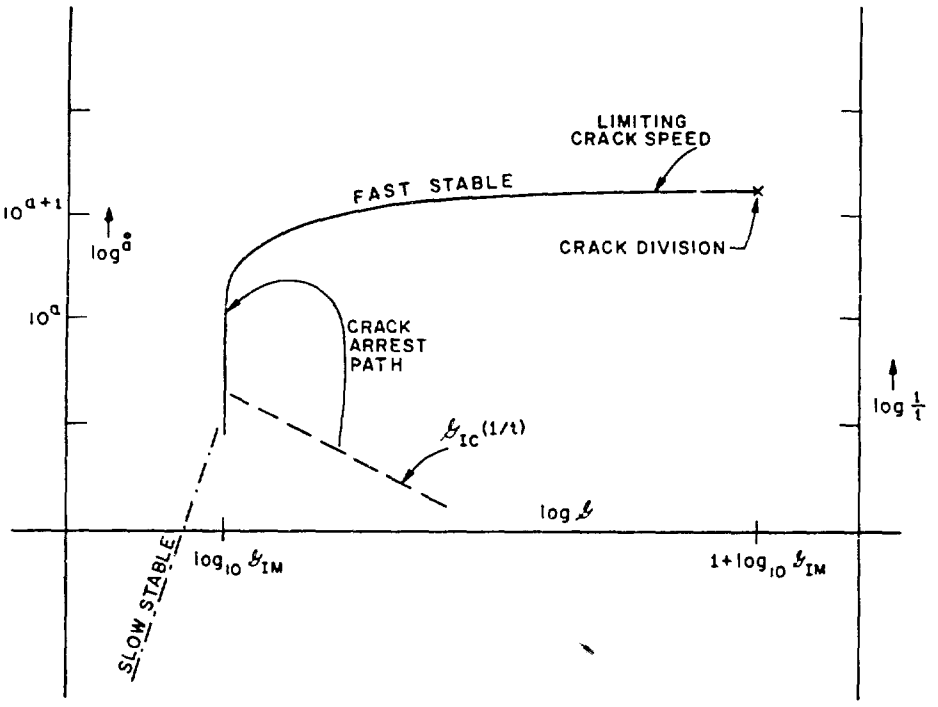

Fig. 7 - Crack extension behaviors as a function of the force $\mathcal{G}$ and at a fixed temperature

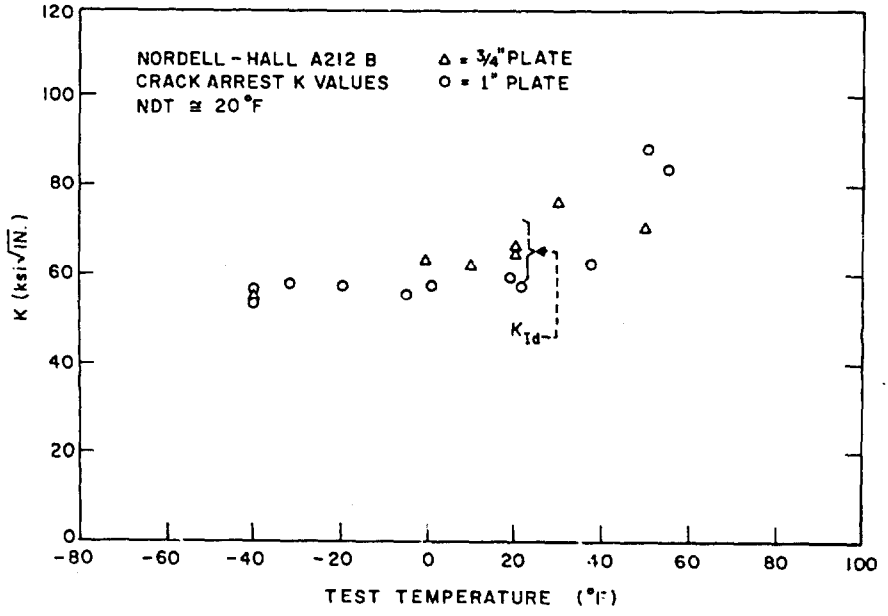

Fig. 8 - Crack arrest K values from wide-plate tests

loading speed a record could be produced showing no load change discontinuities, while the fracture surface still exhibited arrest markings. This means the values of $\mathcal{G}$ (or K) for onset and arrest of rapid fracture had become very nearly equal. In terms of Fig. 8 this means the $\mathcal{G}_{Ic}$ line, extended to high enough loading speeds, was meeting the vertical endpoint portion of the fast-stable behavior curve.

It would be most reasonable to expect that rate-sensitive steels would behave in a similar manner. Evidence for this will be discussed in a later section. For strain-rate sensitive steels the evidence suggests that a loading time about equal to that for a notched bar impact fracture test is fast enough to reduce the fracture toughness to the minimum value.

Fracture Toughness in Relation to Plastic Flow Properties

The two plastic flow properties of primary interest in relation to fracture are yield strength and strain hardening. These may be measured and represented in various ways. The yield property wanted is that which would serve best in estimates, such as $2r_y$, of plastic zone size. For this use, the 0.2% offset uniaxial tensile yield strength, which is most often available, has served satisfactorily.

With regard to strain hardening, the purpose is to assist prediction of the fracture process zone strain ϵ_1 as a critical strain for plastic instability. For this purpose, it is a natural choice to define the measure of strain hardening as the exponent n in the equation

$$\sigma_{TS} = \sigma_0(\epsilon_{TS})^n, \tag{64}$$

where σ_{TS} and ϵ_{TS} are the true stress and true strain, respectively. For a uniaxial tensile specimen this equation predicts plastic instability will occur when $\epsilon_{TS} = n$. Krafft measures n with small cylindrical compression specimens as a function of temperature and strain rate. To obtain isothermal n values it is necessary either to avoid adiabatic temperature rise (by step loadings separated by time intervals) or to correct for the effect of the temperature increase.

To compare n values to K_{Ic} values for equal temperatures and strain rates, Krafft assumes

$$\frac{\dot{\epsilon}}{\epsilon_1} = \frac{\dot{K}}{K_{Ic}} = \frac{\dot{\epsilon}}{n}. \tag{65}$$

This amounts to assuming $\epsilon_1 = n$ as the condition for onset of rapid fracture. The justification for this assumption is found in the results. As illustrated in Ref. 25, a comparison on this basis over a wide range of strain rates and temperatures shows that a trend exists for K_{Ic} to vary in proportion to the isothermal n value. Successful trials have been made with a wide variety of steels and several titanium alloys.

One expects fracture toughness to depend in a joint way upon small defects and plastic flow properties. Krafft's approach assumes the influence of the defects, which assist advance separations in the fracture process zone, can be represented by the K_{Ic} n ratio, a factor assumed to be invariant with temperature and strain rate. This invariance and the simple K_{Ic} n proportionality are, no doubt, oversimplifications which will receive some modification after closer study. Nevertheless, the large degree of success and the information resulting from this approach provide essential guidance for basic research and for certain practical applications as well.

When a series of σ_{YS} versus ε_{TS} curves are made for a ferritic steel as a series of decreasing temperatures, these show regular increases of yield strength with lowered temperature, but the absolute slopes of these curves after yield are quite similar (49). The same observation can be made for a series of increasing strain rates when adiabatic temperature rise is avoided. This means that, if the n-value measure of strain hardening is known for one of these curves, approximate n values for the other temperatures and strain rates can be estimated on the basis of an inverse proportionality of n to yield strength. Combining this procedure with the idea of a direct proportionality between K_{Ic} and n, this means that, given knowledge of a $K_{Ic}(T_0)$ measured at the temperature T_0, the value of $K_{Ic}(T)$ for the temperature T can be estimated from the relation

$$K_{Ic}(T) = \frac{\sigma_{YS}(T_0)}{\sigma_{YS}(T)} K_{Ic}(T_0) . \tag{66}$$

The values σ_{YS} are regarded as 0.2% offset uniaxial tensile yield strengths for the strain rates pertaining to the K_{Ic} tests. Use of Eq. (66) over a very wide range of temperatures and strain rates would not serve well, because Krafft's studies show a closer degree of proportionality of K_{Ic} to n than to $(\sigma_{YS})^{-1}$. Trials indicate that Eq. (66) estimates of the increase or decrease of K_{Ic} due to ±60°F temperature do not show appreciable error. When the range is extended to ±120°F, the results tend to be moderately conservative.

Investigations of σ_{YS} for a steel, as a function of temperature and strain rate in the range from very low temperatures to room temperature, can be nearly represented by a single curve in terms of a speed-temperature equivalence. In fact, Bennett and Sinclair (50) show that data for a variety of metals with crystalline similarity can be fitted to this same curve by a uniform shift of each curve parallel to the σ_{YS} coordinate.

In later sections it will be desirable to estimate σ_{YS} for certain rapid strain rates and at various temperatures from the room temperature static value of σ_{YS}. A recent report by Wessel et al. (51) provided measurements of σ_{YS} for two large-thickness plates of A302B steel and a plate of rotor steel across the temperature range from -320°F to room temperature. Using the basic idea in the Bennett-Sinclair paper, a single curve representation of this data was made (52). A convenient equation with a good fit to this curve was given by the expression

$$\sigma_{YS}\Big|_{T,\,t_0} = \sigma_{YS}\Big|_{-100\,^\circ\mathrm{F},\,t_0} + \frac{14{,}500\ \mathrm{ksi}}{T+459} - 40.4\ \mathrm{ksi}. \tag{67}$$

where T is the temperature in degrees Fahrenheit and t_0 is the load rise time for static (slow) testing and is assumed for later purposes to be 50 sec.

To estimate the σ_{YS} for a shorter load rise time t the temperature-rate equivalence idea leads to the relations

$$\sigma_{YS}\Big|_{T,t} \quad \sigma_{YS}\Big|_{T',t_0} , \tag{68}$$

where

$$\frac{T'+459}{T+459} = \frac{\log\,(2.10^{10}t)}{\log\,(2.10^{10}t_0)} . \tag{69}$$

The frequency constant in this equation is adapted from Ref. 50.

Equation (67) was written in terms of matching the σ_{YS} vs temperature curves at -100°F. This is better than matching the curves at 70°F, because it eliminates effects of strain aging. If the reference temperature is changed to 70°F, the negative term at the right of the equation becomes -13 ksi. Primarily, Eqs. (67), (68), and (69) are intended for use in estimating dynamic yield values at various temperatures in a simple way. It is not possible to include effects of strain aging without a large increase of complexity in the equations. Correspondingly, the tendency of Eq. (67) to predict static σ_{YS} values above 0°F, which are somewhat low, was thought not to be harmful.

A recent paper by Shoemaker and Corten (53) suggests that correlation of K_{Ic} values over a range of temperatures and strain rates might be simplified by going directly to a rate-temperature parameter approach as used by Bennett and Sinclair (50) for correlation studies of yield strength. Reference 53 notes that an approximate proportionality of K_{Ic} to n can be implicit in this method and that an n-value-independent relationship of K_{Ic} to σ_{YS} can in this way be included.

The most prominent influence of plastic flow properties upon fracture toughness is the brittle-ductile transition introduced when the crack-tip plastic zone becomes comparable in size to the dimension of the part parallel to the leading edge of the crack. This was discussed previously. Because of material and testing machine limitations, the critical K for onset of rapid fracture, which is measured and reported, often contains some elevation above K_{Ic} due to plane-stress yielding. If these results correspond to $\beta_c^2 < \pi$, approximate values of K_{Ic} can be obtained from Eq. (13) by taking

$$K_c^2 = K_{Ic}^2 \left(1 + 1.4\ \beta_{Ic}^2\right), \tag{70}$$

where

$$\beta_{Ic}^2 = \frac{1}{B}\left(\frac{K_{Ic}}{\sigma_{YS}}\right)^2. \tag{71}$$

The use of Eq. (70) to predict K_c from a given value of K_{Ic} is subject to a larger uncertainty than its use in the opposite way. However, if conditions representable as $\beta_c^2 < \pi$ or $\beta_{Ic}^2 < 1$ are met, the error of a K_c value obtained in this manner should be tolerable in relation to other uncertainties.

A variety of estimation relationships have been reviewed in this section, because their employment has proved to be useful in checking the general consistency and meaning of fracture testing information of many kinds from a variety of sources. Readers should not infer that these relationships are preferable to possession of the accurate test information, the absence of which motivates their use.

Dynamic Fracture Toughness Measurements and Fracture Transition-Temperature Tests

Figure 8 shows results of crack arrest observations by Nordell and Hall (54) for 1-in.- and 3/4-in.-thick plates of A212B steel. At the NDT of this material, 20°F, the plastic-zone size factor $2r_y$ (plane stress) is about 1/3 in., small enough for the shear-lip borders of the fracture to be small but large enough to allow some plane-stress elevation of the K value. The fact that the results show negligible temperature effect below 0°F may not be significant, because only a small range of temperatures was covered. The upward trend of the crack-arrest K values above 20°F is due to the approach to mid-range fracture transition conditions expected at about 85°F.

These results may be compared to an estimate of a rapid load K_{Ic} from the small-flaw drop-weight impact tests used to find the NDT value for the plate material.

The critical section for the fracture produced in nil-ductility transition (NDT) testing is shown in Fig. 9. The bar is broken in drop-weight impact bending with a notched brittle weld on the tensile side to serve as a representative small flaw. In the original concept the NDT separated the temperature region in which a flat break occurred from the higher-temperature region in which noticeable plastic bending accompanied separation. In the course of test development and standardization it was convenient to make use of the rapid increase in tendency for arrest of lateral cracking, with increase of temperature, through the region of the NDT. Thus, stops were used under the bar, which made these arrests positive, and the failure or success of arrest is critical to the test result. However, in the analytical interpretation it is best to return to the original idea.

As the specimen bends, the notched, brittle weld bead produces a small part-through starting crack. If propagation of this crack occurs prior to yielding at the tensile surface, the quick motion of the crack causes separation without noticeable plastic distortion. At temperatures from 10°F to 30°F above NDT tests with the stops removed have shown that plastic bending does occur. At the NDT the stress level for crack propagation is very nearly σ_{Yd}, the dynamic yield stress for the plate material. By making a fixed arbitrary estimate of the size and shape of the small starting crack, use of the equation for a semielliptical surface crack, as indicated on Fig. 9, gives the result

$$K_{Id} = 0.78 \sqrt{\text{in.}}\ \sigma_{Yd} . \tag{72}$$

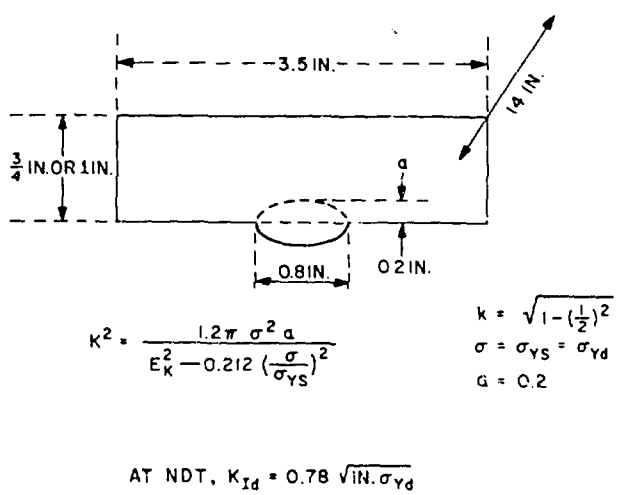

Fig. 9 - Fracture section of NDT test specimen

Examination of typical fractured NDT specimens (by G. Irwin and P. Puzak at NRL) suggested that dimensions, approximately as shown in Fig. 9 could be justified in terms of hesitation lines seen on the fracture surfaces. These dimensions might be adjusted moderately, but the magnitudes given lead to K values which are, so far, consistent with other experimental evidence. The result from Eq. (72) is a K_{Ic} value. However, it might be helpful to have a special designation for the dynamic-crack-arrest or rapid-loading K values, which are considered to represent minimum fracture toughness of the material at the testing temperature. The suggested designation is K_{Id}.

The room temperature σ_{ys} for the material of Fig. 8 was reported as 36 ksi. Assuming a loading time of 0.5 msec for the NDT tests and a loading time of 50 sec for static (slow) measurement of σ_{ys}, use of Eqs. (67), (68), and (69) results in σ_{yd} = 60.4 ksi at the NDT, which was 20°F. Thus, the prediction from Eq. (72) becomes

$$K_{Id} = (0.78)(60.4) \text{ ksi } \sqrt{\text{in.}}$$

$$= 47.1 \text{ ksi } \sqrt{\text{in.}} \tag{73}$$

The values of σ_{fc} for 0.75-in. and 1.0-in. plates were, therefore, 0.81 and 0.61, respectively. Using Eq. (70) to estimate the toughness elevation due to plane stress yielding results in K values of 65 ksi $\sqrt{\text{in.}}$ for 0.75-in. plates and 58 ksi $\sqrt{\text{in.}}$ for 1.0-in. plates. These values agree with the tests results in Fig. 8 somewhat better than might be expected, particularly since neither the Nordell-Hall calculations nor the estimates developed here for comparison have an accuracy likelihood greater than about 10% in the K value.

At the Materials Research Laboratory (Richton Park, Ill.) measurements by Ripling and Crosley are in progress with the objective of K_{Id} determinations using rapid hydraulic loading and a tapered double-cantilever specimen. The procedure employs a rapid-loading surge superimposed on a moderate initial tension on the specimen. Figure 10 shows a set of results which were informally available in October 1966, for specimens of A302B steel. The estimate of K_{Id} from NDT was uncertain, because results of direct NDT testing of the material were not available. From the yield strength and the fact that the material was from a large-thickness plate, an NDT of 20°F was selected for comparison purposes. The estimate of K_{Id} for this choice of NDT is 70 ksi $\sqrt{\text{in.}}$ Assuming inverse proportionality of K_{Ic} to yield strength provided the lower dashed curve of Fig. 10. The measured results lie not far above this curve.

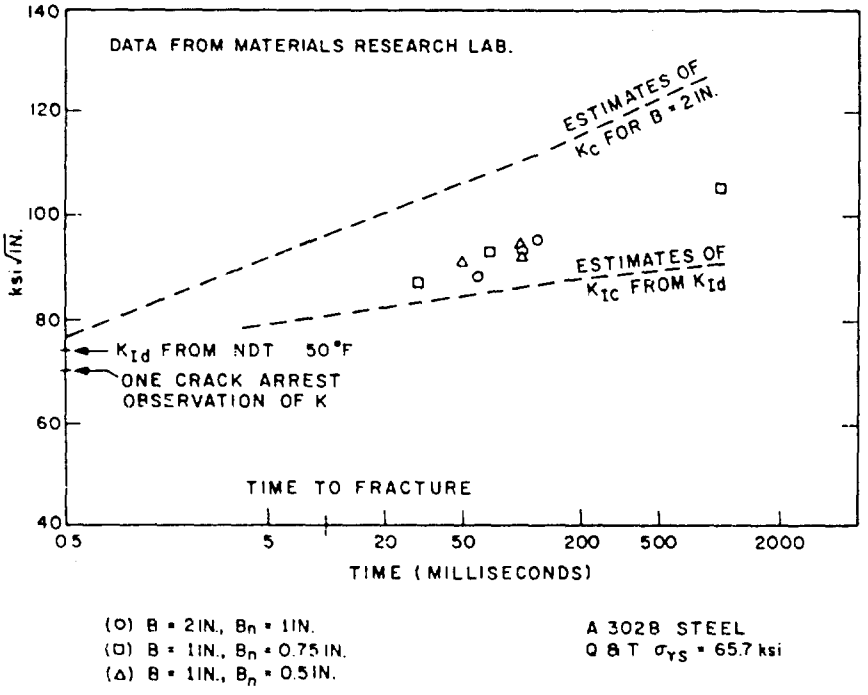

Fig. 10 - Rapid load K_{Ic} values from face-notched double-cantilever specimens (Ripling and Crosley)

To consider whether the specimens were of adequate size, values of $2r_y$ (plane stress) are needed. At 0.5 msec load rise time, the value of K_{Id} is estimated as 85.5 ksi. With K_{Id} estimated as 74 ksi $\sqrt{\text{in.}}$ at 70° F, the value of K_c based upon B = 2 in. for 70°F is 81 ksi $\sqrt{\text{in.}}$ From this, the value of $2r_y$ (plane stress) is 0.29 in. At 50 msec load rise time $2r_y$ (plane stress) has increased to 0.38 in. Assuming the net section thickness should be three times $2r_y$ for adequate constraint, the size of the 2-in.-thick test specimen used in the Ripling-Crosley tests was marginal. However, the specimen size is close to that desired, and the results correspond to expected behavior relative to loading time. Thus, some confidence can be placed in estimating the 70°F value of K_{Id} as about 74 ksi $\sqrt{\text{in.}}$

Several crack arrest events were noted during the tests discussed above. Only for one of these was the load for crack arrest indicated clearly enough to permit a calculation. The result of this single arrest trial provided a K_{Id} value of 70 ksi $\sqrt{\text{in.}}$

Figure 11 shows K_{Id} values estimated for HY-80 steel at the NDT (-150°F), at NDT plus 60°F, and at NDT plus 120°F. Fragments of comparison data were available from Lehigh University (55) and (informally) from Krafft. The experiments at Lehigh University were tests of a wide, 1.75-in.-thick ship-steel plate. The test plate contained a rectangular, welded insert of HY-80 steel in line with the crack starter slot for a trial at crack arrest. At 0°F one trial gave a successful arrest. In a second trial, with the crack much longer at the arrest position, the HY-80 steel separated with a ductile fracture, and no arrest was observed. Rough estimates of the minimum K_c value for crack arrest in the first trial were possible. The conversion to K_{Ic} gave the value 135 ksi $\sqrt{\text{in.}}$ as a minimum estimate, and this is shown in Fig. 11.

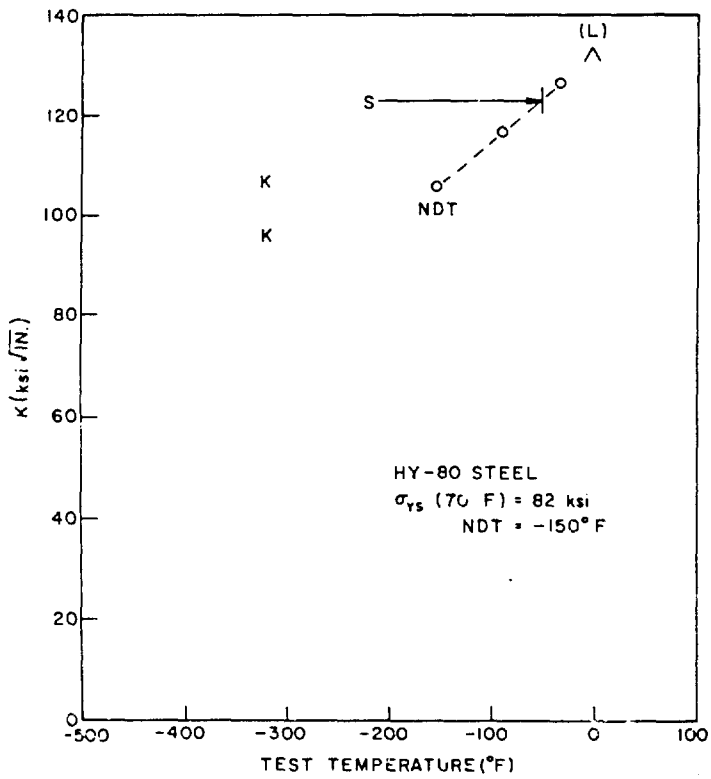

Fig. 11 - Fracture toughness estimates for HY-80 steel

Krafft's measurements of K_{Ic}, indicated by the symbol K in Fig. 11 were with slow-speed loading at -320°F. An n coefficient estimate of the static K_{Ic} at -220°F was available and is shown as the point S in Fig. 11. The short vertical line to the right of S indicates the temperature at which σ_{Yd} for HY-80 would be expected to equal the static σ_{YS} at -220°F. Thus, the estimate of K_{Id} from the point S is in close agreement with the estimates of K_{Id} from the NDT measurement. Results of a direct measurement of NDT for the material used in the Lehigh University tests were not available.

The toughness indicated by the crack-arrest trials discussed above is encouraging. A room-temperature fracture toughness of 140 ksi $\sqrt{\text{in.}}$ may be required for a fracture-safe, 12-in.-wall-thickness, nuclear reactor pressure vessel. This would seem to be obtainable with steels having a toughness quality similar to HY-80.

A variety of crack arrest tests have been employed for crack toughness evaluation led by work of this nature by Robertson at the Admiralty Construction and Repair Establishment. These are well summarized by Tipper (56). Generally, the procedure consists in rapid application of wedge-opening forces to a sharp notch in the specimen. The notch region is chilled to a low enough temperature for brittle fracturing. The balance of the specimen may be held at a fixed gradient of temperature rise. Alternatively, the temperature of test portions of the plate may be placed at a series of uniform temperatures in a sequence of tests. Variations of superimposed tension permit finding a relationship between the machine tensile load and the temperature for successful arrest of the crack. Although, in concept, a fracture mechanics analysis of these tests might be used to determine the K value for crack arrest, the testing plans do not provide for control and measurement of the applied forces to a degree adequate for such calculations. Crude estimates of the wedge-opening forces for certain SOD (Standard Oil Development) tests of 3/4-in. ship-steel plates were made by Wells (57), and values of K (for crack arrest) were found which agree roughly with those of Fig. 8.

By standardization of lateral test dimensions and restriction of testing to a limited range of plate thicknesses, crack arrest tests have served quite usefully for comparative assessments of crack toughness. The recommendations therefrom regarding safe range of operating temperature are generally similar to those from NDT testing.

The test most used for assessment of fracture toughness on a transition-temperature basis is the V-notch Charpy test. So much information has been collected in this form that an attempt at their use for K_{Id} estimates seems desirable even though the foundations for such estimates are far from ideal.

The definition of V-notch Charpy transition temperature which seems best for analysis purposes is the FATT, the temperature at which the side border shear regions occupy half of the fracture surface. Use of a test result corresponding to greater brittleness, say the 12-ft-lb temperature, seems undesirable, because this is known to depend upon notch sharpness and shifts to considerably higher temperatures when a fatigue crack is used at the notch root. The energy level in regions less sensitive to notch sharpness can be used in terms of an analysis suggested by Wells (15). This provides a plausible K_c type estimate but one which is too far from plane-strain to permit use of Eq. (70) to derive a value of K_{Id}. The fracture appearance itself is not truly indicative of relative plastic-zone size, because the run of the crack is too short relative to specimen thickness and does not permit the shear-lip development which would be found in a long crack traversing an equal-thickness plate of the same material.

Two facts which appear useful are as follows.

1. The V-notch Charpy FATT corresponds generally to a 50% shear-fracture appearance for a low-velocity crack in steel plates of 3/4-in. or 1-in. thickness. By assuming $\nu = n$ for each of these two thicknesses, the proportionality of K_{Id} to σ_{Yd} can be estimated using Eq. (70).

2. The V-notch Charpy FATT is often not far from the NDT plus 60°F. From Eqs. (66) and (72),

$$\left(\frac{K_{Id}}{\sigma_{Yd}}\right)_{\text{at FATT}} = 0.78 \text{ in.} \left(\frac{(\sigma_{Yd})_{\text{at NDT}}}{(\sigma_{Yd})_{\text{at FATT}}}\right)^2 . \tag{74}$$

Trials of 1 and 2 above using data typical for A212B, A302B, and HY-80 steels suggested that an approximate estimate of K_{Id} at the FATT is given by

$$K_{Id} = 0.95 \sqrt{\text{in.}}\ \sigma_{Yd} . \tag{75}$$

Except for flaw statistical considerations K_{Id} is a thickness-independent fracture toughness property of the material which, for steels, increases in a regular way with temperature. Transition-temperature results from V-notch Charpy (or NDT) testing can be thought of as assessments of the temperature at which K_{Id}/σ_{Yd} achieves a value within a certain size range. Use of the transition temperature for judging fracture toughness in comparative terms is not, in general, misleading to the metallurgist in his efforts to improve the toughness of the material. Caution is required, however, in applications to design. As the yield strength increases, a design stress which is proportional to the static yield strength becomes a larger fraction of σ_{Yd}. Thus, some flaw tolerance is lost even if the transition temperature remains unchanged. Influences of thickness are discussed later.

Extension of K_{Ic} testing to very large bend tests and to rapid loading has been under discussion and has achieved various degrees of development at a number of laboratories. Progress has been steady but slow, due to the expense of equipment and specimens. A paper giving initial exploratory results was published by Radon and Turner (58). Their work was at Charpy bar size, but it illustrated the successful use of the striking tup as a dynamic weigh bar to furnish load-time records necessary for K-value calculations. Similar work across a range of sizes is in progress at the Naval Research Laboratory.

More study has been given to K_{Ic} testing of very-high-strength steel, aluminum, and titanium alloys than to the rate-sensitive steels of interest for BW and PW nuclear reactor pressure vessels. However, the testing deficiencies are not in the areas of concepts and analysis so much as in matters of equipment and technique. The vessels of interest will be designed sufficiently below the level for general yielding, and the fracture prevention problem will largely concern plane-strain toughness properties and crack situations for which existing methods of fracture mechanics analysis are suitable.

The high values of $(K_{Ic}/\sigma_{YS})^2$ which are of interest indicate that rather large specimen sizes will be required, precracking of the notches will be more difficult, and some testing problems, no doubt, will develop which are not at present foreseen. Within a given size limitation K_{Ic} values can be measured across a range of loading speeds and up to higher temperatures for dynamic loading than for static loading. There are also interpretation difficulties in practical applications. For example, the relative usefulness of static and dynamic fracture toughness is in question with nuclear reactor vessels. However, the entire subject has advanced greatly since the 1955-1960 period. During that period three major fracture problems (deHavilland Comets, heavy-section rotating parts of large steam turbine generators, solid-propellant rocket chambers) assisted fracture mechanics testing developments and at the same time benefited therefrom. Hopefully, the concern over the vessels of interest for this report will contribute and benefit in a similar way relative to rate-sensitive high-toughness metals.

Comments on Crack Opening Dislocation Measurements

In previous comments attention was drawn to the analytical usefulness of the small length factor δ. This is perhaps better called "crack opening dislocation" than "crack opening displacement." The former term has been used at times by Wells and avoids confusion with crack opening measurements at other positions than the actual leading edge of the crack. If a sharp fatigue crack is used at the leading edge of the crack-representing notch in the specimen, some slow crack growth cannot be avoided, even under plane-strain conditions. Thus, it is not clear how a direct measurement would cope with the gauge-positioning problem. In addition, there would be the normal irregularities of the fracture surface.

In trials of direct measurement of δ (59) attention was given primarily to rate-sensitive structural-grade steels, and the leading portion of the notch was a jeweler's hacksaw cut, with no fatigue crack extension. It can be argued that under conditions of moderate ductility the notch sharpness would not cause a significant difference in the fracture load. Static testing was used, and the temperature range covered did not go far below the region of plane-stress to plane-strain fracture transition. At these lower temperatures the δ value, of the order of 10^{-3} in., became comparable to the limits of measurement precision. The strain-rate sensitivity and the notch sharpness tended to suppress slow crack growth, and the hacksaw cut provided smooth surfaces for the gauge. For these reasons, the results of Ref. 58 are of special value from a model-testing viewpoint.

The results verified that the condition for onset of rapid fracturing could be characterized by a critical-opening dislocation value δ_c which was a function of temperature and degree of plane-stress. Aside from considerations of elastic constraint, δ_c did not depend upon the dimensions of the crack and the specimen. Comparison of wide-plate and bend tests permitted examination of the accuracy with which δ_c could be estimated from the plastic bend angles of bars which were too small to prevent general yielding prior to fracture.

The preceding work is summarized in Ref. 15. A more recent review, which also contains additional applications of the δ concept in fracture testing, is provided in a current paper by Wells (60). In this paper Wells derives a method for estimating $\mathcal{G}_c$ from the energy-loss measurement of a Charpy impact test. Of special interest is Wells' comment regarding a relationship of δ to thickness reduction. He reports that Burdekin (BWRA) studied more than 78 measurements of δ in comparison to thickness reduction (just beneath the notch) and found they were equal to within a standard error of 20%.

Assuming δ equal to the thickness reduction, the latter should be about 0.013 in. for a steel with $K = 200$ ksi $\sqrt{\text{in.}}$ and $\sigma_{YS} = 100$ ksi. In the temperature range 200°F to 500°F values for K_{Ic}/σ_{YS} of 2 $\sqrt{\text{in.}}$ or more would be expected for a steel similar in toughness to HY-80. The corresponding thickness reductions would be easily measurable with a precision greater than the fracture-toughness variations inherent in the material. After suitable testing experience methods of correlation should be possible permitting the use of such measurement results to provide approximate values of fracture toughness in terms of K_{Ic} (as well as in terms of δ_c).

Comments on Load Toughening and Strain Aging.

Various testing experiences have indicated that a steel pressure vessel, preloaded to a given pressure at a warm temperature, will not fracture appreciably below that pressure if subsequently tested at a cold temperature (61,62). Trials of this nature, using precracked tensile specimens, by Brothers and Yukawa (63) and by Srawley (NRL), gave a similar indication on an average basis. The scatter of these results might not

encourage absolute confidence in warm preload strengthening relative to low-temperature service. Krafft has noted unexpectedly large values of K_{Ic} in rapid-load K_{Ic} testing for occasional specimens which had been accidentally preloaded at a slow speed, presumably the same effect as the influence of warm preloading.

Since the nuclear reactor vessels of interest will be used at elevated temperature, it would seem that the warm preload would primarily assist a successful proof test. However, if the preload is done at a temperature well above the service temperature, and if the strengthening by crack blunting is verified by a 70°F proof test, confidence in the warm preload strengthening is merited. Furthermore, a substantial advantage relative to fracture safety during service can be obtained. Sonic monitoring during the preloadings might indicate locations of previously unseen flaws. In addition, the cracks should be more visible to ultrasonic inspection after the preloadings than before, and a reinspection at that time would be advantageous.

Room-temperature notched bend test fractures of mild steel (64) were observed to show a segment of sudden brittle fracture if they were precracked and then left unloaded overnight. No such indication of local embrittlement was found when the specimens were broken within an hour or so of the precracking. Observations of this kind are not uncommon, and the embrittlement is considered to be from the influence of strain aging. In the tests discussed in Ref. 64, brittle fracture segments did not appear at lower loads than those used for precracking. However, in fracture trials directed toward K_{Ic} testing, Turner (at Imperial College, University of London) found that a specimen, with a notch which had been compressed at room temperature, broke at -40°F with a K_{Ic} value of about the magnitude observed for crack arrest in similar mild steels. In this case the strain aging occurred after compression normal to the fracture plane, and some residual tensile stress was present.

Tests by Mylonas at Brown University and his "exhaustion of ductility" concept stimulated several British investigations of compressive prestrain damage. Tipper (56) showed that a substantial portion of the compressive-strain embrittlement effect is not due to residual stress by applying 10% compressive plastic strain to a large block of low-carbon structural steel, from which Charpy specimens were later made and tested. When the fracture plane was normal to the direction of compression, the results showed a substantial increase of transition temperature. The original toughness was restored by stress-relief heat treatment. It seems significant that fracture planes parallel to the direction of compression showed only a relatively small increase of transition temperature.

Although steels differ in their strain-aging tendencies, a significant influence on fracture toughness would not be expected for plastic strains less than 3 times the yield strain, regardless of material or fracture-plane orientation. General yielding of this order, say at the throat section of a pressure vessel nozzle, would not be harmful, unless a crack was already present. A substantial amount of strain aging would, then, occur in the local regions close to the leading edge of the crack. During unloading the material closest to the leading edge receives some reverse plastic straining in compression. Thus, a greater damage is expected if the strain aging occurs mainly after rather than before unloading.

A question of interest relating to thick-walled nuclear reactor pressure-vessel safety concerns whether an abnormal fatigue or stress-corrosion crack growth should be expected due to strain-aging embrittlement. Answers to this question should be sought experimentally. The crack growth per cycle observed experimentally could be compared to the size of the crack border strip, in which substantial amounts of reverse plastic straining are predicted by analysis (65).

FRACTURE CONTROL PLANS

Comments on Elimination and Slow Growth of Defects

Among the cracks or sharp reentrant notches present in a large structure, after initial inspections and repairs, a single remaining "worst flaw" would be difficult to select. Granting that all cracks could be clearly "seen," a substantial number might appear comparably dangerous, because of judgment uncertainties which would require disproportionate time and new information for settlement. Real inequalities would undoubtedly exist. However, even if the real inequalities were small, stable crack growth during service would tend to develop large differences in crack size. Due to the high power of K controlling stable crack extension, small differences of size and growth rate are continually amplified so that, eventually, comparatively few cracks emerge as obvious "worst" defects. From service fracture examinations it is clear that there is never more than one winner of this growth race, because the fracture of the structure can always be traced back to a single origin.

Clearly elevation of the initial fracture strength by the location, grinding out, and repairing of cracks has certain practical limits. Removal of the huge cracks found by inspection is obviously necessary and helpful. In the smaller range of crack sizes, questions about the necessity of repair arise which depend upon a number of considerations. At some point the possible damage introduced by the repair practice itself becomes a limiting factor.

The reliability of the structure is greatly improved by improvements in the clarity with which cracks and localizations of impurities are seen by inspection techniques. This reduces the seriousness of the worst remaining overlooked defects and permits sensible decisions regarding repairs. However, even if all cracklike defects were clearly seen, there would be a barrier to improvement of assured strength in terms of judgment uncertainties. In this regard, consideration can be given to methods of using the amplifying effects of slow-stable crack growth to increase the efficiency of the overall inspection process. Inspections during and after proof testing would be of this nature.

If each defect were labeled with some measure S of the limiting strength, which it would impose at the end of N_L hours of service use, the frequency of S would increase regularly with S. Inspection, repair, and trial loadings must give assurance that the value of $S_{min}(N_L)$ for the very worst defect is above the strength S_0 required in service. This means that $S_{min}(N)$ for N at the beginning of operational use must be well above S_0, because the defects tend to move to smaller S values with increasing hours of service.

The level of the $S_{min}(N_L)$ which can be regarded as assured by initial testing and inspection tends to reduce with increase of structural size. In part, this is simply inherent in the probability aspects. In addition, the size and variety of initial defects, prior to inspection, tend to increase with the size and complexity of the structure. Periodic structural inspections, as in the case of commercial aircraft, are very helpful to fracture control. In this practice, one is able to use the amplifying effects of stable crack growth to assist identification of the most serious cracks. The periodic inspection type of control is most reliable when stress corrosion is not of serious importance. After a crack begins to extend with a corrosive type of assistance, the time to the failure point is likely to be less than the period between inspections. Because of uncertainties involved in crack-growth-rate prediction, extension of a fracture control plan to a larger structure is somewhat easier than extension of the plan to a larger value of N_L.

Service fractures due to stress-corrosion crack extension are sometimes observed in which a segment of fatigue cracking from the initial flaw preceded the extension with corrosion assistance. Under steady loads with water or salt water environment, natural cracks produced by fatigue seem to possess a threshold K value below which the corrosive effect does not induce measurable crack extension. Crack extension rates above

this level are rarely studied. Most testing is in terms of total time for the crack to reach propagation size. However, the long times pertain to initial K values which do not exceed the critical K_{ISCC} by an amount which would be significant in reference to large nuclear reactor pressure vessels.

The situation need not be all one of disadvantage regarding water corrosion effects. The tough steel selected for use in very large nuclear reactor pressure vessels should be chosen to have a K_{ISCC} (for water environment) not far below the value of K_{Ic}. In this event, with initial, much lower, K values established by careful quality control, the leading edges of prior cracks might be static long enough for a corrosion-assisted blunting influence to aid continued resistance to crack growth.

Notes prepared for this report by Professor A. A. Wells (Queen's University, Belfast) contained the following comment: "The records of insurance companies in the United Kingdom seem to show that service failures in steam and chemical pressure vessels have mainly occurred as a result of definite accidents or excursions, such as failures of safety valves or of feed water supplies. A relatively thin (1/2 in.) refrigerant vessel dissected after 24 years service, after which the vessel was condemned because cracks had been found (presumably because of improved NDT techniques), showed black oxidation that must have arisen during welding, over the whole of every cracked surface. There was no evidence of crack extension during service. The vessel had not been stress relieved, and it was fractured at the end of its life at a pressure marginally above the hydrostatic test pressure. This single example drawn from the proportionally large population of these vessels may help to explain the dearth of other examples of crack growth during normal boiler service."

The preceding comment was intended to be used only with due caution relative to thick-walled pressure vessels of higher-strength steel in a radiation as well as water environment. No doubt the routine 50% overload customarily used in proof testing British boiler and refrigerant-type pressure vessels does tend to blunt the prior cracks, and the dissected vessel might be a more successful example than others. For nuclear pressure vessels allowance for whatever slow crack growth seems credible must be retained in the fracture control plan. However, the ideas available tend to generate interest in experimental data applicable to the steels to be used in the pressure vessels under consideration. Slow crack growth is of critical importance to fracture safety in this application, and the facts, when known, may show the slow-stable crack growth problem is much smaller than a conservative judgment can accept at the present time.

Fracture Safety in Relation to Crack Arrest

The difficulty of arresting relatively large cracks in thin-walled pressure vessels was recognized and extensively studied in connection with the unfortunate fuselage explosions experienced by de Haviland commercial jet aircraft in 1954 (66). The critical crack size for sheet material similar to the high-strength aluminum-alloy fuselage covering was less than the size of a window opening at the stress level expected for 35,000 ft altitude, even in a flat sheet. Due to inadequate window reinforcements, a small fatigue crack could develop near a corner of a window and, with its effective size enhanced by the poorly stiffened window opening, could attain critical size for propagation before an inspection was likely to reveal its presence. In the investigations following the plane losses a number of such small fatigue cracks were developed at windows during flight simulating tests of additional Comet fuselages, and the bursting of these test fuselages occurred from such cracks in consistency with the above failure sequence.

The emphasis of the Comet-inspired investigations was turned from fatigue toward crack arrest devices by information from U.S. studies of fracture mechanics (67) coupled with the following facts. During the history of passenger aircraft aviation the discovery

of small fatigue cracks during overhaul has never been uncommon. The de Haviland Comet fuselage sheet material was similar in toughness to the USA 7075-T4 aluminum alloy. Previous airplane material experience both in England and in the U.S. was primarily with the much tougher 2024-type aluminum alloy. When the 7075-type material is used in place of the 2024-type material at the same percentage of the yield strength, the combined influence of higher working stress and less toughness is nearly a factor of 10 in terms of critical crack size for crack propagation. The fatigue crack growth rate is increased roughly by a factor of 6 for equal-size cracks. Clearly, the safety of passenger planes prior to 1954 depended more upon overhaul inspections and upon the long service life necessary to grow very large fatigue cracks to critical size, than upon elimination of fatigue cracking.

In the 1953-1957 period (at NRL and NACA) the stresses for propagation of given-size cracks in flat sheets of plastics and high-strength aluminum were compared to the critical hoop membrane stresses in cylindrical sections of these materials containing similar-size axial cracks and subjected to internal pressure. The stress elevating influence of outward bulging of the crack section (due to the internal pressure) was quickly recognized. The effect increased with crack length. By using a lubricated (and strong) cylindrical cover over the cracked portion of the test cylinder, the nominal hoop stress for crack propagation in the cylinder could be made the same as the nominal stress on the flat-plate specimen in tension, for the same size crack. No effort was made at detailed stress-analysis explanations of this special aspect of cracking behavior. However, the magnitude was so large (as much as a factor of 10 in effective critical size) that the outward bulging effect on propagation of long cracks in pressure vessels has been consistently emphasized in NRL technical papers (42,67,68). For the arrest of a long crack in a pressurized container by a riveted stiffener, an arrangement which would provide a local "flat sheet" situation, as well as a stiffener-induced reduction of the stress field, was recommended (67).

A number of U.S. investigations of bursting strength of containers damaged with various-length through-cracks have shown the long-crack bulging influence discussed above. Thus, the results of U.K.-AEA tests, as reported by Nichols (69), were not unexpected. One cannot, of course, accept 6-in.-long to 12-in.-long cracks in a 1-in. wall thickness as modeling 6-in.-long to 12-in.-long cracks in a substantially larger (3 to 12 in.) wall thickness. The increase of effective crack size due to local bulging would be much larger for the 1-in. wall thickness and would be expected to dominate the test results. In addition, the modeling would be poor, because of differences in elastic constraint of the crack.

A fail-safe crack-arresting fuselage design is heavier than one which is not so designed. However, there is some saving in added weight, because the customary design provides strong hoop-direction frames. Thus, when skin attachments to hoop-direction stiffeners are used to arrest longitudinal cracks, the frames, customary to the design, may be satisfactory for this purpose, except for spacing and the positioning of flanges adjacent to the skin.

In modern jet passenger aircraft, through the use of tough (2024-type aluminum) skin material and suitable attachments to frames (or hoop straps), it is possible to arrest cracks with lengths which are several hundred times the thickness of the fuselage wall under service conditions of internal pressure. In case of an accident starting such a crack, the crack would certainly bulge open, and maintenance of a low-altitude pressure in the cabin might be impossible. However, the structure would be safe enough for operation of the airplane to a safe landing. This type of fail-safe crack-arrest design is peculiar to the nature of the aircraft fuselage structure.

A thick-walled steel pressure vessel built for internal liquid pressure containment has no natural reason for hoop direction stiffeners. Furthermore, for the vessels of

interest to this report, through-cracks could not be allowed to reach a length large enough for appreciable outward bulging, because this would permit very rapid escape of liquid and hot vapor. The addition of massive external rings at spacings of about two plate thicknesses would certainly improve the wall strength, particularly if these rings were installed so as to exert external pressure on the cylinder wall. Primarily, the goal of a fail-safe scheme of this kind would be to suppress outward bulging of the cylinder wall along the region of any long through-crack (in a longitudinal seam weld, for example) and to provide enough strength to support the hoop-tension load in the event of such a crack. After some years in service the amount of remaining compression under the rings would be uncertain, and crack arrest under the ring would rest on too small a margin of stress difference to deserve any confidence.

The large-scale fracturing of welded ships was blamed in part upon the continuity introduced by welding which permitted a crack to run directly, without reinitiation at rivet holes, from one large plate into the adjacent plates. Separation of longitudinal rows of deck plates with an overlapping riveted connector has been employed with some success as a crack arresting device. A "tough strip" crack-arresting device for the same purpose has been proposed. In this plan the riveted connector is not used. Instead, the deck plates are joined by welding to a connector of very-high-toughness material, such as HY-80 steel; in either case, successful crack arrest depends upon the stress field force driving the crack, which increases with crack length. Given a large enough stress field force, any crack arrestor will be unsuccessful. The unsuccessful crack-arrest trial with an HY-80 crack arrest strip previously discussed, merely indicated the K_{Ic} for HY-80, at 0°F, was less than 200 ksi $\sqrt{\text{in.}}$

If we regard the pressure vessels of this report as welded regions connected by arresting wall material, the most dangerous regions would be along segments of longitudinal welding and along welds joining the nozzles to the pressure-vessel wall. A conservative crack-arrest plan would be to provide sufficient toughness so that cracks completely through the metal affected by welding would be stable at the expected service stress level. In addition, this crack length would need to be small enough so that the effect of outward bulging near the crack due to internal pressure was small or negligible. Further study of this second requirement is needed. However, we can assume that a crack length as small as twice the plate thickness would be small enough for that purpose. To satisfy the first requirement, the maximum lengths of such cracks must be in correspondence to the equation

$$K_c^2 = \frac{\pi\sigma^2 a}{1 - \frac{1}{2}\left(\frac{\sigma}{\sigma_{YS}}\right)^2} . \tag{76}$$

The crack length is $2a$. Assuming conservative design (stresses well below yield) and K_{Ic} = 170 ksi $\sqrt{\text{in.}}$, a 2-ft-long crack in a 12-in.-thick vessel wall would be stable at stresses below 20 ksi.

Use of ring-rolled cylindrical sections to eliminate longitudinal seam welds was helpful to the fracture strength of steel chambers for solid propellant rockets. Continued consideration of this construction method for application to large BW and PW nuclear reactor pressure vessels seems desirable for purposes of point of view, even if the rings are not solid forgings. The cylindrical portion of the vessel would then consist of rings joined by girth welds, as at the present time. However, the rings, if not solid forgings, would have been plant-welded, inspected, and heat treated to such a high quality level that the welded regions could be regarded as possessing the required crack-arrest toughness.

The Relationship of Fracture Toughness to Pressure-Vessel Design Load in Terms of a Leak-Before-Break Criterion

A criterion sometimes termed "leak-before-break" was proposed in connection with fracture problems of steel solid-propellant rocket chambers for Polaris (69). Methods for K_c-type crack toughness measurement had been accepted, and a statement of how much toughness was "enough" had been demanded by users of the K_c test. The proposal was then made that a crack of twice the wall thickness in length should be stable at a stress equal to the yield strength, or

$$\beta_c = \frac{1}{B}\left(\frac{K_c}{\sigma_{YS}}\right)^2 = 2\pi . \tag{77}$$

On the average, this proposal seemed to correspond to the attainment of full shear fractures. The value 2π in Eq. (77) is obtained by putting $a = B$ and $\sigma = \sigma_{YS}$ in Eq. (76). Using Eqs. (70) and (71), this criterion can also be expressed as $\beta_{Ic} = 1.5$.

Observation of leakage prior to bursting was not actually of importance in the rocket-chamber application. The criterion was simply a reasonable guess which received a large amount of study and trial (42). It was found that, for steels meeting the $\beta_c = 2\pi$ criterion, the design, fabrication, and inspection could generally be done with sufficient care so that the completed chambers would withstand an average hoop stress in the cylindrical section nearly as large as the yield strength of the material, without fracturing (42). Such toughness as could be obtained in the weldments and in the thick-section reinforcements was helpful, but these parts rarely possessed a $\beta_c = 2\pi$ degree of toughness.

For pressure vessels which are tested and used in service at a hoop stress much less than the yield strength of the material, a smaller degree of toughness would be expected to meet with an equivalent degree of success. For such vessels the "leak-before-break" criterion was redefined in relation to K_{Ic} values by Irwin and Sullivan (70) in terms of Eqs. (76), (70), and (71). The requirement $a = B$ was retained, but σ was left undetermined. Thus, the criterion could be met, for any toughness or wall thickness, by a sufficient reduction of σ. From the preceding three equations, one finds

$$\frac{\pi y^2}{1 - \frac{1}{2}y^2} = \beta_{Ic}(1 + 1.4\beta_{Ic}^2) , \tag{78}$$

where $y = \sigma_{YS}$, and, repeating Eq. (71), β_{Ic} is given by

$$\beta_{Ic} = \frac{1}{B}\left(\frac{K_{Ic}}{\sigma_{YS}}\right)^2 . \tag{79}$$

A graph of y as a function of β_{Ic} from Eq. (78) permits determination of a leak-before-break hoop tension stress σ_{LB} from given values of K_{Ic}, σ_{YS}, and B. Throughout the computations, K_{Ic} and σ_{YS} pertain to the applicable temperature and loading speed. The estimates of K_{Ic} from the NDT and FATT kinds of testing are K_{Id} values. These approximate estimates of minimum fracture toughness are appropriate for applications where dynamic conditions can occur either from service loads or weld-zone residual stress effects. Values of σ_{LB} corresponding to these K_{Id} values for three steels are given in Tables 1, 2, and 3. The influence of wall thickness is shown at two temperatures, NDT plus 60°F and NDT plus 120°F. The general trend of the results at each temperature is a decrease of σ_{LB} from the approximate value σ_{YS} (static) by a factor of about 3, as the wall thickness increases from 1 in. to 5 in.

Table 1
HY-80 Steel, σ_{YS} (70°F) = 82 ksi and NDT = -150°F

Estimated Dynamic Values	B (in.)	β_{Ic}	σ/σ_{Yd}	σ_{LB} (ksi)	Static Values
At -90°F	1	0.912	0.693	84	σ_{YS} = 94 ksi
σ_{Yd} = 122 ksi	2.5	0.364	0.358	44	
K_{Id} = 116 ksi $\sqrt{\text{in.}}$	5	0.182	0.243	30	$\sigma_{YS}/3$ = 94/3 = 31 ksi
At -30°F	1	1.25	0.88	99	σ_{YS} = 88 ksi
σ_{Yd} = 113 ksi	2.5	0.50	0.44	50	
K_{Id} = 126 ksi $\sqrt{\text{in.}}$	5	0.25	0.289	33	$\sigma_{YS}/3$ = 88/3 = 29 ksi

Table 2
A302B Steel, σ_{YS} = 62 ksi and NDT = 0°F

Estimated Dynamic Values	B (in.)	β_{Ic}	σ/σ_{Yd}	σ_{LB} (ksi)	Static Values
At 60°F	1.0	0.809	0.630	52	σ_{YS} = 63 ksi
σ_{Yd} = 82.7 ksi	2.5	0.324	0.333	28	
K_{Id} = 74.4 ksi $\sqrt{\text{in.}}$	5.0	0.162	0.229	19	$\sigma_{YS}/3$ = 21 ksi
At 120°F	1.0	1.03	0.761	59	σ_{YS} = 60 ksi
σ_{Yd} = 77.8 ksi	2.5	0.413	0.388	29	
K_{Id} = 79.1 ksi $\sqrt{\text{in.}}$	5.0	0.206	0.260	20	$\sigma_{YS}/3$ = 20 ksi
	8.0	0.129	0.202	16	

Table 3
A212B Steel, σ_{YS} = 36 ksi and NDT = 20°F

Estimated Dynamic Values	B (in.)	β_{Ic}	σ/σ_{Yd}	σ_{LB} (ksi)	Static Values
At 80°F	1.0	0.835	0.647	36	σ_{YS} = 36 ksi
σ_{Yd} = 55.9 ksi	2.5	0.334	0.340	19	
K_{Id} = 51.1 ksi $\sqrt{\text{in.}}$	5.0	0.167	0.232	13	$\sigma_{YS}/3$ = 12 ksi
At 140°F	1.0	1.29	1.10	(55)	σ_{YS} = 33 ksi
σ_{Yd} = 50.1 ksi	2.5	0.518	0.451	23	
K_{Id} = 57.0 ksi $\sqrt{\text{in.}}$	5.0	0.259	0.293	15	$\sigma_{YS}/3$ = 11 ksi

When a fracture-safe operating range is defined in terms of NDT plus 60°F or FATT, such a criterion should be regarded as a general-experience-based rule. It tends to be conservative for wall thicknesses less than 1.5 in., but this conservatism would often be needed. With an increase of wall thickness, the design would be more cautious. Stress relief of 5-in.-wall vessels would be expected. Estimates of allowable stress for dynamic crack instability conditions, as shown in the tables, can be formally developed from the fracture-mechanics-based equations, without regard for experience. However, consideration of factors specific to the individual application is necessary in their use.

The leak-before-break criterion, in $\beta_c = 2\pi$ form, did not appear to be conservative in its application to ultrahigh-strength steel rocket chambers, despite the fact that $\beta_c = 2\pi$ corresponds to a large degree of plane-stress toughening. Very careful design, fabrication, and inspection were required even when the toughness criterion was satisfied. In that application the problem of controlling slow crack extension due to stress corrosion during hydrotesting was seriously underestimated. Very few fractures occurred below design stress in firing trials. Elimination of crack growth due to stress corrosion during hydrotesting would have been most helpful.

The β_{Ic} values in the tables are well below the value necessary for tough plane-stress fracturing. Certainly, for vessels with walls more than 2.5 in. thick, fracture safety in the past has depended much more upon conservative design stress than upon the toughening influence of a brittle-ductile fracture transition.

With reference to thick-walled nuclear reactor pressure vessels, the influence of temperature elevation in terms of the degree of plane-stress toughening is gradual and not very large. No support can be found on that basis for a step-function-type diagram of limiting allowable load, based upon a critical temperature. The allowable-load diagram suggested by this study would be one of gradual increase with temperature to the point where decrease of yield stress with temperature was a limiting consideration. The computation might be made using Eq. (78). However, a simpler plan can be suggested as follows. Available K_{Ic} data for steels over a wide temperature range can be fitted, to a fair approximation, assuming a simple direct proportionality between K_{Ic} and the absolute temperature. Thus, if a decision has been reached on the temperature T_1 at which operational pressure is allowable, a straight line on a load-temperature graph from that point to zero load, at absolute zero temperature, would provide a safe, allowable load diagram for temperatures below T_1. Practices currently used would be applicable at temperatures above T_1.

A fracture of a glass rod or plate normally occurs from a small surface flaw, and a half-circle mirror region can be seen at the fracture origin. This outlines the shape of the crack front when the crack speed reached the limiting velocity, and efforts at crack division began to roughen the fracture surface. Similar half-circle crack-front shapes have been observed in other brittle solids, even when the crack depth is large and the stress on the section reflects some bending.

With regard to the leakage aspect of the leak-before-break analysis, a half-circle would be the expected shape for a crack deepening from one surface into the wall of a nuclear reactor pressure vessel in all regions where the stress is well below the static yield strength. As the surface length approaches $2B$, the stress elevation in the net section beneath the crack would tend to cause relatively fast severing of that part. Thus, the average length of the crack parallel to the wall after breakthrough and start-of-leakage should not exceed $2B$.

In the nozzle throat section the stress favors development of a longitudinal crack in a plane containing the axis of the nozzle, starting at an inside corner. The crack front would have an approximate quarter-circle shape. It seems likely that a leak-before-break design stress would permit arrest with completion of a through-crack on one side

but not if cracks formed simultaneously on both sides of a nozzle. This question could be answered with trials of small-scale models using actual nozzle-throat-section configurations.

The toughness required by Eq. (78) for a 12-in.-wall-thickness pressure vessel can be estimated along the following lines. Assume the steel is such that σ_{ys} (static) is 100 ksi at 70°F, and that an allowable load equal to the operating pressure is wanted at 200°F. Using estimation rules previously discussed, σ_{yd} at 200°F is 110.5 ksi. If we select 31 ksi as representing a design stress (interpreted here as equivalent to the average hoop tension stress σ), the value of y at 200°F is 0.281. From Eq. (78) this corresponds to c_{fc} = 0.240. The required K_{fd} at 200°F is then given by

$$K_{fd} = 110.5 \text{ ksi } \sqrt{0.240 \times 12 \text{ in.}}$$

$$= 187 \text{ ksi } \sqrt{\text{in.}} \tag{80}$$

A value of K_f at 200°F no less than 187 ksi $\sqrt{\text{in.}}$ would be expected for a steel with a toughness similar to that of HY-80. Granting that problems related to heat treatment and welding would be restrictive, a suitable steel with sufficient toughness for the leak-before-break criterion is a reasonable hope, particularly if the yield stress and design stress can be lowered somewhat from the estimates assumed above.

Comments on the NRL Fracture Analysis Diagram

Numerous tests of the transition-temperature kind have received use as providing fracture-toughness information. The moderate differences in the order in which these tests rate the toughness of various steels is not of vital importance in use, because the overall fracture control plan depends upon design, fabrication procedures, and inspection as well as upon the toughness rating of the steel. For any selected method of fracture testing, experience with a given class of structures over a period of time indicates the adjustments which are appropriate and necessary relative to the customarily used toughness evaluations.

In view of the employment complexities of a transition-temperature toughness rating and with the aid of a collection of fracture failure data, Pellini and his associates assembled guidelines for use in terms of their NDT type of fracture testing. The resulting NRL fracture analysis diagram (68,71) was intended to provide guidance for fracture-safe design, as nearly as possible, without reference to loading speed, elastic constraint, and crack location and with only gross estimates of stress level. Uses of the fracture analysis diagram were illustrated. Cautions were provided for increase of plate thickness, low-shear tear strength, quality level of inspection, and opportunities for growth of large flaws under service operating conditions (72).

Approximate methods, applicable to low- and medium-strength steels, can be followed to translate conditions such as NDT plus 60°F and NDT plus 120°F into the design stress level which would satisfy the leak-before-break criterion under dynamic loading, as previously discussed. The results vary with NDT and yield-stress level. On the average, for 3/4-in. and 1-in. thicknesses, the stress thus estimated reaches the static tensile yield strength between NDT plus 60°F and NDT = 120°F, a result which is in fair correspondence to the fracture analysis diagram.

The large flaw sizes suggested for various fractions of the yield strength cannot be taken literally, and few would do so. Otherwise, the practice appears conservative in reference to low-strength steels of about 1-in. section thickness. The practice tends to become marginal for steels of that thickness with σ_{ys} above 100 ksi, and for low-strength steels with section thicknesses greater than 2 in. However, most large welded structures

are designed for stresses well below the yield stress, and, often, the service loads are essentially static. Hence, a large degree of success from using the fracture analysis diagram would be expected and has been experienced.

Relative to the thick-walled pressure vessels of interest in the report, a major handicap in using the method, is that the NDT measurement points for the tough steels of principal interest lie too far below the range of temperatures for service operations. A similar handicap would pertain to all of the presently customary methods of toughness evaluation in terms of a transition temperature.

There is also a scarcity of K_{Ic} data for high-toughness steels, except at low temperatures. Although higher-temperature, large-specimen data of the K_{Ic} type should be available soon, fracture toughness information from direct measurement for high-toughness steels, at temperatures above 200°F, will probably require completion of suitable testing plans based upon one of the plasticity analysis viewpoints previously discussed.

Proof Test Estimates of Critical Crack Size in Relation to Fracture Safe Life

The first interesting question concerns what can be deduced from the fact that a proof test with internal pressure is successfully completed. Estimates will be made here on the basis of a semielliptical surface crack with a depth one-quarter of the surface length of the crack. The equation for K in relation to depth a, tension σ, and tensile yield strength σ_{YS} is

$$K^2 = \frac{3.77\,\sigma^2 a}{1.49 - 0.212\,(\sigma/\sigma_{YS})^2} . \tag{81}$$

Assuming A302B steel, σ_{YS} (static, 70°F) = 60 ksi, and NDT = 10°F, the estimates of σ_{Yd} and K_{Id} at 70°F are 79.8 ksi and 71.5 ksi $\sqrt{\text{in.}}$ Suppose the design stress is 24 ksi and the proof test produces an average hoop tension in the wall of the cylinder portion of 1.25×24 ksi = 30 ksi. Using these data in Eq. (81) a crack size given by a = 2.2 in. would have become unstable at a stress level of 30 ksi. This calculation is on a dynamic basis. On a static basis we assume

$$K_{Ic}\ (\text{static}) = \frac{79.8}{60} \times 71.5\ \text{ksi}\sqrt{\text{in.}}$$

$$= 95\ \text{ksi}\sqrt{\text{in.}}$$

The new estimate of the crack size, shown to be absent by proof testing inspection, is given by a = 5.2 in. Cracks of about 40% greater depth and smaller surface length would be estimated using a semicircle crack shape. Larger cracks could be present if there had been a crack-blunting treatment by warm prestressing. The amount of that size increase would be uncertain and would depend upon the degree of confidence in crack-blunting effect of the warm prestressing.

With regard to regions of the nozzle where the stress is locally elevated, it will be assumed that an additional plastic strain equal to the yield strain occurs across the region containing the crack. When the stress level in this region first achieves 60 ksi tension across the crack, the dynamic basis estimate of the critical size is obtained from

$$(71.5)^2 = \frac{3.77\ (60)^2\, a}{1.49 - 0.212\ (60/80)^2}\ , \tag{82}$$

or

$$a = 0.52 \text{ in.}$$

It would, of course, be inconsistent to assume that continued straining occurs if such a crack is present and is resisted only by the dynamic fracture toughness. On the other hand, to assume a smaller crack and add the influence of plastic strain to the opening dislocation δ amounts to crack blunting, and an onset of fast fracture instability cannot be certainly predicted. An increment of stable extension comparable to δ is more likely.

The critical crack size estimates for base metal cylindrical portions of the vessel were unreasonably large and can be viewed as incredible. However, if the local of these calculations are shifted to a longitudinal weld and if the fracture toughness is assumed, in K-value terms, to be less by 30%, the critical crack sizes are then reduced by a factor of 2. The dynamic calculation estimate then becomes 1.1 in., which is small enough for a significant probability of existence. Furthermore, a weld which joins a nozzle to a shell is subject to some superimposed bending stress to a degree dependent upon the efficiency of the design. Increasing the tensile stress 30% would also halve the sizes of the cracks judged to be critical.

The preceding calculations are, of course, no more than illustrative. For good fracture control each vessel should be studied in terms of the stress analysis, fabrication, and property data applicable to that vessel.

We consider next the critical crack sizes which would be required for failure under operating conditions. For simplicity we assume that the operating pressure is applied at 70°F. We also assume the hoop tension developed is 0.8×24 ksi = 19.2 ksi. To keep the crack sizes within reason we use the reduction by a factor of 2, suggested above. We then find the critical crack size (dynamic) has increased from 1.1 in. to 2.7 in.; and the critical crack size (static) has increased from 2.6 in. to 4.7 in.

Using these sizes, calculations based upon the maximum fatigue crack growth rates, as discussed earlier, indicate that 10^5 or more cycles are needed for fatigue to increase crack growth to unstable size. If an allowance of an additional factor of 2 for 30% increase of stress is made, the critical crack sizes are reduced and the growth rate is greatly increased. However, the required number of cycles is still above 10^4.

In the nozzle regions where plastic straining occurred during proof test and where the stress may be about 60 ksi under operating conditions, an estimate of the above kind is not possible. A reasonable guess at crack growth rate could be made. However, there is no clear way to fix the initial maximum crack size so that the number of growth increments can be estimated. It is quite possible that residual compressive stress from the proof test may provide adequate protection of such regions of highest strain.

The possibility for crack growth to critical size by stress corrosion, in any region of the vessel, must be considered on a different basis. It is, in fact, not possible to guarantee safety relative to moisture-assisted slow growth of the maximum-size surface cracks, unless the material and the cracks are such that a "below K_{ISCC}" situation is always maintained.

Present information gives no positive indication that water plus steady tension causes slow crack growth in A302B vessels, except for conditions of fatigue. The water influence was already represented for fatigue by using the highest growth rate constant C_1 from a previous section of this report. Additional investigations of A302B and of candidate steels for future vessels are necessary relative to water-environment stress-corrosion crack growth. Evidence exists that K_{ISCC} can be increased by crack blunting.

In the present application a substantial degree of crack blunting exists, possibly enough so that this type of stable crack growth need not be a matter of concern.

In the case of the A302B steel vessel discussed in the preceding illustration, the wall thickness was not specified. If the vessel is required to satisfy leak-before-break conditions in the terms of this section, then the value of $y = \sigma_{LB}/\sigma_{Yd}$ is given by

$$y = \frac{24}{79.8} = 0.308 . \tag{83}$$

The corresponding value of β_{Ic} from Eq. (78) is 0.281. Thus,

$$\beta_{Ic} = 0.281 = \frac{1}{B}\left(\frac{71.5}{79.8}\right)^2 \tag{84}$$

and B = 2.76 in.

The small value of B is in part due to stress level and, in part, due to the use of K_{Id} rather than a static K_{Ic}. If the stress level is reduced from 24 ksi (design) to 19.2 ksi (operating), B becomes 4.46 in. The thicknesses corresponding to these two stress levels, if the static K_{Ic} is assumed, are 8.14 in. and 13.9 in. Using the dynamic toughness estimate K_{Id} the 19.2-ksi wall stress would be below the calculated σ_{LB} for an 8-in. wall thickness of the assumed material, at temperatures above some temperature in the neighborhood of 260°F. The nuclear reactor termed Palisades is an example in which the operating pressure is too high for the leak-before-break criterion only in the low-temperature range.

This duscussion cannot propose to settle such questions as whether the leak-before-break criterion should be used or, if so, whether on a dynamic or on a static basis. The primary purpose is to illustrate ways in which such questions can be discussed using macroscopic fracture analysis methods.

Radiation Effects Relative to Fracture Properties and σ_{LB}

Curves of true-stress against true-strain for HY-80 steel, after various neutron exposures, were shown by Chow and McRickard (73). These curves shift upward with an increase of irradiation in much the same fashion as they would do with a decrease in temperature or an increase in strain rate. In the case of similar curves for A302B steel (74) the radiation hardening is accompanied by a decreasing trend in the slopes of the curves. Bearing in mind an approximate proportionality of K_{Ic} to the strain-hardening exponent n these results suggest that a greater influence of irradiation embrittlement would occur for A302B than for HY-80 under the conditions of irradiation which were employed. The above authors estimated the irradiation temperature at 30°C. Measurements of the increase of NDT by Steele and Hawthorne (75) for irradiation temperatures below 450°F provide results in the direction indicated by the strain-hardening behavior.

Previously, attention was directed to the fact that very small defects of the type which interfere with easy glide of dislocations, and thus have major importance to plastic flow properties, tend to influence fracture primarily in an indirect manner through their effect on the plastic flow properties. The defects introduced by radiation are quite small, and it is probable that most of their influences upon fracture toughness can be understood in terms of modification of plastic flow properties. An exception would need to be made for grain boundary weakening due to He (76).

For irradiation below 5×10^{19} n/cm^2 (<1 MeV), assumed here to be the region of major interest for the walls of large BW and PW nuclear reactor pressure vessels, the

stress-strain curves of irradiated steels seem to possess a normal appearance, indicating that K_{Id} estimates along the lines used previously can be employed after irradiation to the same degree as before.

The aspect of major interest is the tendency of an increase of σ_{YS} to accompany an increase of NDT and is best understood in terms of an illustration. As before, the steel is A302. The data were collected by Steele, Hawthorne, and associates (75,77) using material from a 6-in.-thick plate using neutron exposures at temperatures below 250°F. A graph was made of NDT as a function of σ_{YS} (static, 0.2% offset, 70°F) from measurement results obtained after irradiation. The increase of σ_{YS} per 100°F elevation of the NDT was 12 ksi up to 1×10^{19} n/cm^2 (<1 MeV) irradiation, where the NDT had become 230°F. The overall slope corresponded to 15 ksi per 100°F change of the NDT across the range up to 8×10^{19} n/cm^2 irradiation.

The undamaged properties were NDT = 10°F and σ_{YS} (static, 70°F) = 67 ksi. Estimates of the dynamic yield elevation to obtain σ_{Yd} and estimates of K_{Id} as 0.78 $\sqrt{\text{in.}}$ σ_{Yd} gave the results shown in Table 4. The values in parentheses were formally obtainable from the estimation procedure, but the irradiation dosage might be high enough to require a different analysis treatment.

Two methods of estimating the fracture toughness radiation damage for NDT = 230°F are (a) estimating K_{Id} at 10°F for the undamaged material used to estimate K_{Id} at 230°F undamaged using the idea of a direct proportionality between K_{Id} and the absolute temperature and (b) estimating K_{Id} (undamaged) at 230°F on the basis of inverse proportionality to dynamic yield strength. Method (b) would underestimate the damage effect, because the temperature range is too large for this method. Method (a) gave K_{Id} (undamaged, 230°F) = 136 ksi $\sqrt{\text{in.}}$ Thus, the damage influence was a K-value loss of 47%. Method (b) indicated a smaller amount, 30%. Thus, a substantial damage to fracture toughness occurred. It is notable, however, that the elevation of NDT by irradiation is accompanied by an increase of K_{Id} at the NDT.

This aspect was explored additionally by estimating σ_{LB} at NDT plus 60°F. Values of σ_{Yd} and K_{Id} were calculated for each of the three NDT-plus-60°F temperature points. The results are shown in Table 5. Apparently, the increase of σ_{Yd} which accompanies increase of NDT is high enough to enable a nuclear reactor pressure vessel, which did not initially meet a leak-before-break operating pressure criterion at NDT (or NDT plus 60°F), to reach such a condition after substantial radiation damage.

Table 4
A302B Steel, B = 6-in. Wall Thickness, σ_{YS} Static, 70°F = 67 ksi

NDT (°F)	σ_{YS} (ksi)	σ_{Yd} (ksi)	K_{Id} (ksi $\sqrt{\text{in.}}$)
10	67	92.5	72.1
230	100	108.7	84.8
425	134	(134.7)	(105)

Table 5
A302B Steel, B = 6-in. Wall Thickness, σ_{YS} Static, 70°F = 67 ksi

NDT Plus 60°F (°F)	σ_{Ya} (ksi)	K_{Id} (ksi $\sqrt{\text{in.}}$)	σ_{LB} (ksi)
70	86.8	76.0	19.6
290	105.9	87.1	20.0
48.5	(133.7)	(106)	(24.4)

The estimates of σ_{LB} based upon dynamic fracture toughness are normally more conservative than those based upon static fracture toughness. The tensile stress-strain curves for A302B steel after various amounts of irradiation, given in Ref. 77, have an increasing abnormality toward "negative strain hardening" in the dosage range above 0.8×10^{19} n/cm^2. This suggests that the static K_{Ic} would be seriously lowered by the

increased tendency toward plastic instability. The "unhardening" behavior is expected to be time-dependent and may not occur fast enough to have an equally strong influence upon NDT and V-notch Charpy tests.

Static K_{Ic} measurements were made at Bettis Atomic Power Laboratory, using A302B steel and various amounts of irradiation at levels above 10^{19} n/cm^2. These were informally discussed with the author. Estimating back from K_{Id} values based upon NDT after elevation to 230°F and to 425°F, the room-temperature K_{Id} should be about 60 ksi $\sqrt{\text{in.}}$ However, the static measurements are much less than this at room temperature. In the approach of test temperature toward NDT, the static measurements tend to increase rapidly. The size of the test specimen did not permit great confidence in these higher values. A portion of this increase might be from plane-stress yielding. However, the fracture-toughness value approached at NDT would not have exceeded the K_{Id} estimate at NDT in any case.

Granting that more experience may be necessary with K_{Ic} measurements of radiation-damaged steels, it seems probably that, beyond some dosage limit, a conservative calculation of fracture strength may depend more upon the static K_{Ic} value than upon the dynamic value. This aspect has only recently appeared and requires careful investigation.

REFERENCES

1. Rankin, A.W., and Moriarty, C.D., "Acceptance Guides for Ultrasonic Inspection of Large Rotor Forgings," ASME paper 55-A-194

2. DeForest, D.R., Schabtach, C., Grobel, L.P., and Seguin, B.R., "Investigation of the Generator Rotor Burst at the Pittsburgh Station of Pacific Gas and Electric Co.," ASME paper 57-PWR-12

3. Irwin, G.R., "Notes for March 24, 1959, meeting of ASTM Committee in New York," (ORNL Library and NRL Mechanics Div. have copies)

4. Irwin, G.R., "The Leading Edges of Fracture Mechanics," ASME Thurston Lecture 1966, ASME Trans (forthcoming)

5. Wells, A.A., "The Mechanics of Notch Brittle Fracture," British Welding Res. Vol. 7 (Apr. 1953)

6. Wells, A.A., and Post, D., "The Dynamic Stress Distribution Surrounding a Running Crack," Trans. SESA 16(No. 1):93 (1958) (Discussion by G. R. Irwin)

7. Irwin, G.R., "Fracture Dynamics," in "Fracturing of Metals" (ASM Symposium 1947) ASM Cleveland (1948), pp. 147-166

8. Orowan, E., "Fundamentals of Brittle Behavior of Metals," Symposium on Fatigue and Fracture of Metals, New York:Wiley, p. 139, 1952

9. Clark, A.B.J., and Irwin, G.R., "Crack Propagation Behavior," Exp. Mech. (June 1966)

10. "Fracture Toughness Testing and Its Applications," ASTM Spec. Tech. Publ. 381 (1965)

    a. McClintock, F.A., and Irwin, G.R., "Plasticity Aspects of Fracture Mechanics," pp. 84-113

10. b. Paris, P.C., and Sih, G.C., "Stress Analysis of Cracks," pp. 30-83

c. Tiffany, C.F., and Masters, J.N., "Applied Fracture Mechanics," pp. 249-277

d. Srawley, J.E., and Brown, W.F., Jr., "Fracture Toughness Testing Methods," pp. 133-198

e. Kies, J.A., Smith, H.L., Romine, H.E., and Bernstein, H., "Fracture Testing of Weldments," pp. 328-356

11. Irwin, G.R., "Crack Extension Force for a Part-through Crack in a Plate," Trans. ASME 29E:651 (1962)

12. Irwin, G.R., "Plastic Zone Near a Crack and Fracture Toughness." 7th Sagamore Ordnance Materials Res. Conf., Aug. 1960, Proc. publ. by Syracuse Univ., 1961

13. Irwin, G.R., "Fracture Mode Transition for a Crack Traversing a Plate," Trans. ASME 82(No. 2):417-425 (1960)

14. Clark, W.G., Westinghouse Research Lab. report, forthcoming. (Results reported at ASTM E-24, Sub. I, Mtg. June 1966)

15. Wells, A.A., "Notched Bar Tests, Fracture Mechanics and the Brittle Strengths of Welded Structures," IIW Houdremont Lecture, British Welding J. 12:2 (Jan. 1965)

16. Barenblatt, G.I., Advan. Appl. Mech. 7:55 (1962). (There were previous papers by Barenblatt in Russian Journals.)

17. Dugdale, D.S., J. Mech. Phys. Solids 8:100 (1960)

18. Bilby, B.A., Cottrell, A.H., and Swinden, K.H., Proc. Roy. Soc. A 272:304 (1963)

19. Irwin, G.R., "Fracture Mechanics Applied to Adhesive Systems," in "Treatise on Adhesion and Adhesives," R. Patrick, editor 1:254 Dekker (1967)

20. McClintock, F.A., and Hult, J.A.H., Proc. 9th Int. Congress on Appl. Mech. (Brussels, 1956) Vol. 8, p. 51

21. Walsh, J.B., and Mackenzie, A.C., J. Mech. Phys. Solids 7:247 (1959)

22. Koskinen, M.F., Trans. ASME 85D:585 (1963)

23. Rice, J.R., "The Mechanics of Crack Tip Deformation and Extension by Fatigue," Brown U., Div. of Eng. Report, May 1966

24. Rice, J.R., "Stresses Due to a Sharp Notch in a Work Hardening Elastic-Plastic Material Loaded by Longitudinal Shear," Brown U., Div. of Eng. Report, Dec. 1965

25. Krafft, J.M., Appl. Mater. Res. 3:88 (Apr. 1964)

26. Williams, J.G., and Turner, C.E., "The Plastic Instability Viewpoint of Crack Propagation," Appl. Mat. Res. 3:144 (1964)

27. Krafft, J.M., "Role of Local Dissolution in Corrosion-Assisted Cracking of Titanium Alloys," Report NRL Progress, Mar. 1967, p.8

28. Johnson, H.H., and Willner, A.M., "Moisture and Stable Crack Growth in a High Strength Steel," Appl. Mater. Res. 4(No. 1):34 (Jan. 1965)

29. Paris, P.C., "The Fracture Mechanics Approach to Fatigue," in "Fatigue - An Interdisciplinary Approach," Syracuse University Press, p. 107, 1965

30. Donaldson, D.R., and Anderson, W.E., "Crack Propagation Behavior of Some Airframe Materials," Proceedings of the Crack Propagation Symposium, Cranfield, England, Sept. 1961

31. Paris, P., and Erdogan, F., "A Critical Analysis of Crack Propagation Laws," Transactions of A.S.M.E., J. Basic Eng., Series D, 85(No. 4) (Dec. 1963)

32. Brothers, A.J., and Yukawa, S., "Fatigue Crack Propagation in Low-Alloy Heat-Treated Steels," Transactions of ASME, in J. Basic Eng., Paper No. 66-MET-2 (to be published, 1966)

33. Carman, C., and Katlin, J., "Low Cycle Fatigue Characteristics of High Strength Steels," Transactions of A.S.M.E., J. Basic Eng., Paper No. 66-MET-3 (to be published, 1966)

34. Clark, W., and Wessel, E., private communication of data on A302B steel (Westinghouse Research Laboratories)

35. Piper, D., Smith, S., and Carter, R., "Corrosion Fatigue and Stress Corrosion Cracking in Aqueous Environment," A.S.M. National Metal Congress, Oct. 31, 1966

36. Crooker, T., Morey, R., and Lange, E., "Low Cycle Fatigue Crack Propagation in Quenched and Tempered Steels Under Corrosive Environments," NRL Report 6196, Sept. 1964 (See also subsequent-quarterly reports of Metallurgy Division of NRL)

37. Crooker, T., and Lange, E., private communication of data on A302B steel (NRL)

38. Wei, R.P., Talda, P.M., and Li, C.Y., "Fatigue Crack Propagation in Some Ultra-High-Strength Steels," Proceedings of the ASTM Fatigue Crack Propagation Symposium, 1966 (forthcoming)

39. Brown, B.F., "A New Stress-Corrosion Cracking Test Procedure for High-Strength Alloys," Mater. Res. Std. (ASTM), 1965 (See also subsequent NRL Reports by Brown, et al.)

40. Rolfe, S.T., Novak, S.R., and Gross, J.H., "Stress-Corrosion Testing of Ultraservice Steels Using Fatigue Cracked Specimens," presented at the Symposium on Stress Corrosion Testing, ASTM, in Atlantic City, New Jersey, June 27-28, 1966

41. "Fracture Testing of High-Strength Sheet Materials; a Report of a Special ASTM Committee," ASTM Bulletin (No. 243):29 (1960)

42. Irwin, G.R., "Structural Aspects of Brittle Fracture," Appl. Mater. Res. 3:65 (Apr. 1964)

43. Sternberg, E., and Sadowsky, M.A., "Three-Dimensional Solution for the Stress Concentration Around a Circular Hole in a Plate of Arbitrary Thickness," J. Appl. Mech. 16:27 (1949)

44. Wundt, B., informal communication

45. Harris, D.O., and Dunegan, H.L., "Fracture Toughness of Beryllium," Trans. ASTM (forthcoming)

46. Ripling, E.J., Mostovoy, S., and Patrick, R.L., "Measuring Fracture Toughness of Adhesive Joints," Mater. Res. Std. 4:129 (Mar. 1964)

47. Mostovoy, S., and Ripling, E.J., J. Appl. Polymer Sci. 10:1370 (1966)

48. Yoffe, E.H., "The Moving Griffith Crack," Phil. Mag. 42:739 (1951)

49. Smith, R.L., Moore, G.A., and Brick, R.M., "Mechanical Properties of Metals at Low Temperature," Proceedings of the NBS Semicentennial Symposium, 1951. Washington:Govt. Print. Off., 1952

50. Bennett, P.E., and Sinclair, G.M., "Parameter Representation of Low Temperature Yield Behavior of Body Centered Cubic Transition Metals," ASTM paper 65-MET-11, 1965

51. Wessel, E.T., Clark, W.G., and Wilson, W.K., "Engineering Methods for the Design and Selection of Materials Against Fracture," Westinghouse Res. Lab. Rpt. to Army Tank-Automotive Center, June 24, 1966

52. Irwin, G.R., "The Leading Edges of Fracture Mechanics," ASME 1966 Thurston Lecture, Trans. ASME (forthcoming)

53. Corten, H.T., and Shoemaker, A.K., "Fracture Toughness of Structural Steels as a Function of the Rate Parameter, $T \log (A/\dot{\epsilon})$," ASME paper 66-WA/MET-8 (1966)

54. Nordell, W.J., and Hall, W.J., "Two Stage Fracturing of Welded Mild Steel Plates," Univ. of Ill. Report, Curl Eng. Dept., Oct. 1963

55. Gerridge, D.W., and Slutter, R.G., "The Brittle Behavior of High Strength Steel Weldments," Lehigh Univ., Fritz. Eng. Lab. Rpt. 200.61.364.8, Apr. 1965

56. Tipper, C.F., "The Brittle Fracture Story," Cambridge, England:Cambridge University Press, 1962

57. Wells, A.A., "Strain Energy Release Rates for Fractures Caused by Wedge Action," NRL Report 4705, Mar. 1956

58. Radon, J.C., and Turner, C.E., "Note on the Relevance of Linear Fracture Mechanics to Mild Steel," J. Iron Steel Inst. 204:842 (1966)

59. Burdekin, F.M., and Stone, D.E.W., J. Strain Anal. 1:145 (1966)

60. Wells, A.A., "Fracture Control of Thick Steels for Pressure Vessels," IIW Meeting, Dusseldorf, Apr. 1967

61. Wells, A.A., "Welded Ferritic Steel Construction for Intermediate Low-Temperature Service," ASTM STP-302, p. 21, 1962

62. Irvine, W.H., Quirk, A., and Bevitt, E., "Fast Fracture of Pressure Vessels," J. Brit. Nucl. Energy Soc. 3:31 (Jan. 1964)

63. Brothers, A.J., and Yukawa, S., "The Effect of Warm Prestressing on Notch Fracture Strength," Trans. ASME, J. Basic Eng. 85D:97 (Mar. 1963)

64. Irwin, G.R., "Fracture Dynamics," in "Fracturing of Metals," ASM Cleveland, 1948

65. Rice, J.R., "The Mechanics of Crack Tip Deformation and Extension by Fatigue," preprint No. 36, ASTM Meeting, June 1966

66. De Havilland Official Rep. on "Comet" Failures, 1955

67. Irwin, G.R., Kies, J.A., and Smith, H.L., "Fracture Strength Relative to Onset and Arrest of Crack Propagation," Proc. ASTM 58:640 (1958)

68. Pellini, W.S., and Puzak, P.P., "Practical Considerations in Applying Laboratory Fracture Test Criteria to the Fracture Safe Design of Pressure Vessels," NRL Report 6030, Nov. 1963

69. Nichols, R.W., Proc. Roy. Soc. A285:104 (1965)

70. Irwin, G.R., and Sullivan, A.M., Proc. Roy. Soc. A285:141 (1965)

71. Puzak, P.P., and Pellini, W.S., Welding J. 35:275-S (June 1956)

72. Pellini, W.S., Goode, R.J., Puzak, P.P., Lange, E.A., and Huber, R.W., "Review of Concepts and Status of Procedures for Fracture-Safe Design of Complex Welded Structures Involving Metals of Low to Ultra-High-Strength Levels," NRL Report 6300, June 1965

73. Chow, J.G.Y., and McRickard, S.B., "Low-Temperature Embrittlement of Iron, Iron Alloys, and Steels by Newtron Irradiations," ASTM STP 380:120 (1965)

74. Trozera, T.A., and Flynn, P.W., ASTM STP 380:342 (1965)

75. Steele, L.E., and Hawthorne, J.R., ASTM STP 380:289 (1965)

76. Barnes, R.S., ASTM STP 380:58 (1965)

77. Steele, L.E., Hawthorne, J.R., Serpen, C.Z., Watson, H.E., and Klier, E.P., "Irradiation Effects on Reactor Structural Materials — 1 May - 31 July 1965," NRL Memorandum Report 1638, Aug. 15, 1965

Appendix A

RECOMMENDATIONS

PROPOSED INVESTIGATIONS AND TECHNIQUE DEVELOPMENT

1a. Investigate material crack paths and K values for cracks in high-stress regions at or near a nozzle. Such studies might employ a model constructed of a brittle, transparent material with stable crack extension assisted by moisture, or a model constructed of a low-toughness metal with stable crack extension produced by fatigue.

1b. Investigate the residual, compressive-stress type of protection which might be provided to such regions from the proof-testing method.

2. Develop ultrasonic techniques appropriate for finding and estimating sizes of transverse cracks.

3. Establish control and inspection techniques which insure absence of significant center-line weakness in electroslag weldments.

4a. Investigate stable-water-assisted crack growth rate for steels of interest using pressures, temperatures, and radiation typical of service conditions.

4b. Study the possibility of suppressing crack growth by means of warm preload crack blunting, if this stable growth rate is not negligible.

5. Investigate the influence of loading speed on K_{Ic} and on isothermal strain hardening in relation to the study of radiation hardening and embrittlement near and above a dosage of 10^{19} n/cm^2 (<1 MeV). A strong effect on both measurements is probable, due to the unstable relaxation of hardening (from large amounts of radiation) in the presence of increasing plastic strain. Time-rate sensitivity in this hardening relaxation would be expected. The dynamic K_{Ic} (or K_{Id}) may be larger than the static K_{Ic}, and some revision of methods for assessing the degree of radiation damage may be necessary.

SUGGESTED TESTS AND THE LEAK-BEFORE-BREAK CRITERION

1. Large-Thickness Toughness Tests

It is strongly endorsed that sharp notch tests should be performed on the materials developed for service, over the desired temperature range, at full section thickness. The bend test is favored, in view of its reasonable static load requirement, suitability for impact loading, and convenient comparison with the drop-weight NDT test. However, fatigue notches would be preferred; to obtain clear conditions for fracture mechanics analysis, a combination of slow bend tests and impact tests would also be desirable. It is vital that these tests, both static and dynamic, should be autographically instrumented for load, displacement, and either COD or transverse contraction at the notch root.

2. Intermediate-Thickness Substandard Toughness Tests

It will only be possible to test limited numbers of full-thickness specimens as part of a material evaluation program. However, Charpy-V specimens may prove to be too small for adequate routine production control of toughness at the selected level. It is considered that the evaluation program should contain half-thickness or quarter-thickness tests with which a reasonable full-thickness correlation might be obtained using COD mechanics methods. These tests should also be fully instrumented.

3. Small-Scale Local Toughness Tests

It is possible that certain microstructural combinations associated with welded joints will give rise to low-toughness zones. If large programs of in situ tests of such joints are not to be mounted, there should be an available sampling procedure using small-scale tests of subdivided joints to screen for low-toughness regions. This alternative is recommended, and it is considered that a small-scale test, such as the precracked Charpy test, should be further developed for the purpose. Instrumentation for autographic recording of load and displacement would be advisable to permit extraction of relevant fracture mechanics data. The same procedure could be used to monitor the effects of irradiation.

4. Slow Defect Growth and the Hydrostatic Test

It would appear, from studies of fatigue growth rate data and the thresholds for stress corrosion (and creep rupture cracking), that these factors will not be as important for the thick reactor pressure vessel steels as they are for high-strength steels and that slow extension of defects in service will not, therefore, be extensive. In this connection, it would seem to be more desirable to develop the technique of proof of vessels at intervals by hydrostatic test than to rely completely upon nondestructive flaw detection in service. The philosophy of proof test would comprise (a) overpressurization at an elevated temperature before repetition at an ambient or low temperature, to minimize the risk of loss by fracture during proof test and (b) determination of the period of validity of the proof test on the basis of: overpressure factor, or estimated rate of slow growth of the defects of toughness deterioration.

5. Full-Scale Vessel Test

If it is decided to test a full-scale vessel representative of thick material, it is recommended that the nozzle/sphere configuration should be employed, since the intersection region is considered to be the most critical in terms of the presence of crack defects. The test should be performed under a pulsating pressure to nucleate a natural crack defect at the most critical region, and it should be associated both with periodic applications of overpressure and measurements of slow growth of flaws, to provide a basis for proof test qualification in service.

6. Leak-Before-Break Criterion

It is recommended that the leak-before-break criterion of fracture should be retained, in spite of the increases in thickness and yield strength of reactor steels, because of the extra degree of sensitivity to defect sizes at stress concentrations that would otherwise arise. This is regarded as practicable if the precracked Charpy energy level can reach the level given by

$$\mathcal{G}_{Ic} \quad 0.56 \frac{W}{A} ; \tag{A1}$$

hence,

$$W = 0.116 \frac{\sigma_y^2 B}{E} . \tag{A2}$$

For A533 steel the maximum thickness is 12 in., and the minimum yield strength is 50,000 lb/in.^{2}; therefore,

$$W = 116 \text{ ft-lb.}$$

For A542 steel the maximum thickness is 8 in. and the minimum yield strength is 85,000 lb/in.^{2}; therefore, W = 223 ft-lb. These values are regarded as possible of achievement.

Appendix B

FRACTURE ANALYSIS UNDER CONDITIONS OF GENERAL PLASTIC YIELDING

GENERAL YIELDING IN A PRESSURIZED CYLINDER WITH A LONGITUDINAL CRACK

An effect which may be important in relatively thin cylinders and spheres concerns the crack extension force supplement from the bulging effect of internal pressure in the crack region. When the crack length is more than $3B$, experiments have shown substantial amounts of bulging. Theoretical analyses by Folias* suggest that the crack extension force ($\mathcal{G}$) ratios between through-cracks of given length $2a$, in shells and flat plates, may be expressed in the form

$$\frac{\mathcal{G}(\text{shell})}{\mathcal{G}(\text{flat plate})} = 1 + q\,\frac{a^2}{RB}\cdot\frac{a^2}{RB} < 1. \tag{B1}$$

where the constant q is 1.9 for spheres and 1.6 for cylinders, R is the midthickness radius, and B is the thickness. Folias expresses reservations concerning additional terms which are neglected in the analysis. Nevertheless, the trend is well represented for cracks for which a^2/RB does not greatly exceed 1.

Assume radius R, thickness B, crack length $2a$, internal limit pressure p, and yield stress σ_{YS}. Consider a beam element adjacent to the slit and parallel to it, loaded with axial tension $pR/2$ and distributed load $2pa$ per unit width. The bending moment at each of the three plastic hinge points is $pa^2/4$, but the limiting bending in the presence of tension may also be shown to be

$$\frac{pa^2}{4} = \frac{\sigma_{YS}}{4}\left[B^2 - \left(\frac{pR}{2\sigma_{YS}}\right)^2\right]. \tag{B2}$$

This may be regrouped as follows, in terms of the ratio of the hoop-to-yield stress $pR/B\sigma_{YS}$ and the dimensionless quantity BR/a^2, the solution of which is given by

$$\frac{pR}{B\sigma_{YS}} = \frac{BR}{a^2}\left[1 - \frac{1}{4}\left(\frac{pR}{B\sigma_{YS}}\right)^2\right] \tag{B3}$$

and

$$\frac{pR}{B\sigma_{YS}} = 2\left[\sqrt{\left(\frac{a^2}{RB}\right)^2 + 1} - \frac{a^2}{RB}\right]. \tag{B4}$$

At the limit pressure p plastic bending will take the form of bulging deflection, which will cause the axial tension to increase. This will diminish the limit moment until a stage of membrane longitudinal tension is eventually established, limited in turn only at the uniaxial yield stress. When this state is reached, there will be no remaining capacity to resist shearing in the radial plane at the ends of the crack, and tearing will therefore be anticipated. Thus, the plastic hinge bending may be established as a true, general yielding condition for the cylinder. In Table B1 strength factors are compared for the linear elastic calculation and the plastic limit calculation above.

*E. S. Folias, Intern. J. Fracture Mech. 1(Nos. 1 and 2) (1965).

Table B1
Relative Strength Factors

a^2/RB	Linear Elastic Calculation	Plastic Limit Calculation
0	1	—
0.5	0.745	—
0.75	0.675	1
1.0	0.62	0.83
1.5	0.54	0.60
2	0.49	0.46
3	0.40	0.32
5	0.33	0.19

As the crack increases in length the plastic limit on strength becomes even more pronounced than that computed by linear elastic fracture mechanics methods. The dependence of both upon the same dimensionless ratio a^2/RB lends considerable confidence to the assertion that these crack bulging effects will be negligible for shorter cracks of the leak-before-break type for which

$$\frac{a^2}{RB} \leq \frac{B}{R} << 1 . \quad (B5)$$

THE EFFECT OF LOCAL YIELDING AT NOZZLES ON CRACK EXTENSION FORCE AT A CRACK

When the stress system is wholly elastic, the small defect may be assumed to lie in the field of stress with the magnitude equal to the remote stress times the stress concentration factor (scf) for the nozzle. When local yielding at the nozzle has commenced, the stress will be limited at uniaxial yield σ_Y, but the strain will increase more than proportionally to the applied stress σ. The crack-extension-force supplementation may be estimated from the strain value, through the crack opening displacement estimated, in turn, using the strip yield model.

To determine the plastic strain field, the circular hole in an infinite plate under biaxial tension stress σ at infinity with plane stress may be considered. Let the hole radius be r and the plastic zone radius be R. For any radius a consider $R > a > r$. Within the plastic ring, the hoop stress is σ_Y and the radial stress σ_a is given, from equilibrium considerations, as

$$\sigma_a = \sigma_Y\left[1 - (r/a)\right] \text{ or, at radius } R,\ \sigma_R = \sigma_Y\left[1 - (r/R)\right]. \quad (B6)$$

At the boundary, with the elastic ring, the hoop stress σ_θ in the elastic and the plastic regions must be

$$\sigma_\theta = 2\sigma - \sigma_Y\left[1 - (r/R)\right] = \sigma_Y,\ r/R = 2\left[1 - (\sigma/\sigma_Y)\right]; \quad (B7)$$

hence,

$$\sigma_R = \sigma_Y\left[2(\sigma/\sigma_Y) - 1\right]. \quad (B8)$$

The hydrostatic stress in the plastic zone is

$$\frac{\sigma_Y + \sigma_R + 0}{3} = \frac{\sigma_Y}{3} [2 - (r/a)] \tag{B9}$$

and the deviator stresses are

$$\bar{\sigma}_\theta = \frac{\sigma_Y}{3} [1 + (r/a)] \quad \bar{\sigma}_a = \frac{\sigma_Y}{3} [1 - (2r/a)] . \tag{B10}$$

Thus,

$$\frac{e_a}{e_\theta} = \frac{\bar{\sigma}_a}{\bar{\sigma}_\theta} = \frac{1 - (2r/a)}{1 + (r/a)} . \tag{B11}$$

But, for radial displacement u, $e_\theta = u/a$ and $e_r = du/da$, so that

$$\frac{e_a}{e_\theta} = \frac{a}{e_\theta} \left(\frac{de_\theta}{da} + 1 \right) = - \frac{3r/a}{1 + (r/a)} + 1 . \tag{B12}$$

The solution to this is

$$e_\theta = A [1 + (r/a)]^3 . \tag{B13}$$

At the elastic/plastic boundary

$$e_\theta = \frac{\sigma_\theta - \nu\sigma_R}{E} = \frac{\sigma_Y}{E} \left(1 + \nu - \frac{2\nu\sigma}{\sigma_Y} \right) ,$$

so that in the plastic region

$$e_\theta = \frac{\sigma_Y}{E} \left(1 + \nu - \frac{2\nu\sigma}{\sigma_Y} \right) \left(\frac{1 + \frac{r}{a}}{1 + \frac{r}{R}} \right)^3 . \tag{B14}$$

or, at the edge of the hole,

$$e_\theta = \frac{\sigma_Y}{E} \frac{8 \left(1 + \nu - \frac{2\nu\sigma}{\sigma_Y} \right)}{\left(3 - 2 \frac{\sigma}{\sigma_Y} \right)^3} . \tag{B15}$$

The ratio between this value and the corresponding value without yielding is given by

$$\frac{e_{\theta(\mathrm{plastic})}}{e_{\theta(\mathrm{elastic})}} = \frac{4 \left[(1 + \nu) \frac{\sigma_Y}{\sigma} - 2\nu \right]}{\left(3 - \frac{2\sigma}{\sigma_Y} \right)^3} . \tag{B16}$$

from which the strain limitation arising from surrounding elastic material is evident, even when the plastic zone has grown to large size. Table B2 gives several values of interest for this ratio.

The COD, hence the crack extension force and the stress field parameter, can be estimated for a radial surface crack of very short length c by assuming that the extent of the yield zone is identical with that for the circular opening. The value obtained may be compared with the linear/elastic equivalent

$$\mathcal{G}_0 = \frac{\pi(2\sigma)^2 c}{E} \quad . \tag{B17}$$

Now, the strip yield model gives rise to a COD value

$$\mathcal{G}_1 = \sigma_{YS}\delta = \frac{8(\sigma_Y)^2 c}{\pi E} \ell n \left(\frac{R-r}{c}\right) \quad , \tag{B18}$$

whence,

$$\frac{\mathcal{G}_1}{\mathcal{G}_0} = \frac{8}{\pi E}\left(\frac{\sigma_Y}{2\sigma}\right)^2 \ell n \left(\frac{R-r}{c}\right) \quad . \tag{B19}$$

several values of which are listed in Table B3 for cracks of length r/n, from which it would appear that Eq. (B17) is suitable for calculations for small cracks without correction.

Table B2
Ratios of Elastic to Plastic Stress and Strain

$\frac{\sigma}{\sigma_Y}$	$\frac{\sigma_{elastic}}{\sigma_{plastic}\ (2\sigma/\sigma_Y)}$	$\frac{R}{r}$	$\frac{e_{e(plastic)}}{e_{e(elastic)}}$
0.5	1.0	1.0	1.0
0.6	1.2	1.25	1.08
0.7	1.4	1.67	1.23
0.8	1.6	2.5	1.49
1.0	2.0	—	2.8

Table B3
Comparison of Linear Elastic and Strip Yield Model

$\frac{2\sigma}{\sigma_Y}$	$\frac{R}{r} - 1$	$\mathcal{G}_1/\mathcal{G}_0$		
		$n = 5$	$n = 10$	$n = 20$
1.0	0	—	—	—
1.2	0.25	0.126	0.516	0.905
1.4	0.67	0.50	0.785	1.07
1.6	1.5	0.60	0.86	1.08

For intermediately longer cracks a first approximation to the crack extension force is obtained from the alternative assumption that the circumferential plastic strain at the inside edge of the opening is wholly accommodated as crack opening displacement, at a pair of diametrically opposite edge cracks. This incremental value of COD is large compared with the preyield value, and leads to

$$\delta\sigma_Y = \sigma_{YS}\left(K'\pi r \frac{\sigma_Y}{E}\right) = K' \frac{\pi\sigma_Y^2 r}{E} \quad , \tag{B20}$$

where, from Eq. (B15), K' is given by

$$K' = \frac{8\left(1 + \nu - \frac{2\nu\sigma}{\sigma_Y}\right)}{\left(3 - 2\frac{\sigma}{\sigma_Y}\right)^3} - 1 \tag{B21}$$

with several values given in Table B4.

ratio δ_1 / δ_2. For rate-sensitive materials, the loading speed and the ratio of static-to-dynamic fracture toughness would be important additional factors. The analysis, at this point, faces enough elements of uncertainty so that an appeal to experimental results for guidance would be desirable.

In the case of large nuclear reactor pressure vessels, loading would be slow enough, even in the proof test, to suggest that crack extension would be resisted by the static K_{Ic}. For A302B steel at 70°F one might assume K_{Ic} = 90 ksi $\sqrt{\text{in.}}$ and σ_{YS} = 65 ksi. For these values, a = 0.86 in. would produce onset of rapid fracture when the general tension across the region of the crack first reached $\sigma = \sigma_Y$. If the crack present is smaller and reaches instability with $\delta_1 = \delta_2$, the value of a is given by

$$\delta_c = \delta_1 + \delta_2 = \left(\frac{\sigma_{YS}}{E}\right) \frac{\pi}{4} \left(\frac{90}{65}\right)^2 ,$$

$$\delta_1 = 2.24 \left(\frac{\sigma_{YS}}{E}\right) a ,$$

$$\delta_2 = q_1 \left(\frac{\sigma_{YS}}{E}\right) a ,$$

or

$$a = \frac{1.92 \text{ in.}}{2.24 + q_1} .$$

Selection of q_1 larger than 2.24 would mean that cracks with values of a less than 0.46 in. would produce onset of rapid fracture. For example, if q_1 = 4, the critical value of a is 0.31 in. The relative infrequency of proof test failures at pressures which produce tensile yield at local regions of nozzles, coupled with inspection uncertainties, suggests the proper value of q_1 is in the range of 2 to 4. A small crack, which achieves a value of $K^2 < K_{Ic}^2$ during the attainment of general yielding in the region of the crack, is expected to extend only by a stable increment of growth in the balance of the loading cycle. The unloading cycle would leave this crack in a state of residual compression, a condition likely to protect the crack from additional slow growth during subsequent loadings to smaller internal pressure.

WORK REQUIREMENT FOR FRACTURE OF A SHARPLY NOTCHED BAR IN BENDING

From investigations of plastic slip fields by Green and Hundy* the deformation near the root of the notch (for nonwork hardening, fully plastic bending) occurs on slip lines which are arcs of circles centered beneath the notch at the distance 0.45 d_N, where d_N is the net ligament size. Wells (60) assumes from this result that the value of δ_2 after substantial bending and a stable crack growth of x is approximately given by

$$\delta = 0.45 \, (d_0 - x) \theta , \tag{B25}$$

where θ is the plastic bend angle of the bar, d_0 is the original ligament depth at x = 0, and δ_1, for elastic strain components, is assumed negligible compared to δ_2.

*A.P. Green, and B.B. Hundy, "Initial Plastic Yielding in Notch Bend Tests," J. Mech. Phys. Solids 4:128-144 (1956).

Table B4
Estimates of K' and K''

σ/σ_Y	K'	K''	σ/σ_Y	K'	K''
1.0	0.08	0.45	1.4	0.49	1.6
1.2	0.23	0.82	1.6	1.8	∞

The larger values K'' (Table B4) represent the coefficients obtained if plastic behavior is neglected, but the cracks are assumed to extend between $\pm R$ and are subject to the remote stress field of magnitude σ.

These assessments show that crack extension force values for small radial crack defects at a nozzle are not significantly greater when plastic deformation occurs at the inner periphery than when it does not.

ALTERNATIVE DISCUSSION OF SMALL CRACK IN A FIELD OF GENERAL YIELD

When the plastic zone at the leading edge of the crack is separated from the free edges of the specimen by a large linear-elastic domain, the crack opening dislocation δ is proportional to $\mathcal{G}\,\sigma_Y$ through a near-unity proportionality constant. The definition of δ employed in verifying the relationship would be in terms of the integral of y-direction strains around the elastic-plastic boundary.

After general yielding the same definition is applicable in a formal way. However, after the plastic zone contacts the free edges of the specimen, a simplified method of analysis is possible. Consider, for example, the case of a small surface crack in a nozzle throat region, where analysis predicts a zone of yielding which is confined but is large compared to the crack size. The portion of δ established prior to general yield of this region can be estimated as

$$\delta_1 = \mathcal{G}_1/\sigma_Y , \tag{B22}$$

where $\mathcal{G}_1$ is the plasticity adjusted value of $\mathcal{G}$ corresponding to a general tension across the region equal to σ_Y. Beyond this point we assume that the plastic flow pattern around the crack scales in proportion to the crack size and tends to concentrate the effect of tension direction yielding near the crack into an increase in δ. To represent the influence of a plastic strain equal to σ_Y/E, the effect in terms of additional δ value might be estimated as

$$\delta_2 = q_1 a \frac{\sigma_Y}{E} , \tag{B23}$$

where q_2 is a near-unity proportionality factor.

If the surface length of the crack is $4a$, the adjusted linear analysis gives

$$\delta_1 = 2.24a \frac{\sigma_Y}{E} . \tag{B24}$$

Whether a δ value which would be large enough for onset of rapid fracture in the elastic range will produce more than an increment of stable extension depends upon the

If δ retains a critical value δ_c as x increases, we have the relationship

$$d\delta = 0.45\ (d_0 - x)\, d\theta - 0.45\ \theta\, dx = 0\ . \tag{B26}$$

Thus, during increase of x

$$d\theta = \frac{\theta\ dx}{(d_0 - x)} = \frac{\delta_c\ dx}{0.45\ (d_0 - x)^2}\ . \tag{B27}$$

The bending moment for a unit-thickness bar which would be consistent with the basic assumptions is approximately

$$M = \frac{\sigma_{YS}}{4}\ (d_0 - x)^2 . \tag{B28}$$

Calculation of the work in terms of

$$W = \int_{0\,(a\,t\ x=0)}^{\delta=\delta_c} M\, d\theta + \int_{x=0}^{x=d_0} M\, d\theta \tag{B29}$$

gives the result

$$W = 1.11\ \sigma_Y\ \delta_c\ d_0 \tag{B30}$$

or

$$W = 1.11\ \mathcal{G}_c\ d_0\ . \tag{B31}$$

Wells (60), for reasons not clearly explained, assumes that

$$d\theta = \frac{\delta_c\ dx}{(0.45)^2 (d_0 - x)^2} \tag{B32}$$

during increase of x and finds that

$$W = 1.91\ \mathcal{G}_c\ d_0\ , \tag{B33}$$

where W is the total work per unit bar thickness.

Since the intuitive, expected result is $W = \mathcal{G}_c\, d_0$, the answer with the smaller coefficient appears to be the most acceptable calculation method.

The preceding total fracture work calculation leading to Eq. (B31) suggests that Eq. (B25) might be used to estimate values of δ_c when the fracture of a notched bar occurs after general yielding. A discussion of applications of this idea is given in Ref. 16.

Security Classification

DOCUMENT CONTROL DATA - R & D

Security classification of title, body of abstract and indexing annotation must be entered when the overall report is classified)

1. ORIGINATING ACTIVITY (Corporate author)

Naval Research Laboratory
Washington, D.C. 20390

2a. REPORT SECURITY CLASSIFICATION

UNCLASSIFIED

2b. GROUP

3. REPORT TITLE

BASIC ASPECTS OF CRACK GROWTH AND FRACTURE

4. DESCRIPTIVE NOTES (Type of report and inclusive dates)

A final report on the problem.

5. AUTHOR(S) (First name, middle initial, last name)

G.R. Irwin, J.M. Krafft, P.C. Paris, and A.A. Wells

6. REPORT DATE	7a. TOTAL NO. OF PAGES	7b. NO. OF REFS
November 21, 1967	76	77

8a. CONTRACT OR GRANT NO.	9a. ORIGINATOR'S REPORT NUMBER(S)
NRL Problem F01-18	NRL Report 6598
b. PROJECT NO. USAEC Oak Ridge, Tenn.,	
c. ltr ACT:WT of 9 Aug. 1966	9b. OTHER REPORT NO(S) (Any other numbers that may be assigned this report)
d.	

10. DISTRIBUTION STATEMENT

This document has been approved for public release and sale; its distribution is unlimited.

11. SUPPLEMENTARY NOTES	12. SPONSORING MILITARY ACTIVITY
Sponsored by AEC, Oak Ridge, Tenn.	(See item 11 on this form)

13. ABSTRACT

A near approach to absolute fracture safety in boiling water (BW) and pressurized water (PW) nuclear reactor pressure vessels requires a very conservative fracture control plan. Such a plan must assume that any plausible cracklike defect, which has not been proved absent by inspection, may exist in the vessel. Requirements for design, materials, and inspection may then be established in a conservative way relative to estimates of progressive crack extension behavior. These estimates are assisted by elastic and plastic methods of analysis of cracks in tension. Approximate methods of assigning K_{Ic} values to measurements of crack toughness in terms of a brittle-ductile transition temperature are valuable in reviewing methods of fracture control which have received trial in the past, such as the NRL fracture analysis diagram and the leak-before-break toughness criterion.

DD FORM 1 NOV 65 1473 (PAGE 1)

S/N 0101-807-6801

Security Classification

14 KEY WORDS	LINK A		LINK B		LINK C	
	ROLE	WT	ROLE	WT	ROLE	WT
Brittle-ductile transition						
Crack growth rate						
Crack stress field						
Critical crack size						
Elastic-plastic analysis						
Fracture analysis diagram						
Fracture-dominant failures						
Fracture toughness (static and dynamic)						
Leak-before-break criterion						
Linear stress analysis						
Plasticity analysis						
Pressure vessels						
Progressive crack extension						
Radiation effects						
Strain aging						
Stress corrosion						
Strip-yield-zone concept						
Temperature equalization time						
Yielding-dominant failures						